Instituto Superior de Engenharia do Porto

DEPARTAMENTO DE ENGENHARIA GEOTÉCNICA

Spatiotemporal changes of urban groundwater vulnerability and safeguard zones in the fractured hard-rock aquifers of Porto city (NW Portugal): A GIS-based methodological essay

Reem Mansour

2022

(página propositadamente em branco)

Instituto Superior de Engenharia do Porto
DEPARTAMENTO DE ENGENHARIA GEOTÉCNICA

Spatiotemporal changes of urban groundwater vulnerability and safeguard zones in the fractured hard-rock aquifers of Porto city (NW Portugal): A GIS-based methodological essay

Alterações espácio-temporais da vulnerabilidade das águas subterrâneas urbanas e perímetros de protecção nos aquíferos cristalinos fracturados da cidade do Porto (NW Portugal): Um ensaio metodológico baseado em SIG

Reem Mansour

Nº 1202047

*Dissertação apresentada ao Instituto Superior de Engenharia do Porto (ISEP) para cumprimento dos requisitos necessários à obtenção do grau de **Mestre em Engenharia Geotécnica e Geoambiente**, realizada sob a orientação da Doutora Maria José Afonso, Professora Adjunta no Departamento de Engenharia Geotécnica do ISEP e da Doutora Liliana Freitas, Investigadora no Laboratório de Cartografia e Geologia Aplicada do ISEP.*

*Dissertation submitted to the 'Instituto Superior de Engenharia do Porto' (ISEP) to fulfil the requirements to obtain the **Master's Degree in Geotechnical and Geoenvironmental Engineering** carried out under the guidance of Dr. Maria José Afonso, Adjunct Professor at the Department of Geotechnical Engineering of ISEP and Dr. Liliana Freitas, Researcher at the Laboratory of Cartography and Applied Geology of ISEP.*

(página propositadamente em branco)

Júri

Presidente

Doutor Helder Gil Iglésias de Oliveira Chaminé
Professor Coordenador com Agregação, Departamento de Engenharia Geotécnica, Instituto Superior de Engenharia do Porto

Doutor João Paulo Meixedo dos Santos Silva
Professor Coordenador, Departamento de Engenharia Geotécnica, Instituto Superior de Engenharia do Porto

Doutora Maria José Coxito Afonso
Professora Adjunta, Departamento de Engenharia Geotécnica, Instituto Superior de Engenharia do Porto

Doutor José Augusto Alves Teixeira
Professor Auxiliar, Departamento de Geografia, Faculdade de Letras da Universidade do Porto

Doutora Liliana Filipa da Silva Freitas
Investigadora, Laboratório de Cartografia e Geologia Aplicada, Instituto Superior de Engenharia do Porto

*A dissertação de **mestrado em engenharia geotécnica e geoambiente** (MEGG) foi apresentada e defendida em prova pública, por **Reem Mansour**, em 9 de Novembro de 2022 mediante o júri nomeado, em que foi atribuída, por unanimidade, a classificação final de **15 (quinze) valores**, cuja fundamentação se encontra em acta. Todas as correções pontuais determinadas pelo júri, e só essas, foram efectuadas.*

To my family, my teachers, my home country Syria, and my second home Portugal…

(página propositadamente em branco)

Acknowledgments

I would like to express my sincere gratitude to my esteemed advisers, Professor Maria José Afonso (DEG and LABCARGA|ISEP) and Dr. Liliana Freitas (LABCARGA|ISEP), for providing me with invaluable supervision, sharing bibliography and data, and support throughout my Master's dissertation.

Additionally, I would like to thank Professor Helder I. Chaminé (DEG and LABCARGA|ISEP) for his treasured support, brainstorms, and mentorship over the last 2 years.

My gratitude extends to the Global Platform for Syrian Students[1] for the funding opportunity to undertake my advanced studies at the Department of Geotechnical Engineering at the School of Engineering ("Instituto Superior de Engenharia do Porto", ISEP), Polytechnic of Porto (P.Porto). Without their tremendous support, it would be impossible for me to complete my MSc.

My appreciation also goes to my husband, family, and friends for their encouragement and support throughout my studies.

[1] *https://www.globalplatformforsyrianstudents.org/*

(página propositadamente em branco)

Keywords

Urban fractured hard-rock aquifers, Spatiotemporal changes, Groundwater vulnerability, Safeguard zones, GIS.

Abstract

This study presents a spatiotemporal analysis of changes in groundwater vulnerability and the safeguard zones using an integrated, multidisciplinary, and GIS-based approach. The fractured hard-rock aquifer of Porto city in the surroundings of Paranhos and Salgueiros spring galleries was used as an experimental case study where the TIME–INPUT method was used for assessing the intrinsic vulnerability and the Time-Dependent model was used for assessing the sanitary safeguard zones. Two scenarios were compared: the end of the XIXth century when the water was still used for drinking, and there were no sanitary sewers, and the present day in the XXIst century, after the city's urban expansion. The vulnerability and the safeguard zones were completely assessed using flow travel time components, and the results are based on travel times rather than categories of unitless numbers. Dug-wells data were used to estimate the thickness of the fissured zone, the saturated zone, and the unsaturated zone. The historical land use map was reconstructed using a historic map from 1892. Then, GIS models were built to predict the recharge, groundwater vertical and horizontal travel time, and surface travel time. Several updated elements have been added to enhance the calculation of vulnerability in urban areas, such as the maps of hydraulic networks. The study shows that the TIME-INPUT method and the Time-dependent model apply to urban fractured hard-rock aquifers. The results indicate that the land use in the study area has changed over time with rapid growth in urbanization, and the most affected factor by this change are the recharge (INPUT Factor) and surface travel time. Areas around tectonic lineaments are the most vulnerable, and the overall spatiotemporal changes in vulnerability and the safeguard zones are small in the study area between the past and present time.

(página propositadamente em branco)

Palavras-Chave

Aquíferos fraturados urbanos, Alterações espácio-temporais, vulnerabilidade das águas subterrâneas, perímetros de proteção, SIG.

Resumo alargado

Este estudo apresenta uma análise espácio-temporal das alterações na vulnerabilidade das águas subterrâneas e nos perímetros de proteção, utilizando uma abordagem integrada, multidisciplinar e simplificada baseada em SIG. O aquífero granítico fraturado da cidade do Porto (NW de Portugal) na envolvente das galerias subterrâneas que conduzem a água das nascentes de Paranhos e Salgueiros foi utilizado como caso de estudo experimental. Dois cenários temporais foram usados para comparar as mudanças nas zonas de vulnerabilidade intrínseca e de proteção antes e após a expansão urbana e o consequente crescimento da cidade. No cenário histórico, de finais do século XIX, as águas das nascentes de Paranhos e Salgueiros eram usadas para consumo humano e não havia um sistema integrado de esgotos, e o cenário atual, século XXI, em que se analisaram as infraestruturas hidráulicas em pleno funcionamento (Rede de abastecimento público de água, saneamento e pluvial). O método TIME–INPUT foi utilizado para avaliar a vulnerabilidade intrínseca. Os principais fatores envolvidos neste método são o tempo de fluxo (TIME) da água desde a superfície até atingir a zona saturada, com um peso de 60%, e o valor da recarga subterrânea (INPUT), com um peso de 40%. Esta ponderação ligeiramente empírica, atribuindo ao tempo uma maior importância do que a recarga. Em contraste com outros métodos de avaliação, a vulnerabilidade é expressa em tempo real e os valores de entrada são reais e não valores adimensionais. Os dados de base para calcular o tempo de fluxo são a espessura e a condutividade hidráulica de cada nível da zona não saturada. A influência dos lineamentos tectónicos foi utilizada como fator de correção, uma vez que estes diminuem o tempo de fluxo. O fator recarga é classificado como fator de correção. Valores baixos de recarga correspondem a valores altos de fatores de correção, aumentando assim o tempo, enquanto valores altos de recarga reduzem o tempo e, assim, aumentam a vulnerabilidade. Para avaliar o fator recarga, foram usados vários fatores, incluindo a Geologia/Hidrogeologia, os declives, o uso do solo, a densidade de lineamentos tectónicos e a densidade da rede de drenagem. Além disso, para melhorar o cálculo do fator recarga em áreas urbanas no cenário atual, foram igualmente utilizados os parâmetros hidráulicos e sanitários, densidade da rede de água potável, densidade da rede de saneamento e densidade da rede de águas pluviais.

O modelo Time-Dependent foi usado para avaliar os perímetros de proteção. Este modelo inclui componentes de fluxo horizontal e vertical da água subterrânea e considera ainda uma componente de fluxo superficial. O tempo de fluxo vertical através da zona não saturada foi calculado usando o método TIME-INPUT. O tempo de fluxo horizontal na zona saturada foi estimado usando a ferramenta Euclidian Distance no ArcGIS Spatial Analyst e assumido para a velocidade do fluxo o valor inicial de 1 m/dia proposto por Devlin. O tempo de fluxo superficial, que é uma função da topografia, da geologia e do uso do solo no seio da bacia hidrográfica, foi previsto usando o método de velocidade NRCS. Seguidamente, o tempo total de fluxo foi calculado combinando as componentes dos tempos de fluxo.

A vulnerabilidade e os perímetros de proteção foram avaliados usando as componentes do tempo de fluxo. Para estimar a espessura das zonas não saturada, saturada e fraturada foram usados dados de poços existentes em 1908. O mapa histórico de uso do solo foi reconstruído usando um mapa histórico de 1892. Seguidamente, os modelos SIG foram construídos para prever a recarga, os tempos de fluxo vertical e horizontal da água subterrânea e o tempo de fluxo superficial.

Os resultados baseiam-se nos tempos de fluxo e não em números adimensionais. Desta forma, o nível de subjetividade na avaliação da vulnerabilidade é reduzido, pois a hierarquização e a parametrização da vulnerabilidade foram parcialmente evitadas. As áreas com minores tempos de fluxo são mais vulneráveis. Seguidamente converteu-se o mapa do tempo total de fluxo obtido num mapa de perímetros de proteção.

O uso do solo, na área em estudo, sofreu alterações ao longo do tempo. Desde o passado, no século XIX, até ao presente, no século XXI, ocorreu um rápido crescimento urbano. Foi possível comprovar, que os valores dos parâmetros mais afetados pelas alterações do uso do solo, foram a recarga e o tempo de fluxo superficial.

Os resultados obtidos indicam que a componente de tempo de fluxo vertical total é inferior a 12 dias e que as áreas em próximas aos lineamentos tectónicos são as mais vulneráveis, por apresentarem os valores menores de tempo de fluxo. No entanto, as alterações espácio-temporais gerais em termos de vulnerabilidade e área de proteção foram pequenas na área de estudo, entre passado e o presente. Considerando que as características hidrogeológicas da área de estudo não sofreram alterações significativas entre o passado e o presente, não houve alterações espácio-temporais no tempo de fluxo horizontal, apresentando este um valor máximo de cerca de 1 ano e 4 meses (491 dias). No entanto, na maior parte da área, o tempo de fluxo horizontal é inferior a 50 dias, e na envolvente das nascentes de Paranhos e Salgueiros pode atingir os 100 dias. O tempo de fluxo superficial máximo na área de estudo é de 1 h no passado e de 0,5 h atualmente, o que significa que este tempo se torna mais rápido com o aumento da urbanização. Quanto ao tempo total de fluxo, este apresenta valores semelhantes aos do tempo de fluxo horizontal, com um valor máximo de cerca de 1 ano e 4 meses (489 dias). Na maior parte da área o tempo total de fluxo é inferior a 50 dias, e na envolvente das nascentes de Paranhos e Salgueiros pode atingir os 100 dias. As áreas envolventes aos lineamentos tectónicos apresentam os menores valores de tempo de fluxo e, portanto, os níveis de vulnerabilidade mais elevados.

As mudanças espácio-temporais gerais nas zonas de vulnerabilidade e de proteção foram pequenas na área de estudo entre o tempo passado e o presente.

Este estudo mostrou que o método TIME-INPUT e o modelo Time-Dependent se podem aplicar a aquíferos urbanos fraturados, e a metodologia proposta baseada em SIG pode ser aplicada com diferentes níveis de dados, mesmo com limitação de dados. No entanto, com a possibilidade de melhorá-lo e melhorar a qualidade da aquisição de dados, o método torna-se mais flexível e o nível de incerteza na previsão diminui.

Table of Contents

Table of Figures

List of Tables

(página propositadamente em branco)

Chapter I: Introduction

(página propositadamente em branco)

"Life is divided into three terms – that which was, which is, and which will be. Let us learn from the past to profit by the present, and from the present, to live better in the future. ". William Wordsworth (1770-1850)

"All models are wrong, but some are useful". George E. P. Box (1919-2013)

1.1. Overview

History matters in aquifers since what happened in the past has its legacies in the present (Martin et al., 2017, 2021). Therefore, historical reconstruction and recreation of the past conditions of aquifers are important for understanding the past and resolving long-ago problems (Clement, 2011). It is also essential for providing estimates of contaminant concentrations in drinking water and identifying the impacts of land uses and contamination on the groundwater used for drinking water in the Past (Swartz et al., 2003; Guan et al., 2009).

Throughout history, most settlements relied on springs and shallow wells for reliable, clean potable water. However, the accelerated urbanization and transformation from undeveloped spaces to urban environments, along with urban land-use practices, put tremendous and highly complex pressure on groundwater sources, resulting in spatial and temporal changes in the landscape. These alterations then impact urban ecosystems, including urban waters and their aquatic ecosystems, and change the hydrological urban water cycle and the quantity and quality of urban water (Hibbs, 2016; McGrane, 2016).

To analyze how urban development could affect groundwater quality and contribute to changing the vulnerability of the urban aquifer to contamination over time, a reconstruction of the historical groundwater vulnerability maps of aquifers can be useful since groundwater vulnerability maps can identify areas susceptible to contamination. They are also important for delineating water source protection areas and assessing groundwater contamination risks and quality protection (Witkowski et al., 2007, 2020).

Climate, geology, geomorphology, land use/cover, hydrogeochemistry, hydraulics, and human activities play a significant role in groundwater sustainability in urban areas as they control groundwater infiltration, recharge, and vulnerability (Freitas, et al., 2019a). Based on this, for mapping historical urban aquifer vulnerability, it is important to understand the hydrological conceptual site model of the study area, which describes the natural and anthropogenic factors that govern the movement of groundwater in the subsurface. It can answer questions related to the behavior of the groundwater system in the past and how it will change in the future as natural and anthropogenic influences are combined (Kresic & Mikszewski, 2012).

A Geographic Information System (GIS), which is a computer system that analyzes and displays geographically referenced information and uses data that is attached to a unique location, is increasingly becoming popular in mapping and visualizing groundwater vulnerability, reconstruction of land uses (Albuquerque et al., 2013) and even modelling and analyzing groundwater flow (Jani, 2012). GIS can be a rapid and simplified solution to model groundwater flow using minimal input data and basic modelling procedures (Schilling & Wolter, 2007).

Because of their wide extent, crystallized basement rocks are commonly used as a source of groundwater, but their yields are generally small, and the low storage makes boreholes prone to drying up during droughts. In addition, the disposal of wastewater on-site to the subsurface in an unsanitary manner can also be a problem for cities (Morris et al., 2003).

In this study, the reconstruction of the maps will be based on GIS. An integrated, multidisciplinary, and simplified GIS-based methodology will be conducted to reconstruct groundwater vulnerability in urban areas. This methodology will be applied in the urban area of Porto, which is one of the oldest cities in Europe and is settled on the granitic hill slopes of Douro riverbanks.

Several studies have been published in the urban area of Porto related to mapping and visualizing the vulnerability and safeguard zones of the historical groundwater system (Afonso et al., 2016; Freitas et al., 2019a,b; Meerkhan et al., 2021). In those studies, the vulnerability was estimated as dimensionless numbers using the following methods: DRASTIC (Aller, 1985), GOD (Foster, 1987; Foster et al., 2002), AVI (Van Stempvoort et al., 1993), SI (Francés et al., 2001; Ribeiro et al., 2017); DRASTIC-Fm (Denny et al., 2007), SINTACS (Civita, 1994, 2008, 2010), DISCO (Pochon et al., 2008), and DISCO-Urban (Meerkhan et al., 2021).

However, in this study, the vulnerability is expressed in real-time instead of dimensionless numbers, and the vulnerability maps were created using two approaches, the Input-Time method developed by Kralik & Keimel (2003) and the Time-Dependent Model (TDM) (Živanović et al., 2016). The Input-Time method calculates aquifer vulnerability regarding groundwater vertical travel time and recharge amounts. At the same time, the Time-Dependent model (TDM) delineates groundwater protection zones in terms of groundwater travel time (vertical and horizontal travel time) and surface water travel in areas where surface runoff is predominant.

Considering the time lag associated with contaminant transport is important in effective vulnerability studies since when contaminants take longer to reach the groundwater table or the groundwater receptor, the more dilution, retardation, and attenuation they have. Besides, in fissured aquifers, the relationship between attenuation and fracture flow must be considered carefully (Robins et al., 2007). It is important to understand the effective pathways of recharge

where the contamination attenuation occurs (Ó Dochartaigh et al., 2005) since the travel time, attenuation capacity and quantity of contaminants are a function of the subsoils that overlie the groundwater, the type of recharge and the thickness of the unsaturated zone through which the contaminant moves (Lee et al., 2020).

Moreover, both mapping methods, Input-Time, and TDM, have the advantage that they allow evaluation of the parameters recharge and travel time separately, and therefore, the results are more easily verified, and the evaluation process is more transparent. In addition, they have universal practical applications in porous media as well as in complex fractured and karstified groundwater bodies (Kralik & Keimel, 2003). Therefore, they are widely applicable and can be used to initial and further characterise groundwater bodies in the European Water Framework Directive (Kralik & Keimel, 2003). Nevertheless, these methods need an update and modification to best reflect the characteristics of our study area, an urban area in a fissured aquifer system. Accordingly, some aspects of recharging in urban areas and the characteristics of fractured rock aquifers will be considered when calculating groundwater vulnerability.

1.2. Research problems, objectives, and questions

For more than six centuries, the water supply of Porto city was provided by fountains supplied by numerous springs. Throughout the centuries, several underground galleries were excavated on fissured granitic rock masses to capture the water of springs and protect it from contamination (e.g. Afonso et al., 2010, 2020). However, over the years, urbanization and anthropogenic activities changed the quality and quantity of these urban heritage sources. As a result, they are no longer of drinking quality. Figure 1 illustrates the urban growth around the *Paranhos and Salgueiros* springs and the corresponding increase in groundwater demand between 1700 and 1892 (Morais & Galvão de Carvalho, 2018).

Reconstructing the maps of groundwater vulnerability and groundwater travel time of contaminations in the aquifers in an urban area is important to understand the changes in sensitivity of the water sources to human and/or natural impacts and the alteration of groundwater protection zones. With regards to this and taking the lack of historical field data into account and considering the difficulty of building fate and transport models of groundwater and contaminants, a simplified GIS-based technique is used to reconstruct the historical maps and determine the vulnerability's vulnerability change over time.

This study aims to visualize and understand the history of groundwater, which was the most important source of fresh water in the urban area of Porto (Afonso et al., 2016), and make the invisible visible throughout achieving the study's main objectives, which are:

I. Developing a simplified GIS-based model to reconstruct the historical groundwater travel time, recharge, vulnerability, and safeguard zones in the urban fissured aquifers in the city of Porto in the historical period, the beginning of the XXth century, when the galleries were still used for drinking, and there were no sanitary sewers or water supply system (e.g., Afonso 2011, Afonso et al. 2018) and comparing the results to the current situation after the urban expansion and growth of the city has occurred; and

II. Understanding the spatiotemporal changes of groundwater travel time components (The vertical travel time, the horizontal travel time, and the surface travel time) between the past and the present day and how vulnerability and safeguard zones have changed based on these components.

Additionally, the research aims to answer the following questions:

I. What are the most important factors when mapping and modelling groundwater travel time, recharge, vulnerability, and safeguard zones in urban fissured aquifers?; and

II. What are the spatial-temporal changes in land uses, groundwater flow, and vulnerability in the urban area of Porto between the XIXth and the present day?

Research contributions include updating the parameters of the TIME-INPUT method and the Time-Dependent Model (TDM), so they can best fit groundwater modelling in urban fractured hard-rock aquifers.

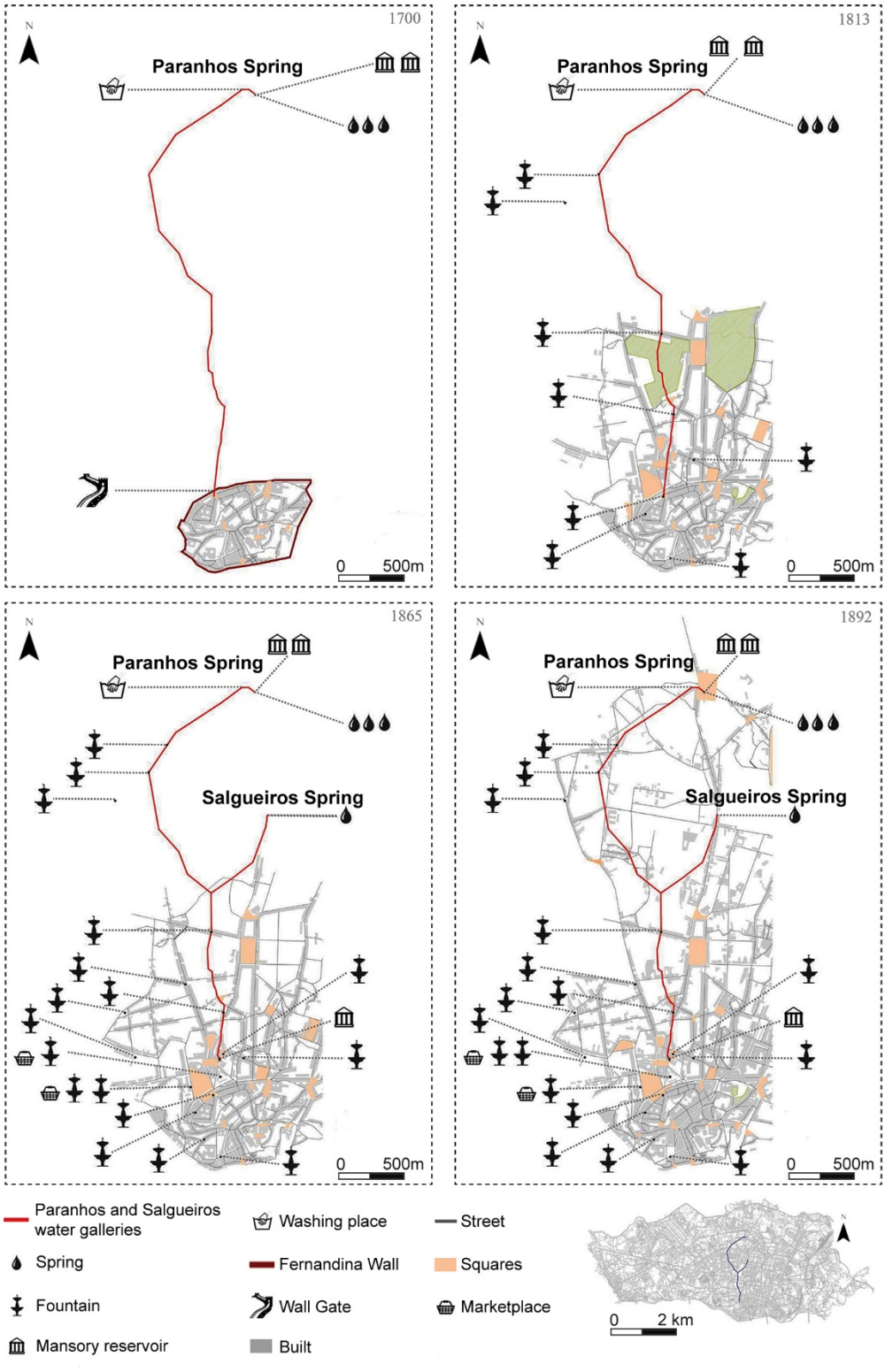

Figure 1. The urban growth around the Paranhos and Salgueiros springs and the corresponding increase in groundwater demand between 1700 and 1892 (after Morais & Galvão de Carvalho, 2018).

1.3. Research outlines

This study is divided into five chapters: Chapter I is a general introduction to research problems, objectives, questions, and contributions. Chapter II is a literature review of the spatiotemporal changes in urban hydrogeology and how to apply the TIME-INPUT vulnerability and the Time-Dependent Model (TDM) in urban and fractured hard-rock aquifers. In Chapter III, the geographical and historical background of the studied area is presented, and the research methodology is described. Chapter IV is an identification of the study's outcomes and results. Chapter V, the final chapter, contains the main conclusions and suggestions for future research.

Figure 2 illustrates the outline and structure of this study, from the goals to the methodology and the main results to be found.

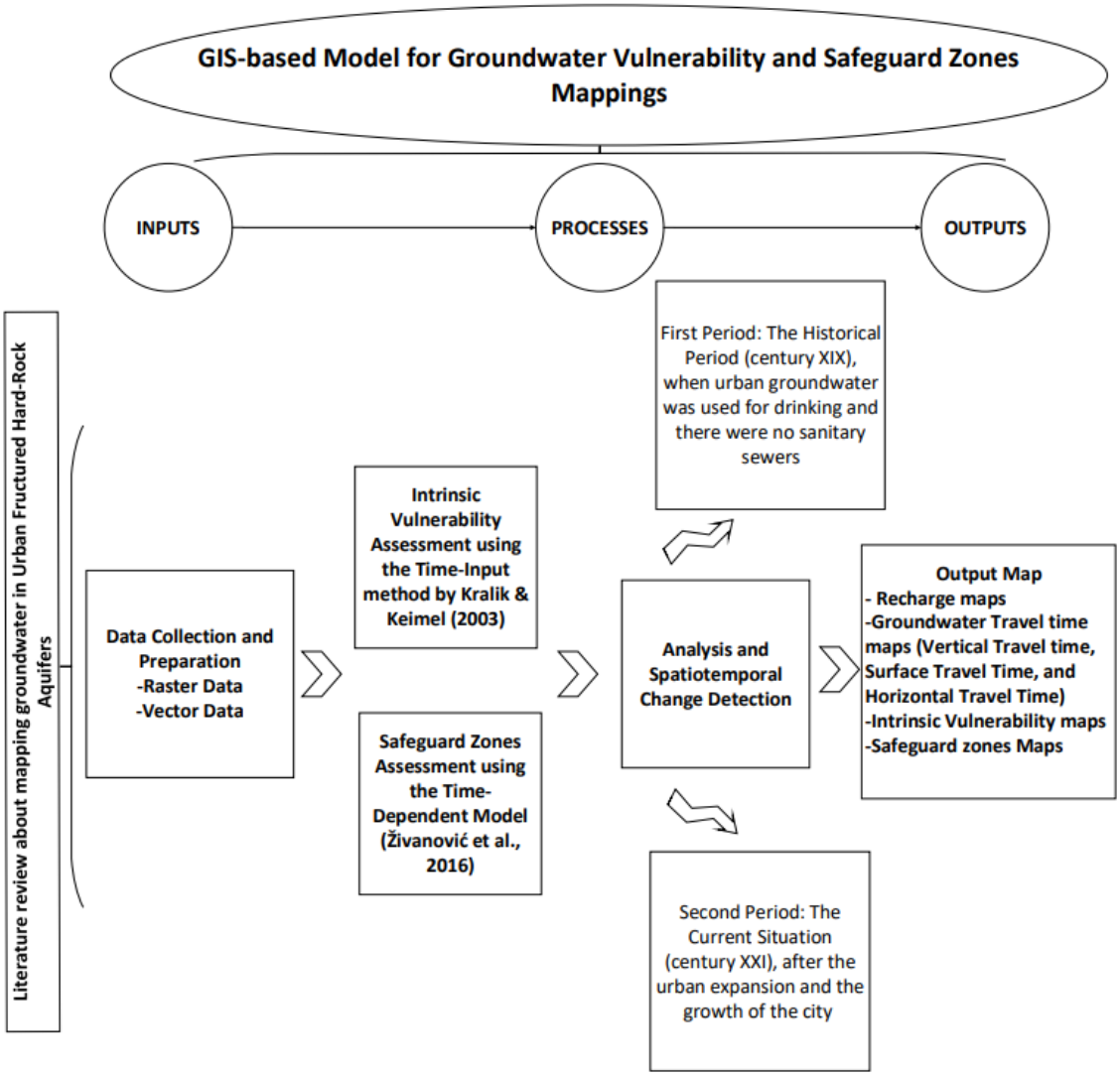

Figure 2. Research outlines.

Chapter II: Literature Review

(página propositadamente em branco)

2.1. Introduction

Urbanization is a global phenomenon, with 55% of the world's population living in urban areas, which is expected to increase to 68% by 2050. (UN-DESA-PV 2019). Consequently, urban sprawl is growing rapidly, dramatically impacting catchment hydrology. Impervious surfaces and constructed drainage systems are the primary causes of the change in hydrology, with increases in peak flows, annual runoff volumes, and flow variability, along with decreased infiltration and shorter lag times (Fletcher et al., 2013).

The importance of groundwater beneath cities is rising, with implications for scientific, economic, social, legal, and political issues, and in many cities, the interaction of groundwater systems and urban environments has begun an urgent challenge to face. This is related to many factors, including cities' horizontal and vertical expansion, the increasing population, climate change, water scarcity, and groundwater degradation (Lubis, 2018). A city's groundwater impacts depend both on its location and economic status, and by using urban groundwater, less pressure may be placed on conventional freshwater sources. On the other hand, not using this groundwater may lead to flooding and structural damage to underground structures (underground railway systems, basements, underground parking areas, etc.). While water is often scarce, water demand in cities is large and, in many cases, increasing with time. Even when its quality makes it unsuitable for drinking, groundwater can be used after treatment for several alternative purposes. This would reduce the need for high-quality water (Vázquez-Suñé et al., 2005).

Urban hydrology has emerged as a distinct branch of hydrogeology (Vázquez-Suñé et al., 2005). The research of urban groundwater has to deal with a high complexity of water flow and contaminant transport for different reasons since urban areas, in many cases, developed in geologically interesting and often complex environments close to rivers, hills and other features (e.g. salt water springs and hot springs) which make an investigation a challenge, in addition, to the high spatial heterogeneous pattern of surface sealing and vegetation which affects groundwater recharge processes and the subsurface infrastructure, such as the water supply system and the sewage system, which introduces both spatial and temporal variability of water and contaminant flow (Schirmer et al., 2013). Urban hydrogeology can be identified as a science for investigating groundwater at the hydrological cycle and its change, water regime, and quality within the urbanized landscape and zones of its impact (Lubis, 2018).

Several specific factors must be considered when dealing with groundwater in urban areas. Urbanization significantly affects the natural water cycle in terms of quantity and quality. In particular, the main contributors to recharge and discharge differ from those in natural systems.

Moreover, water can affect underground structures and infrastructure characteristics of cities such as basements, public transport services (trains, underground railways, etc.), and utility conduits, and according to Vázquez-Suñé et al. (2005), the main space-time issues related to the changes in the quantity and quality of groundwater in urban areas are:

- Groundwater cycle is directly linked to the history of urbanization;
- Fluctuations in groundwater levels related to the anthropogenic activity;
- Severe groundwater pollution caused by human activities; and
- The presence of underground structures, either permanent or temporary (e.g., construction sites).

Groundwater vulnerability assessment of urban areas is a challenging task in the fast trend of urbanization around the globe and quantifying groundwater fluxes. In addition, modelling becomes challenging due to a lack of data, planning (actions typically occur in response to emergencies rather than planning), and communication between the scientific community and city managers (Vázquez-Suñé et al., 2005).

The next chapter reviews spatiotemporal changes in groundwater in urban areas because of the urbanization process, the data required for reconstructing historical groundwater maps, and the vulnerability and safeguards zone mapping focused on applying the TIME-INPUT vulnerability and Time-Dependent model in urban fractured hard-rock aquifers.

2.2. Spatiotemporal changes of Urban Groundwater

Historically, groundwater originates as precipitation that infiltrates at the ground surface and percolates down to the water table, at the top of the surface where groundwater occurs (Figure 3) (USGS, 2018a). Water is constantly added to the system by recharge from precipitation, and water is constantly leaving the system as discharge to surface water and as evapotranspiration (Alley et al., 1999). A groundwater system can be considered the earth’s plumping system (Poeter et al., 2020), consisting of a mass of water flowing through the pores or cracks below the Earth's surface. This mass of water is in motion, possibly very slowly, and it is still part of the water cycle, which is the continuous exchange of water between land, water bodies, and the atmosphere (USGS, 2018a).

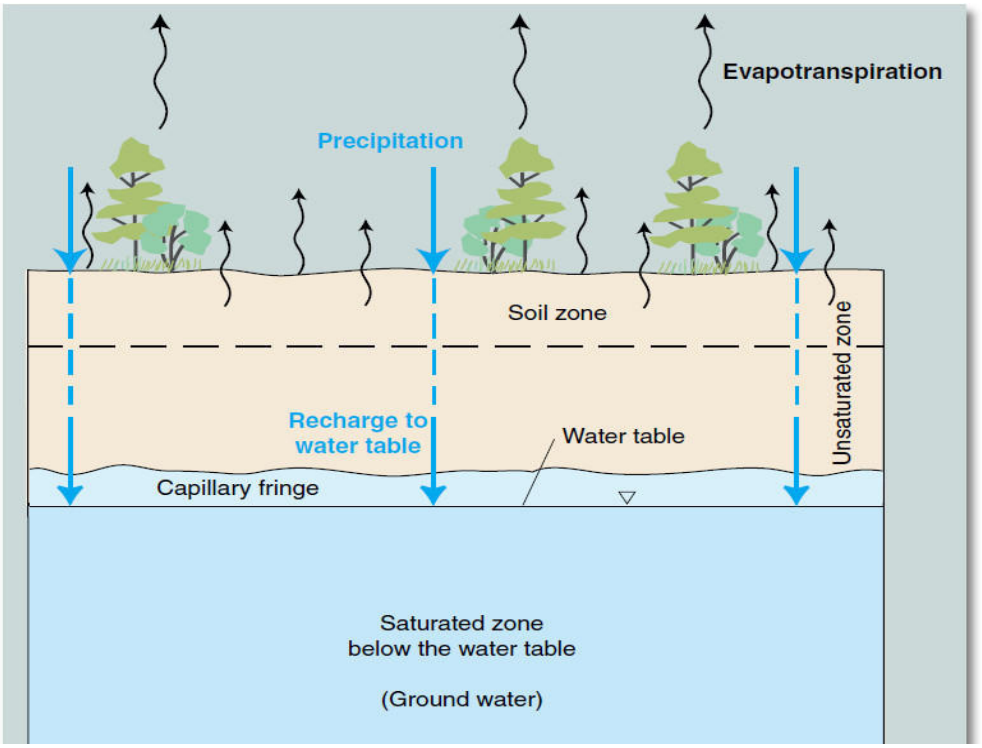

Figure 3. Basic visualization of groundwater (USGS, 2018).

When precipitation moves below the ground surface, it is called infiltration. Water from a short rain event only infiltrates to a shallow depth, but long, gentle rains infiltrate deeper, sometimes reaching the water table. In fractured rock, water moves through cracks, while in porous media, water moves through spaces between granular particles. Flow processes are the same in both systems, but the character of the geologic material differs (Poeter et al., 2020) (Figure 4).

Groundwater is an important part of the freshwater cycle, and it moves continuously through interconnected void spaces in porous media and fractured media, as well as large passageways from the areas of recharge to the areas of discharge. The driving force for groundwater movement is measured in terms of the hydraulic head, which represents the fluid pressure potential and elevation potential. It is also referred to as the piezometric or potentiometric head. Contour maps of the hydraulic head, and piezometric or potentiometric maps, which can be constructed from water-table elevations, can be used to infer groundwater flow directions (USGS, 2018a).

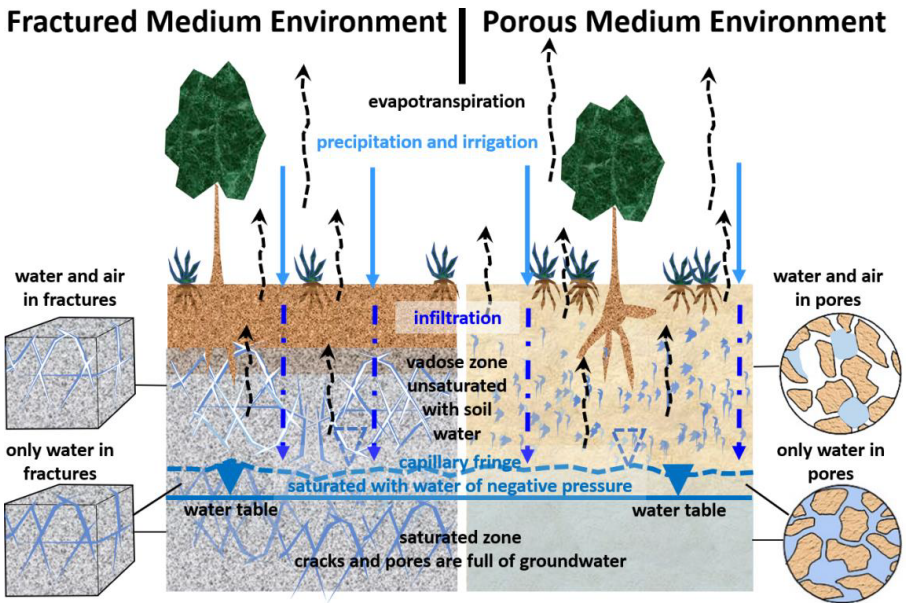

Figure 4. Schematics show infiltration through the unsaturated zone to the capillary fringe and the water table, where it recharges the groundwater. Water in the unsaturated zone generally moves downward as infiltration (blue arrows) or upward as evapotranspiration (Poeter et al., 2020).

Figure 5 shows water flow in large aquifers, the vertical flow in the unsaturated zone, and the horizontal flow in the saturated zone. The travel time of groundwater can vary between days to centuries according to the hydrogeological properties. It can also be noticed that shallow aquifers in recharge areas are generally unconfined, but elsewhere and at greater depths, groundwater is often partially confined by low permeability strata (an aquitard) or fully confined by overlying impermeable strata (an aquiclude). In confined conditions, water may be encountered under pressure, and when wells are drilled, it rises above the top of the aquifer, even as far as the ground surface, to a level called the potentiometric surface (Morris et al., 2003).

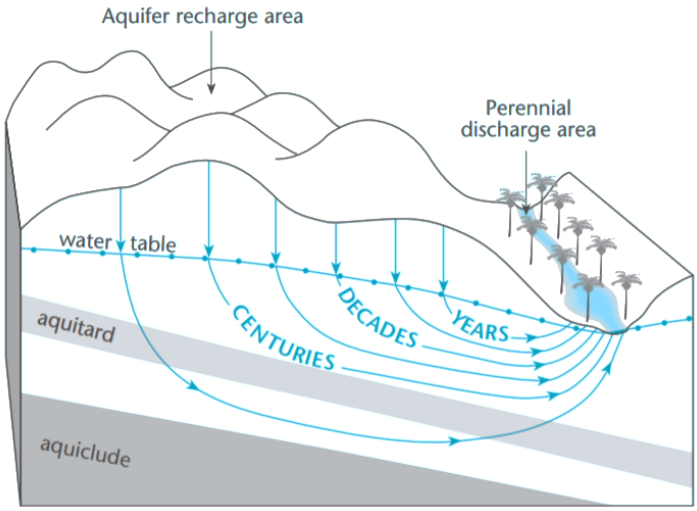

Figure 5. Groundwater flow system in a large aquifer(Morris et al., 2003).

Groundwater flow rates are an important factor for contaminants that degrade over time and in controlling disease-causing micro-organisms such as some bacteria, viruses, and protozoa. Through fracture systems, velocities can be much higher where flow depends on factors like aperture or fracture network density (Morris et al., 2003).

However, the urbanization and transformation from undeveloped spaces to urban environments result in spatial and temporal changes in the landscape, and these alterations then impact urban ecosystems, including urban waters and their aquatic ecosystems, and result in changing the hydrological urban water cycle and the quantity and quality of urban water. (Hibbs, 2016; McGrane, 2016). Figure 6 illustrates the water cycle before and after urbanization.

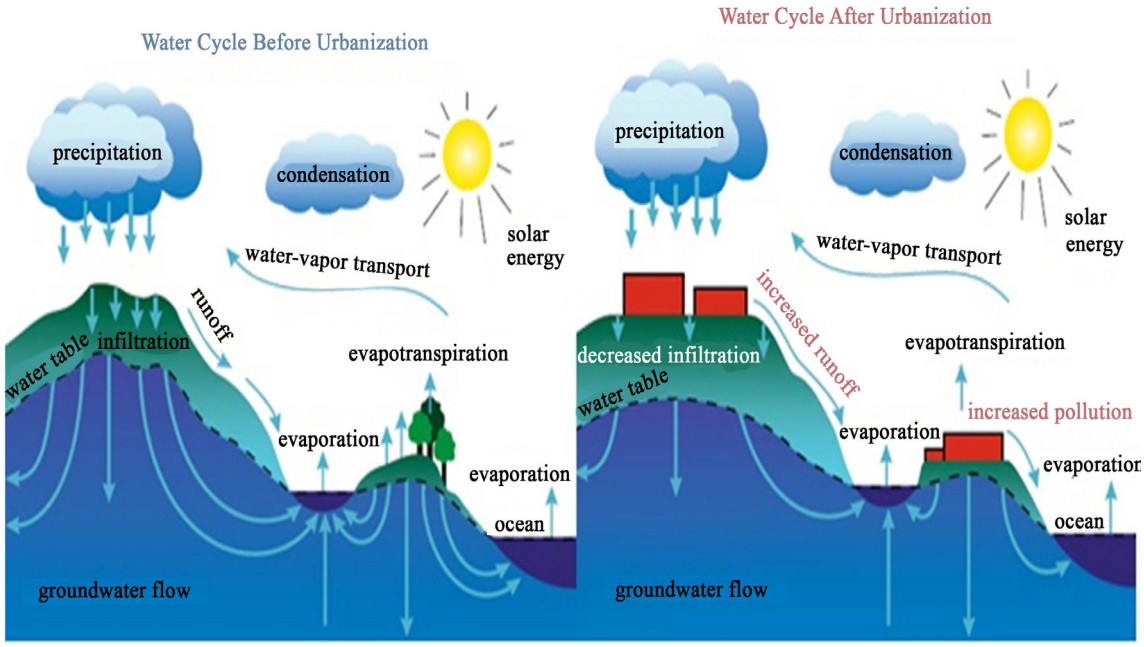

Figure 6. Water cycle diagram showing different processes involved before (left) and after (right) urbanization (Gatwaza et al., 2016).

Urbanization started with cutting trees and building houses, some with sewers, others with septic tanks, and drilling water wells. All these actions affected the water system, resulting in more storm runoff and erosion because there is less vegetation to slow water as it runs downhill. More sediment is washed into streams. Flooding can occur because water-drainage patterns are changed (USGS, 2018b). Then, urbanisation's growth ends with adding more roads, houses, and commercial and industrial buildings. The impacts on the water system include an increment in wastewater discharged into local streams. Then, new water supply and distribution systems are built to supply the growing population. Reservoirs may be built too to supply water, and some

stream channels are changed to accommodate building construction. Industries might drill some deep, large-capacity wells. The increase in impervious surfaces, which do not allow water to seep into the ground, means less water will soak into the ground, which means that the water table will have less water to recharge. This will lower the water table (Figure 7). Some existing wells will not be deep enough to get water and might run dry. Besides, too many large wells can lower the water level. This can cause other wells to run dry, can cause saltwater to be drawn into drinking-water wells, and can cause land that was formerly "held up" by underground water to subside, resulting in sinkholes and land subsidence(USGS, 2018b).

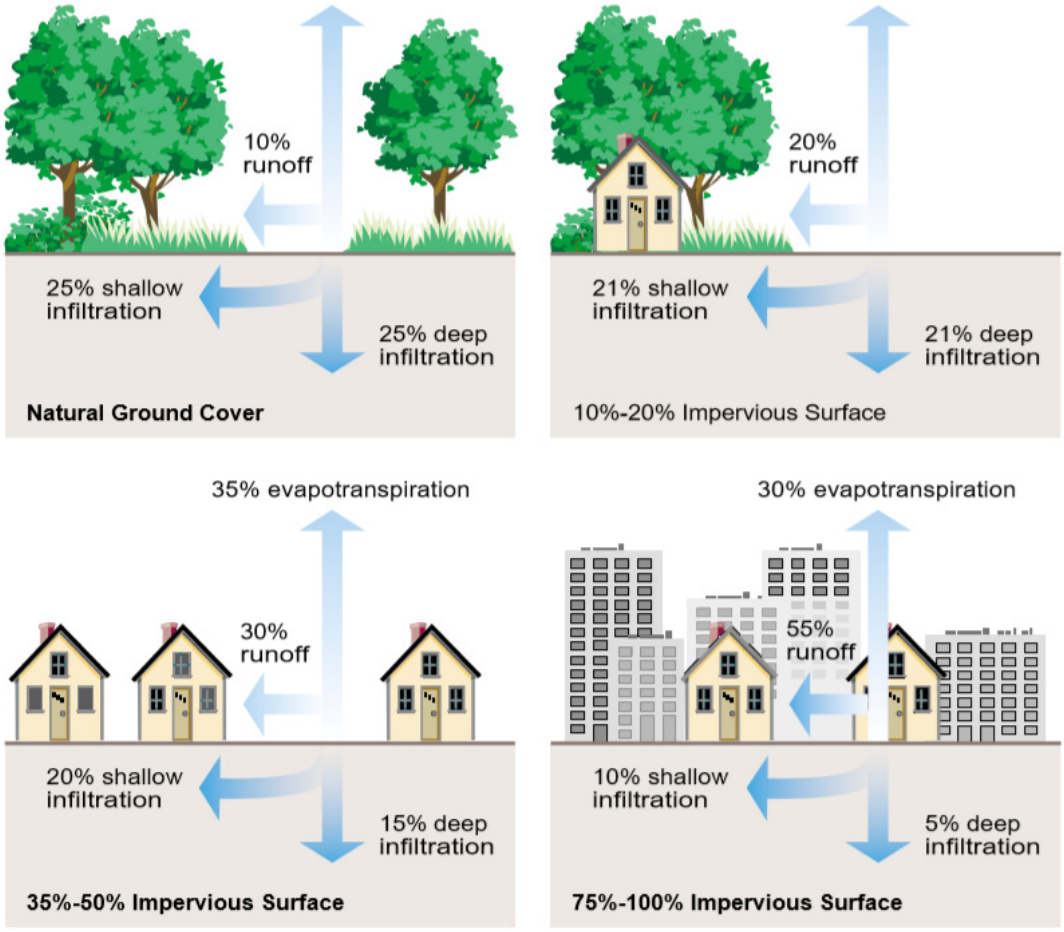

Figure 7. Influence of urbanization on different components of the water cycle (Hack, 2020).

Although urbanization reduces direct recharge from precipitation, it creates new pathways and sources of water for recharge, including leaking water mains, sewers, septic tanks, and soak ways. The net effect often increases recharge to pre-urbanization rates or higher in dry climates and cities with high densities and large imported water supplies (Lerner, 1990). Figure 8 shows the effects of urbanization on urban recharge.

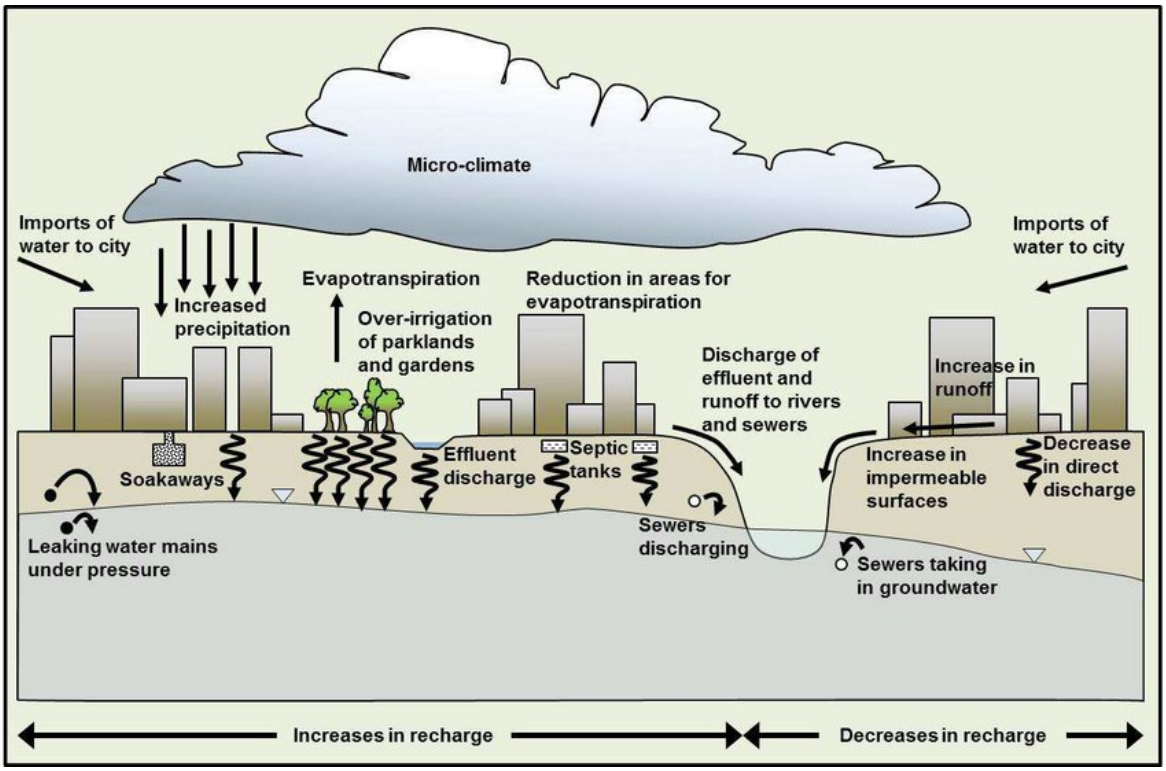

Figure 8. Urban effects on groundwater recharge (Acreman et al., 2012).

Understanding the massive influence of urbanization on the total water balance is essential to comprehending the deterioration of urban water resources and maintaining the quality and quantity of urban water supplies, which is widely acknowledged as a challenging undertaking involving several spatial and temporal scales(Schirmer et al., 2013). Figure 9 summarizes the effects of urbanization on water balance, while Table 1 summarizes the physical hydrogeological effects of urbanization (Hibbs & Sharp Jr, 2012).

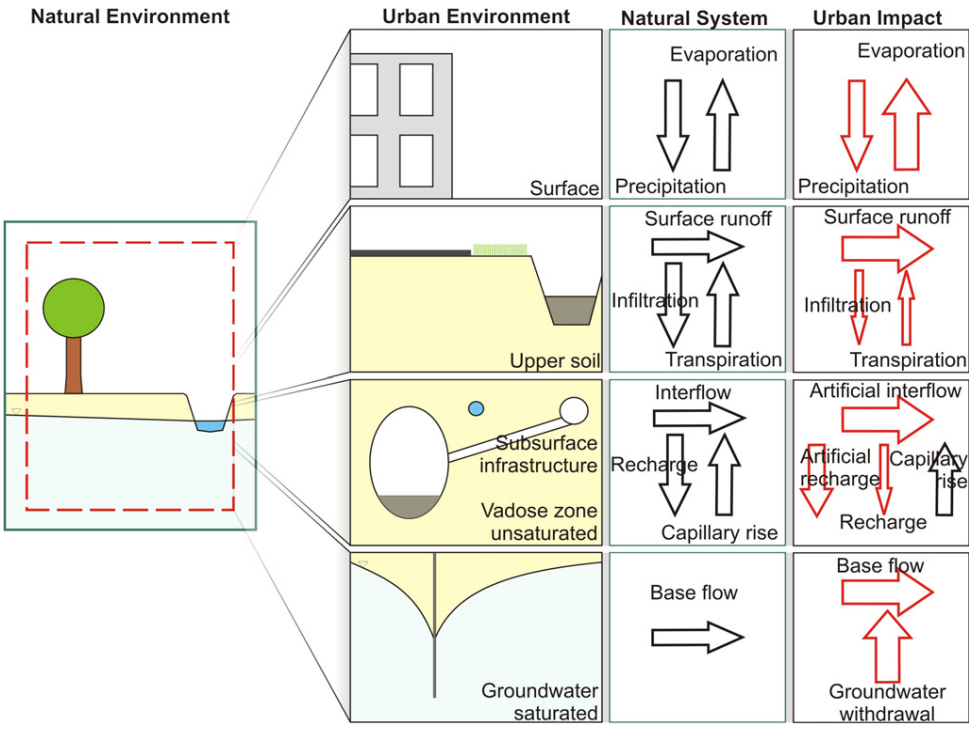

Figure 9. Simplified urban impact on the water balance. The red arrows represent water flow that has been modified or newly introduced by urbanization (Schirmer et al., 2013).

Table 1. Physical hydrogeologic effects of urbanization (Hibbs & Sharp Jr, 2012).

1. Impervious cover and storm sewers increase:	a. Surface water runoff and flooding b. Limiting direct recharge
2. Changing recharge by:	a. Loss of direct recharge b. Leaky water and sewer systems c. Irrigation return flow d. Changing urban vegetation e. Artificial recharge, including aquifer storage and recovery
3. Changing permeability and porosity fields from:	a. Compacted urban soils b. Increased porosity c. Increased potassium (K) from the reticulations
4. The altered permeability and porosity fields:	a. Serve as French drains to control water table rises b. Affect recharge locations and rates c. Make groundwater remediation and prediction of plumes difficult
5. Effects of pumpage can lead to:	a. Declining water levels b. Subsidence, which can alter surface drainage patterns c. Saltwater intrusion d. Upcoming of poorer quality water e. Diminished stream flows

In addition to the physical changes that occur from urbanization, including increased recharge from leaking utilities, change in irrigation and return flows, and modification of subsurface flow channels from underground infrastructure, there are also chemical changes, including groundwater and soil contamination from point and non-point sources, water quality impacts from storm drains, and modern and legacy impacts from urban development. It is, therefore, vital to understand the causes and effects of these changes to address the critical and growing environment and water resource issues in urban areas (Hibbs, 2016).

As well as the flow components of the urban water cycle, attention must also be paid to fluxes of materials and energy carried by air, water, or human activity, as Figure 10 shows. This includes wet and dry atmospheric pollutants, acidity (originating from burning fossil fuels), trace metals, and mercury agricultural chemicals (particularly pesticides and herbicides). In addition, other pollution sources include transportation, construction, use of building materials, road maintenance, elution or corrosion of hard surfaces, soil erosion, deficient solid waste collection, and others (Marsalek, 2014).

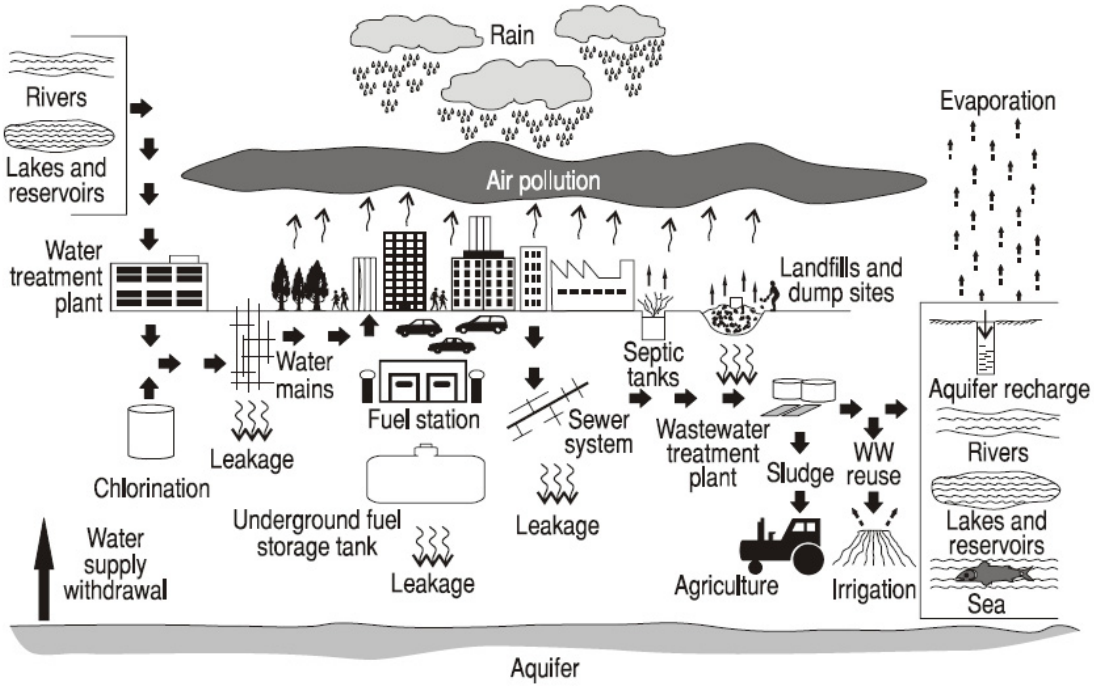

Figure 10. Urban water contaminations (Marsalek, 2014).

2.3. Weathered crystalline/hard-rock aquifers

Crystalline rocks, including igneous rocks (e.g., granite, diorite) and metamorphic rocks (e.g., gneiss, granulite, quartzite, marble, schist, phyllite), usually belong to the group of hard rocks. Hard rocks have low primary porosity (intergranular porosity) and low primary permeability.

However, weathering and fracturing can impart secondary porosity and permeability to varying degrees. They are also known as fractured rocks because their hydraulic properties are primarily controlled by fracturing. Hard rocks generally have anisotropic and heterogeneous properties, unlike sedimentary rocks (Singhal, 2008). Table 2 contains a comparison between granular and fractured hard rock aquifers.

Table 2. Comparison between granular and fracture hard rock aquifers (adapted from Singhal, 2008).

Aquifer Characteristics	Aquifer Type	
	Granular Rock	**Fractured Rock**
Effective Porosity	Mostly primary	Mostly secondary through joints, fractures, etc.
Isotropy	More isotropic	Mostly anisotropic
Homogeneity	More homogeneous	Less homogeneous
Flow	Laminar	Possibly rapid and turbulent
Flow predictions	Darcy's law usually applies	Darcy's law may not apply, but cubic law is applicable
Recharge	Dispersed	Primary dispersed with some point recharge
Temporary head variation	Minimal variation	Moderate variation
Water quality variation	Minimal variation	Greater variation

Hard rocks are characterized by rock discontinuities of different sizes, from a few mm-sized joints to large fault zones and lineaments. The main discontinuities of rocks are foliation, fractures (joints), faults, and lineaments, and the main location of groundwater movement is along these discontinuities. Rock discontinuities and their spacing, aperture size, and orientation determine the porosity and permeability of such rock masses. If an open joint or fracture is not filled with weathered or broken rock, it may be a potential passage for groundwater movement. However, its permeability is greatly reduced when filled with clayey material, such as smectite or montmorillonite. Filling materials also influence the movement of solutes out of fractures and into the porous matrix. (Singhal, 2008).

According to Lachassagne et al. (2011), the fracture permeability of hard rock aquifers is not dependent on tectonics or unloading. However, weathering processes and the storability and hydraulic conductivity of hard rock groundwater resources are determined by these weathering processes, which create weathering profiles. As a result, hard-rock aquifers develop mainly within the first 100 m below the ground surface. Figure 11 shows weathering profile layers' geological structure and hydrodynamic properties.

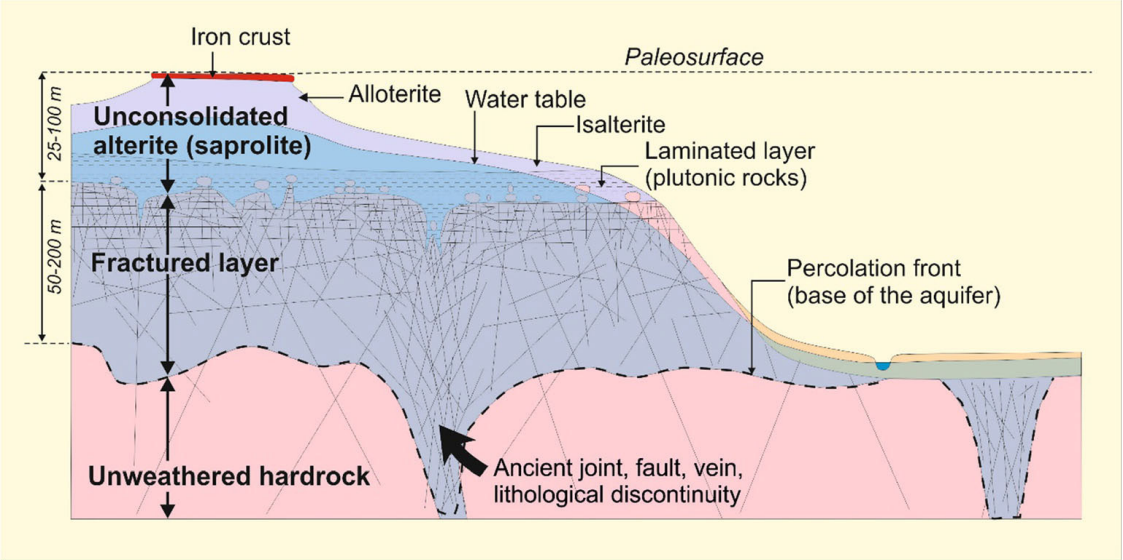

Figure 11. Conceptual model of a weathering profile in hard rocks (Lachassagne et al., 2021).

From top to bottom, the layers are:

a. An iron or bauxitic crust may be absent. In locations preserved from erosion and recharged by heavy rainfall, the iron or bauxitic crust may give rise to small, perched aquifers with springs that behave like epikarsts;

b. The saprolite, alterite or can be called (regolith). The material is generally clay-rich and derived from the in-situ decomposition of bedrock several tens of meters thick, where the layer has not been eroded. In nonplutonic rocks, the saprolite layer is commonly divided into two subunits, the alloterite, and the isalterite;

c. The stratiform fractured layer has dense fracturing in the first few meters and a decreased density with depth. This layer is approximately two times the thickness of the saprolite in places where the saprolite has not been eroded, and it can reach over 100 m thick in some places. As the fracture density decreases with depth towards the base of the weathering profile, the hydraulic conductivity of hard rock aquifers declines; and

d. The fresh basement is only permeable where deep fractures and faults exist. However, even if these fractures are as permeable as the fractures of the stratiform fractured layer, their density decreases with depth and laterally. Accordingly, the fresh basement is considered impermeable with negligible storability for catchment-scale water resources studies.

Development of a weathering profile tens of meters thick must have enough time for effective hydrogeological development; this takes millions to tens of millions of years, and the

demonstration and recognition of this conceptual model of hard-rock aquifers have enabled understanding of the functioning of such aquifers and has facilitated a comprehensive corpus of applied methodologies in hydrogeology and geology (Lachassagne et al., 2021).

Crystalline rocks form important shield areas in different parts of the world, covering about 20% of the land surface. The main characteristics of crystalline rocks, according to Singhal & Gupta (2010):

- These rocks develop different landforms and drainage characteristics depending on their structural and lithological characteristics and climatic conditions;
- The main source of groundwater in these terrains is the weathered horizon (regolith);
- The groundwater potential of the regolith depends upon its thickness, lithology, permeability, and climatic conditions;
- The potential of deeper massive rocks depends upon the intensity of fracture characteristics, including degree and interconnectivity;
- The yields of wells in crystalline rocks are usually low, which depends on rock weathering, topography, and rock structures (fractures and lineaments);
- Water quality depends on rock compositions; TDS is usually less than 300 $mg.L^{-1}$;
- Near-surface water has low TDS, but the salinity generally increases with depth; and
- The crystalline rocks form potential repositories for the disposal of radioactive waste, which requires detailed hydrogeological investigations.

2.4. Data for historical reconstruction of urban hydrogeological maps

According to Schirmer et al. (2013), there are numerous forms of information as well as evaluation methodologies required for assessing urban groundwater quantity and quality, including:

a. Water balancing and water flow

In urban hydrogeology, information about the amount of water flowing into, within, and out of groundwater is crucial. In this manner, it is needed to understand the groundwater's different ways of recharging. Additionally, the groundwater travel time and the residence time in reactive zones are important parameters to describe contaminant turnover on a large scale.

b. Spatiotemporal distributions of contaminant concentration

It is important to deeply analyse their risks to understand the spatiotemporal distribution of urban contaminations. It is also important to derive exposure scenarios for (eco)toxicological risk assessment.

c. Contaminant loads

Loads of contaminants flowing into, within, and out of an urban groundwater body combine the information on water flow and contaminant concentrations. Load determination within the groundwater allows the estimation of attenuation, e.g., when considering flow through sequential control planes. Moreover, quantifying the contaminant load into and from groundwater allows the weighting of the relevance of different contaminant pathways. For toxicological assessments, contaminant loads are needed to understand cumulative effects on ecosystems. Cumulative effects result from gradual changes in the water bodies, such as accumulation of nutrients and toxicants in and released from sediment, and occur only after the cumulative changes rise above a critical threshold level. Short-term changes and small-time scales are not important for cumulative effects. The main interests here are the loads and substance fluxes over long periods.

d. Implementation of integrated modelling approaches

Since only part of the groundwater system can be measured, water and contaminant flow and transport models are indispensable. The urban groundwater compartment interacts closely with the unsaturated zone, sewage systems, and surface water. Depending on the task, groundwater models often must be coupled to the other compartments. This can be done by loose coupling, where the output of one model, e.g., a model of wastewater flow and exfiltration, is input for the groundwater model. This task can become complex if different compartments influence each other in both directions.

Moreover, reconstructing land use and land cover, the geographic area that recharges the groundwater, is an important factor to consider in urban hydrogeological studies, as groundwater quality and quantity are profoundly affected by recent and historical land use and land cover at both the regional and local levels. Therefore, it is crucial to understand historical land use/land cover and compare it to current and projected land use/land cover. Around the world, three trends in land use and human-induced changes in land cover have disrupted natural hydrological cycles (Kresic & Mikszewski, 2012):

i. Conversion of forests to agricultural land is commonly practised in developing countries;

ii. Land used for other purposes is converted into urban land because of rapid urbanization in undeveloped and developing countries; and

iii. A rapid decentralization of cities (i.e., suburbanization) and reforestation of former agricultural land, particularly in the USA and developed countries.

Historical reconstruction of past land-use and land-cover changes is crucial to understanding long-term human-environment interactions. The reconstructions can be done using historical documents containing land-cover data, historical maps, and pictures that offer visual and spatial quantitative land-cover information, natural archives, especially when historical records are missing or lacking, and historical reconstruction models that have been gradually developed from empirical models to mechanistic ones, or reconstruction method based on multiple-source data and multidisciplinary (Yang et al., 2014). Table 3 reviews the historical reconstruction methods of land use/land cover and their advantages, constraints, and suitable spatial and temporal scales.

In urban areas, determining relevant hydrologic factors and developing an accurate conceptual site model presents a special challenge. These include rerouted streams and fill streambeds, which may result in complex groundwater flow patterns that are hard to predict based on the current land surface topography. Considering these complicated factors is particularly important for interpreting the present shapes of groundwater contaminant plumes. In addition, some artificial hydrographic features are usually poorly described (or not at all) in conceptual site models, including stormwater and drainage ditches, stormwater collection basins, leaking sewers, water lines, and infrastructure tunnels. These can all have local or regional impacts on groundwater recharge, discharge, and flow directions (Kresic & Mikszewski, 2012).

Chaminé et al. (2014) emphasized the importance of historical hydrogeological inventory through GIS mapping to problem-solving in urban groundwater systems since water resources have hugely impacted the socioeconomic sustainability and development of urban areas. Moreover, these authors emphasized that the use of a multidisciplinary and transdisciplinary approach (e.g., historical documentation, archaeological hydraulic structures, subterranean geology, groundwater ecotoxicology, geomicrobiology, and urban groundwater studies) leads to an accurate assessment and protection of aquifers in urban areas, as well as contributes definitively to a reliable understanding of the impact of climate variability on water resources.

The hydrotoponymy and mapping of the historical sources of groundwater are also crucial to assessing the development of urban groundwater through history. Freitas et al. (2014) shed light on the importance of coupling hydrotoponymy and GIS Cartography to examine hydrohistorical issues, namely hydrogeographic, hydrotoponymical and hydrogeological features, to assess the evolution of the urban groundwater system.

Table 3. Review of historical reconstruction methods (Yang et al., 2014).

Reconstruction Method	Advantages	Constraints	Suitable spatial and temporal scales
Reconstruction based on historical documents	i. Accessible data ii. A huge amount of land-cover information and a great variety iii. Widely used in numerical reconstruction	i. Time-consuming to collect ii. Fragmentary iii. Inaccurate and missing information iv. Qualitative or semi-quantitative data v. Different meaning from that of today vi. Recorded in administrative units with fuzzy spatial information	i. Millennium timescale ii. From regional to national scales
Reconstruction based on historical maps and pictures	i. Visual information ii. Abundant spatial quantitative information	i. Errors, inconsistencies, and inaccuracies ii. Geometrical irregularities iii. Un-unified land cover classification iv. Missing certain boundaries in some classes of land covers	i. Centennial timescale ii. Regional scale
Reconstruction based on natural archives	i. Providing accuracy ii. spatial details of land use iii. With a long period	i. Not easily available ii. With great limits on the certain land-cover type	i. Millennial timescale or longer ii. Regional scale
Model-based reconstruction	i. Driving forces and driving mechanism of land use ii. Quantitatively spatial land cover	i. High-quality data acquisition and input parameters ii. Incomplete reconstruction system iii. Few historical land-cover datasets with high spatial accuracy	i. From decadal to millennial timescales ii. From regional to global scales
Reconstruction based on multiple-source data and multidisciplinary analysis	i. Multiple perspectives ii. Complementing missing data and verifying reconstruction results	i. Difficult to various couple types of data ii. Few all-round researchers with multidisciplinary backgrounds	i. Unlimited

Freitas et al. (2019b) highlighted the importance of GIS-based mapping on urban groundwater systems. They emphasized the key role of ground field surveys at several scales, a representative hydrological inventory, and an integrated groundwater mapping in conceptualizing the urban groundwater system (Figure 12).

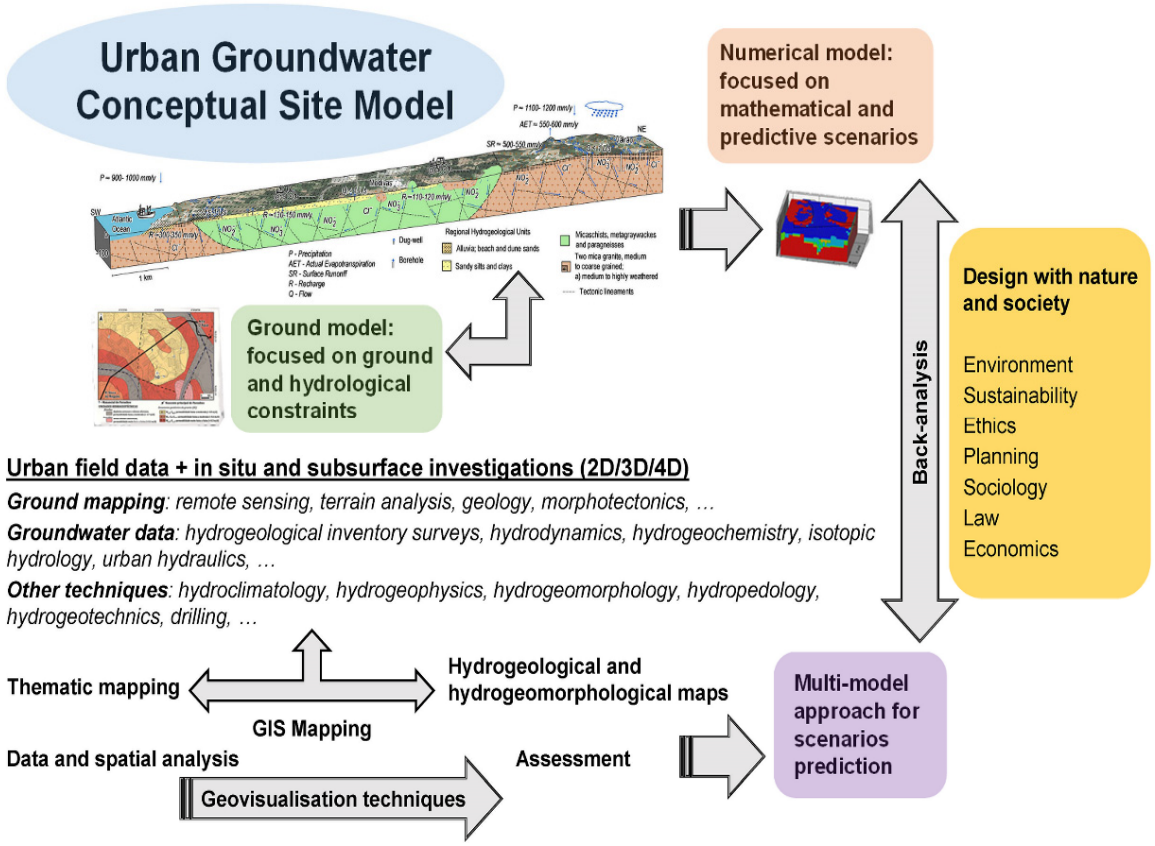

Figure 12. The importance of GIS-based mapping on urban groundwater systems (Freitas et al., 2019b).

In addition, Freitas et al. (2020) identified the importance of vulnerability GIS-mapping, monitoring, and infiltration/recharge of water resources, and the delineation of the environmental protective background as key issues in evaluating, planning, managing, and decision-making for urban water systems. These authors set up a methodology to conceptualize the site model for a small-scale urban area. Finally, Afonso et al. (2016) pointed out the importance of a vulnerability assessment in urban areas. They developed a multidisciplinary approach to estimate urban groundwater vulnerability to contamination in Porto's urban area, combining hydrogeology, hydrogeochemistry, subterranean hydrogeotechnics, groundwater ecotoxicology, and isotope tracers.

2.5. Groundwater vulnerability

Groundwater is the most important potable water resource in many areas of the world, and its protection and sustainable management are of fundamental importance. Therefore, assessing the vulnerability of groundwater to adverse effects of human activities is one of the most important problems in applied hydrogeology.

The term 'vulnerability' was first used in hydrogeology in the 1970s in France (Albinet & Margat, 1970), and as a term referring to the relative vulnerability of aquifers to anthropogenic pollution, this term was initially used without any attempt to define it. From the late 1980s, there were various attempts to formalize the definition of the expression and to develop related mapping systems, including DRASTIC (Aller, 1985), GOD (Foster, 1987), AVI (Stempvoort et al., 1993), ISIS (Civita & De Regibus, 1995), GLA (Hölting et al., 1995), PI (Goldscheider et al., 2000), SINTACS (Civita, 2008), and others. Each of these methods attempted to simplify complex processes in a scientifically correct way but involved a variety of contributing factors, varying degrees of simplification, and subjective professional judgment. Table 4 illustrates the development of the various definitions of vulnerability (Machiwal et al., 2018).

In this context, groundwater vulnerability assumes that the physical environment protects groundwater against natural and human impacts, particularly considering contaminants entering the subsurface. Therefore, some land areas are more prone to contamination than others (Witkowski et al., 2020).

Figure 13 illustrates the flowchart for building a vulnerability map using the DRASTIC Index. At the same time, Figure 14 shows the flowchart for building a vulnerability map in the GOD Index, and Table 5 defines classes of aquifer pollution vulnerability associated with activities on the land surface overlying any given location. Generally, there are two types of groundwater vulnerability assessments and maps: (Wachniew et al., 2016)

i. Intrinsic vulnerability is based on the assessment of natural climatic, geological, and hydrogeological attributes; and

ii. The vulnerability relates to a specific contaminant, contaminant class, or human activity and is mostly assessed regarding the groundwater system's risk of exposure to contaminant loading.

Recharge, soil properties, lithology and thickness of the unsaturated zone, and depth to water table are the key attributes of both intrinsic and specific vulnerability. However, contaminants from point sources often enter the groundwater system beneath the soil profile (e.g.,

underground oil tanks, septic tanks), and the role of soil as an attenuation medium is then bypassed (Wachniew et al., 2016).

Table 4 Definitions of groundwater vulnerability (adapted from Machiwal et al., 2018).

Definition	Source
"Aquifer vulnerability is the possibility of percolation and diffusion of contaminants from the ground surface into natural water-table reservoirs, under natural conditions".	Margat (1968)
"Vulnerability is the degree of endangerment, determined by natural conditions and independent of the present source of pollution".	Olmer & Rezac (1974)
"Vulnerability is the risk of chemical substances – used or disposed of on or near the ground surface – influencing groundwater quality".	Villumsen et al. (1984)
"Aquifer pollution vulnerability as the intrinsic character of the strata separating the saturated aquifer from the immediately overlying land surface which determines its sensitivity to adversely affecting a surface applied (anthropogenic) contaminated load".	Foster (1987)
"Groundwater vulnerability is the sensitivity of groundwater quality to anthropogenic activities which may prove detrimental to the present and/or intended usage-value of the resource".	Bachmat & Collin (1987)
"Vulnerability of a hydrological system is the ability of this system to cope with external, natural and anthropogenic impacts that affect its state and character in time and space".	Sotornikova & Vrba (1987)
"Groundwater vulnerability is a measure of the risk placed upon the groundwater by human activities and the presence of contaminants … Without the presence of contaminants, even the most susceptible groundwater is not at risk, and thus, is not vulnerable".	Palmquist (1993)
"Groundwater vulnerability is the tendency or likelihood for contaminants to reach a specified position in the groundwater system after introduction at some location above the uppermost aquifer".	National Research Council (1993)
"Vulnerability is an intrinsic property of a groundwater system that depends on the sensitivity of that system to human and/or natural impacts".	Vrba & Zaporozec (1994)
"Groundwater vulnerability is defined as the tendency or likelihood of contaminants reaching the groundwater system after introduction at the surface and is based on the fundamental concept that some land areas are more vulnerable to groundwater contamination than others".	Majandang & Sarapirome (2013)

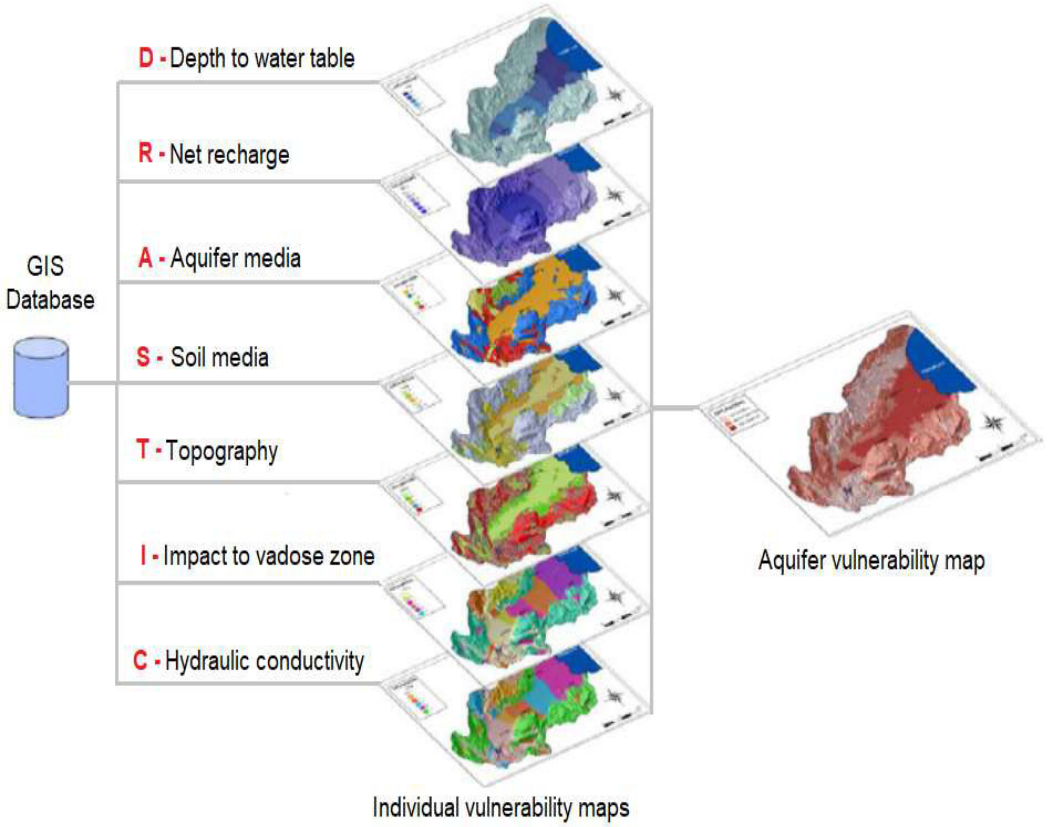

Figure 13. Flowchart for building a vulnerability map in DRASTIC Index (Barbulescu, 2020).

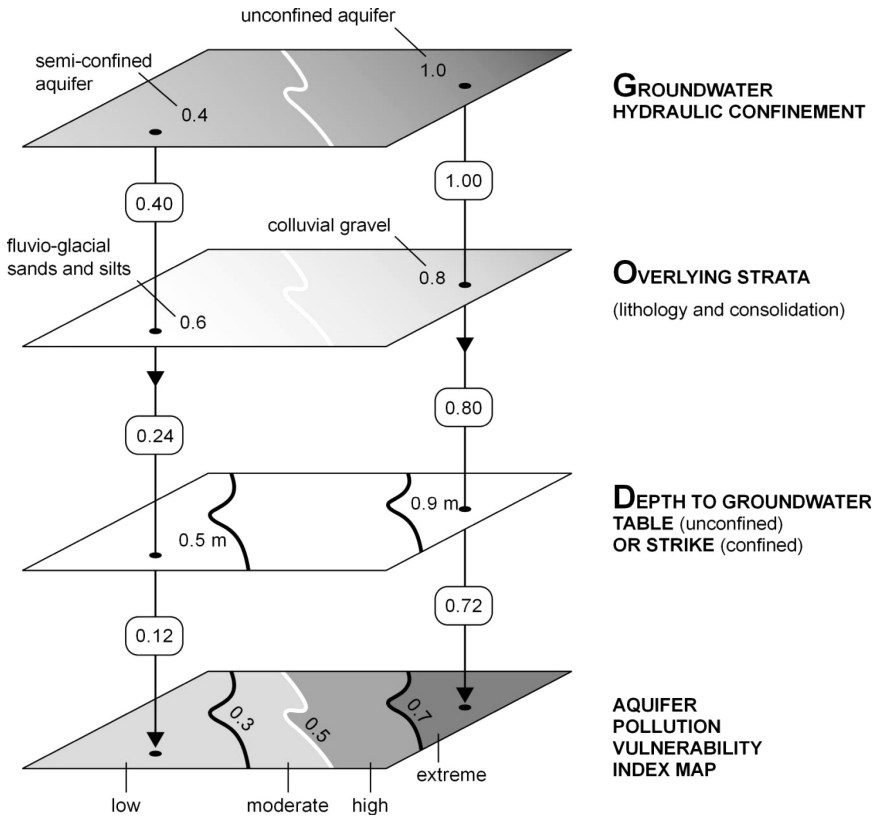

Figure 14. Flowchart for building a vulnerability map in GOD Index (Foster et al., 2007).

Table 5. Definition of vulnerability classes associated with activities on the land surface overlying any given location (Foster et al., 2007).

Vulnerability Classes	Corresponding definition
Extreme	Vulnerable to most water pollutants with relatively rapid impact in many pollution scenarios
High	Vulnerable to many pollutants, except those strongly absorbed or readily transformed, in many pollutions scenarios
Moderate	Vulnerable to some pollutants but only when continuously discharged or leached
Low	Only vulnerable to conservative pollutants in the long-term when continuously and widely discharged or leached
Negligible	Confining beds present with no significant vertical groundwater flow (leakage)

According to Foster et al. (2007), the key factor in pollution vulnerability assessment and mapping is to classify the (essentially intrinsic) characteristics of the strata overlying the saturated aquifer (vadose zone or confining beds) according to their physio-chemical characteristics to retain and degrade potential water pollutants and consequently contribute to contaminant attenuation capacity and physical properties, which can reduce the rate of vertical water infiltration. Besides, Foster et al. (2007) refer that the possibility of developing preferential flow paths in the vadose zone (Figure 15) must be thoroughly considered (usually because of fracturing) and their significance in increasing aquifer pollution vulnerability.

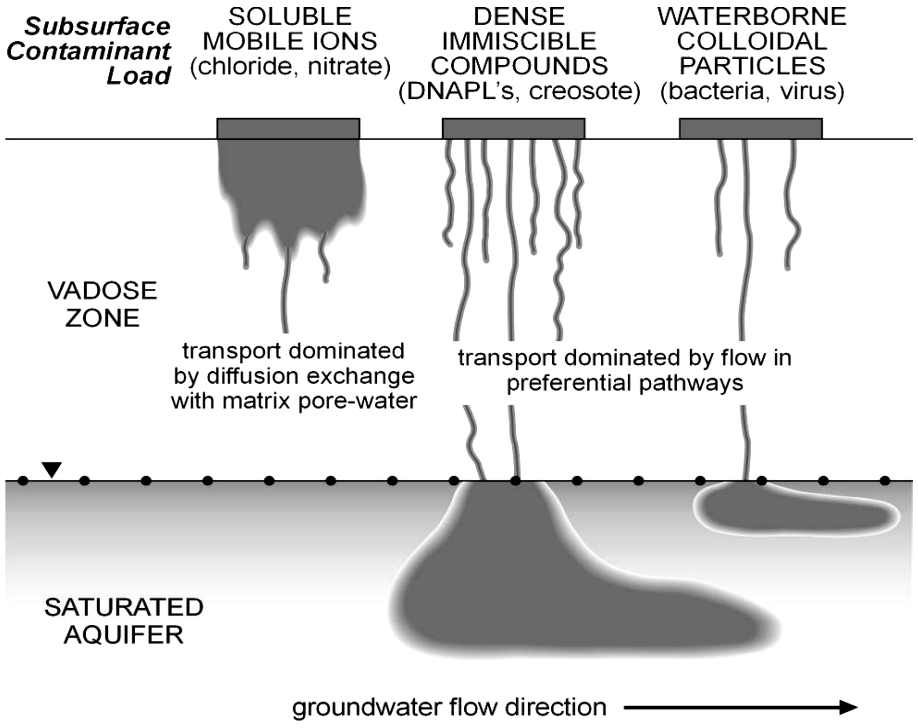

Figure 15. Development of preferential flow in the vadose zone and its significance for aquifer pollution (Foster et al., 2007).

This concept of groundwater vulnerability aims at identifying and prioritizing the most vulnerable areas/regions of a basin that can cause groundwater contamination and provides a scientific basis for groundwater protection and land use planning. The European approach to groundwater vulnerability is based on an 'Origin-Pathway-Receptor/Target' model (Machiwal et al., 2018) with differentiating between groundwater as a 'resource' (aquifer storage) and groundwater as a 'source' (e.g., production well or spring), (Figure 16).

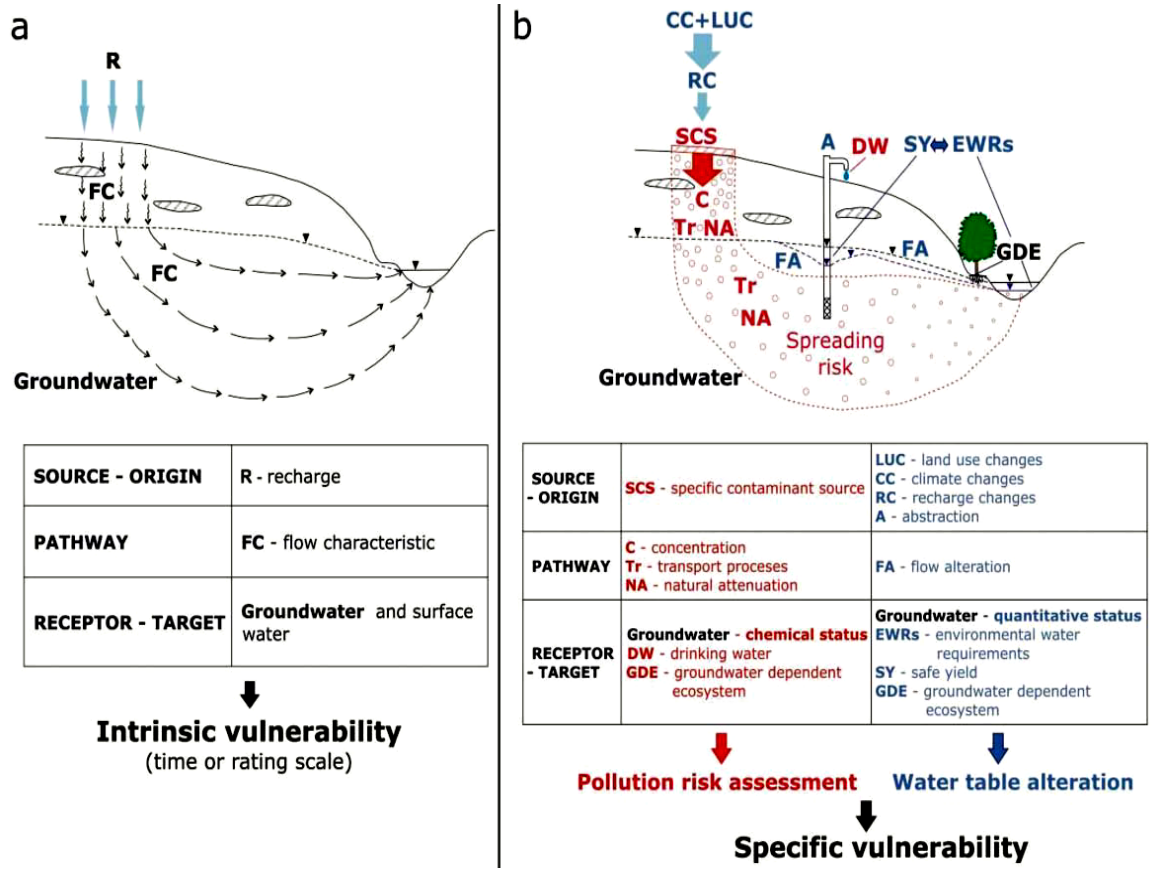

Figure 16. Basic concepts define the (a) intrinsic and (b) specific vulnerability (Wachniew et al., 2016).

The goal of 'resource protection' is to safeguard the entire underlying aquifer, while that of 'source protection' is to prevent a production well or spring from contamination. On a quantitative basis, three main aspects of vulnerability assessment (Machiwal et al., 2018):

i. time of travel for a contaminant to reach the target from the origin;

ii. contaminant attenuation along the pathway; and

iii. duration of contamination at the target.

Foster et al. (2013) pointed out that maps of aquifer pollution vulnerability have proven to be useful in communicating between hydrogeologists and those involved in planning water and land resources. However, it should not be forgotten that vulnerability assessments inherently include a

significant level of uncertainty and cannot readily be independently calibrated, although they reflect the best available synthesis of information. Nevertheless, as a second remark, aquifer pollution vulnerability maps can be used as screening tools to determine where deeper hydrogeological investigations are most needed and prioritized protection measures to deal with a potential groundwater pollution event.

A fundamental difficulty in assessing groundwater vulnerability is the complexity of groundwater systems. The intertwined processes of groundwater flow and pollutant transport occur in three spatial dimensions, in the inherently heterogeneous and anisotropic geological media, over a great range of distances and times, and are typically nonstationary. Also, the pressures on groundwater quality have complex or unknown spatial and temporal distribution characteristics. The vulnerability of a particular groundwater receptor is, therefore, a complex function of the following (Wachniew et al., 2016):

- spatial and temporal distribution of pressures, for example, location of source areas of pollution, pollutant loads, fertilization levels, location of pumping wells and their pumping regimes, patterns of land-use change;
- distribution of water flow paths in the groundwater body;
- dilution, retardation, attenuation, and transformations of contaminants in the subsurface that affect their levels at the receptor; and
- rates at which impacts of pressures propagate along the flow paths, that are, time lags associated with the responses of the receptor to the commencement or cessation of pressures.

According to Machiwal et al. (2018), the main approaches for evaluating the vulnerability of groundwater to pollution are:

i. Vulnerability is evaluated by considering only soil and unsaturated-zone media without taking into account transport processes occurring in the saturated zone, i.e., aquifer media;

ii. Considering groundwater flow and transport processes in the aquifer up to a certain extent and is based on the delineation of wellhead protection zones for groundwater supply systems; and

iii. a holistic approach for assessing aquifer vulnerability is considering soil and unsaturated-zone media as well as the saturated zone.

These three approaches have been used in developing methods for assessing aquifer vulnerability, briefly discussed below, along with their modifications. Broadly, there are three types of methods for aquifer vulnerability assessment (Machiwal et al., 2018), as Figure 17 shows:

i. GIS-based qualitative methods;

ii. process-based methods (quantitative methods), including simulation modelling; and

iii. statistical methods, including artificial intelligence (AI) methods.

Qualitative methods and statistical tools aim to assess 'intrinsic vulnerability', whereas simulation models aim to determine 'specific vulnerability'.

On the other hand, Wachniew et al. (2016) divided the methods to assist vulnerability into two categories:

i. subjective methods where various physical factors of vulnerability are rated, usually as layers of information within a GIS system; and

ii. objective methods allow for predicting groundwater responses to pollution using statistical or physically based approaches.

The complementary nature of both approaches can be seen, for example, in the European approach(Zwahlen, 2003) and the Polish approach (Witczak et al., 2014). Wachniew et al. (2016) also mentioned that it is virtually impossible to avoid using educated guesses in most cases due to the limited availability of data.

In urbanized areas, groundwater contamination and vulnerability are of major concern that need to be addressed. Therefore, several models are modified to best fit the urban area by including anthropogenic influence, land use impact, and nitrate effects as a model parameters, namely Alam et al. (2014), Pórcel et al. (2014), Singh et al. (2015), Findell et al. (2017), and Albuquerque et al. (2021).

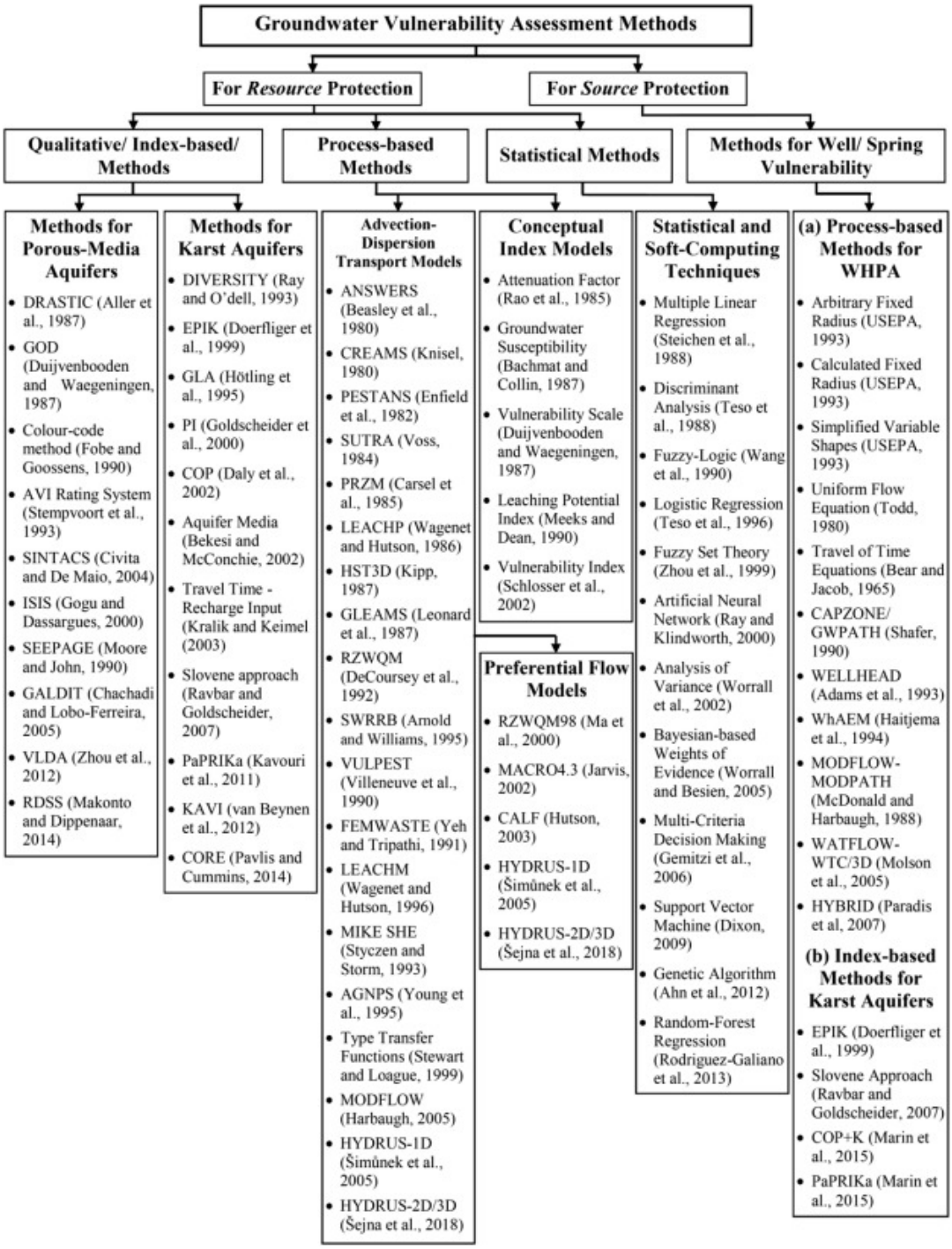

Figure 17. Groundwater Vulnerability assessment methods (Machiwal et al., 2018).

2.6. Groundwater vulnerability in fractured hard-rock aquifers

Despite being rich in groundwater resources, assessing hard-rock aquifers in many areas is difficult, given their strong heterogeneity. However, the delineation of such aquifers is essential for the estimation of groundwater reserves. In addition, the vulnerability of hard-rock aquifers is controlled by the weathered/fractured zones because it is where most of the groundwater reserves are contained (Hasan et al., 2019).

Ó Dochartaigh et al. (2005) clarified that the effective pathways where the contaminant attenuation occurs vary according to the characteristics of the aquifer creating the receptor. These variations, and the parameters controlling groundwater vulnerability assessments in each case, are described below and shown in Figure 18. It is assumed that significant attenuation does not occur when the water table lies within a bedrock aquifer with mixed intergranular/fracture flow or fracture flow only. The pathways usually consist only of superficial deposits overlying the bedrock aquifer in these cases. As a result, the effective pathway within the vulnerability assessment is shorter than the total pathway length. When the water table is in a superficial aquifer (this refers to high permeability superficial deposits that are at least partially saturated), the pathway consists of only the unsaturated superficial deposits above the water table. Effective pathway length equals total pathway length. Where a superficial aquifer overlays a bedrock aquifer, the uppermost water table in the superficial aquifer is considered the receptor. A pathway consists of the unsaturated bedrock overlying the water table and overlying superficial deposits in bedrock aquifers with the predominant intergranular flow. Therefore, the effective pathway is equal to the total pathway length and the effective pathway thickness, and the permeability, clay content, and groundwater flow type of the geological material making up the effective pathway control the groundwater vulnerability assessment.

In addition, Ó Dochartaigh et al. (2005) followed the following guidelines to ensure that the matrices were developed following scientific principles:

Groundwater is most vulnerable in areas where point recharge can bypass superficial deposits and where fractured unsaturated bedrock allows rapid groundwater flow to the water table.

All bedrock is liable to fracturing to some degree. Therefore, protection from thick and/or low permeability superficial deposits is required to significantly reduce vulnerability, even where bedrock has a significant intergranular porosity.

Superficial deposits can also be fractured, and their thickness and properties are often variable over short distances. As such, mapped thicknesses greater than 3 m are required to reduce vulnerability significantly.

The capacity of the soil to attenuate contaminants and affect groundwater vulnerability is only assumed to be significant where superficial deposits are absent or are less than 1 m thick.

The classes of vulnerability assessment in Scotland concerning the frequency of contamination activity and the travel time of contaminants through the pathway, as Table 6 shows (Ó Dochartaigh et al., 2005).

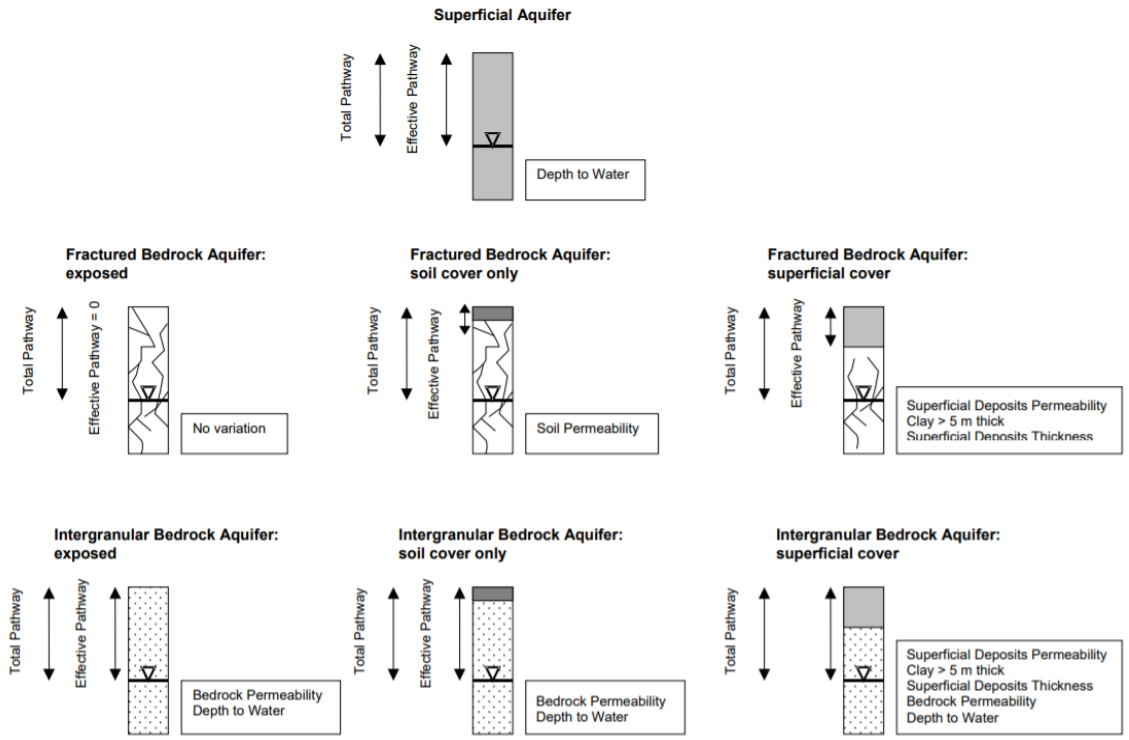

Figure 18. Groundwater vulnerability scenarios show the pathway attributes and determining vulnerability classes (Ó Dochartaigh et al., 2005).

Table 6. Vulnerability classes concerning the frequency of contamination activity and the travel time of contaminants through the pathway (Ó Dochartaigh et al., 2005).

Vulnerability class	Description	Relationship to the frequency of contamination activity	Travel Time
5	Vulnerable to most water contaminations with immediate impact in many cases.	Vulnerable to individual events	Rapid
4	Vulnerable to those contaminants not readily adsorbed or transformed.		
3	Vulnerable to some contaminants, but many are significantly attenuated		
2	Vulnerable to some contaminants, but only when continuously introduced		
1	Only vulnerable to conservative contaminants in the long-term when continuously and widely introduced.	Vulnerable only to persistent activity	Very slow

Robins et al. (2007) pointed out that the relationship between attenuation and fracture flow must be considered carefully because, in many situations, attenuation can take place in the soil horizon

and continue to some extent in poorly dilated factures below. However, the transport process between the surface of the ground and the water table seems to be fast. Even thin soils may contain some organic carbon, which provides an active zone for ion exchange and sorption. However, the soil can easily be bypassed (e.g., from contaminant sources such as septic tanks, etc.), or the soil may be absent. Robins et al. (2007) also suggest that, as a precaution, fractured rocks should be considered vulnerable until they can be proven otherwise.

Lee et al. (2020) noted that little contaminant attenuation occurs in the bedrock. Consequently, the travel time, attenuation capacity, and quantity of contaminants are a function of the following natural geological and hydrogeological attributes of any area:

i. the subsoils that overlie the groundwater (most important);

ii. the type of recharge – whether point or diffuse; and

iii. the thickness of the unsaturated zone through which the contaminant moves.

In this regard, it is important to evaluate the recharge and the travel time in the effective pathways where the contamination attenuation occurs in fractured aquifers. The Input-Time method developed by Kralik & Keimel (2003) to evaluate groundwater vulnerability according to the travel-time (TIME) from the surface to groundwater and the amount of precipitation (INPUT) as groundwater recharge can be useful in fractured aquifers as it allows evaluation of the physical parameters TIME and INPUT separately.

2.7. The original TIME-INPUT vulnerability method

The TIME-INPUT method was developed by Kralik & Keimel (2003) to evaluate groundwater vulnerability, especially in a mountainous area. Its main factors are (1) the travel-time (TIME) from the surface to groundwater (about 60%) enhanced by (2) the amount of precipitation input as groundwater recharge (INPUT; about 40%). Figure 19 visualizes the factors influencing Input and Time (Kralik & Keimel, 2003).

The weighting is empirical and gives the travel time slightly higher importance than the groundwater recharge. Unlike the other schemes, vulnerability is expressed in real-time and input values are in real quantities instead of dimensionless numbers (Kralik & Keimel, 2003).

The TIME-INPUT method has the advantage that it allows the evaluation of the physical parameters TIME and INPUT separately. Moreover, it has universal practical application in porous as well as in complicated fractured and karstified groundwater bodies. It is widely applicable,

transparent, and quality-assured. It can be used for an initial and further characterization of groundwater bodies in the sense of the European Water Framework Directive (Kralik & Keimel, 2003).

Preconditions:

There are three main preconditions to the TIME-INPUT method (Kralik & Keimel, 2003):

i. Potential contaminants are believed to behave similarly to an ideal tracer and move like infiltrating water (specific vulnerability assessment is not considered);

ii. The main target of a vulnerability assessment is the surface of the uppermost groundwater body (i.e., resource protection), which enables a consistent investigation of the total recharge area. For the protection of wells or springs (source protection), the distance to the source and the lateral movement in the saturated zone is considered; and

iii. the "mean bad conditions" of a hydrological year are assessed preferentially; therefore, the mean conditions of periods with rapid travel-times and high water input are investigated (extreme events are not considered).

Intrinsic vulnerability calculating

The two main factors, travel time and input, are combined by the simple equation:

Vulnerability =TIME(s)*INPUT (mm)

Vulnerability is mainly expressed as travel time-classes, measured in seconds [s], modified by the input correction factor (f) based on groundwater recharge, measured in millimetres per year [mm].

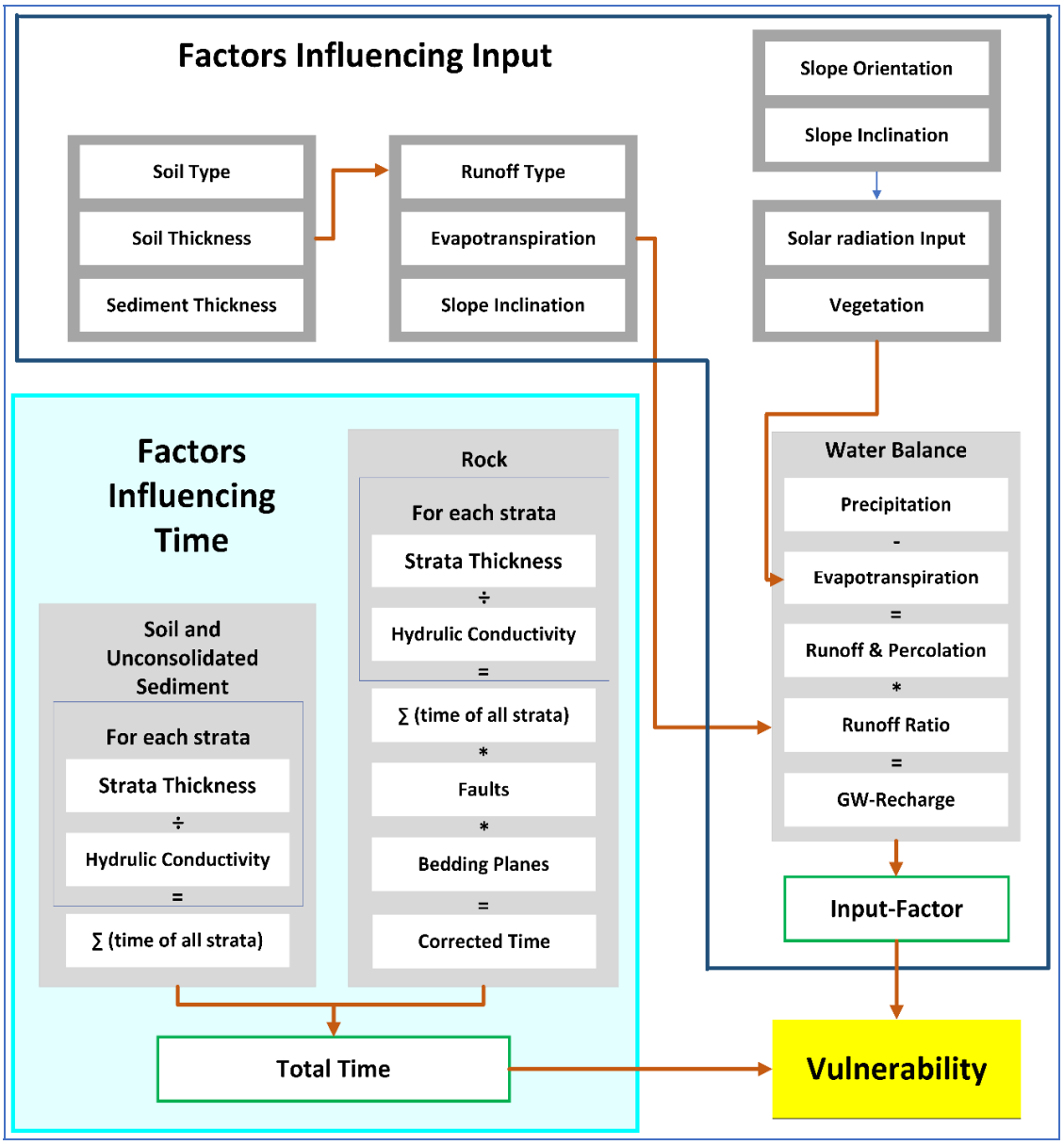

Figure 19. Flow chart of factors influencing the vulnerability assessment using the TIME-INPUT method (modified from Kralik & Keimel, 2003).

Travel time calculating

To determine the first main factor, travel TIME, it is necessary first to know the thickness of each layer (the overlying unconsolidated deposits and the different strata of the bedrock). Then, the mean hydraulic conductivity of each stratum needs to be determined with sufficient precision. In rock strata, particularly in bedded formations, the hydraulic conductivity will be much enhanced by faults, the inclination of bedding planes towards the groundwater, and karstification features like swallow holes, etc. (Figure 20) (Kralik & Keimel, 2003).

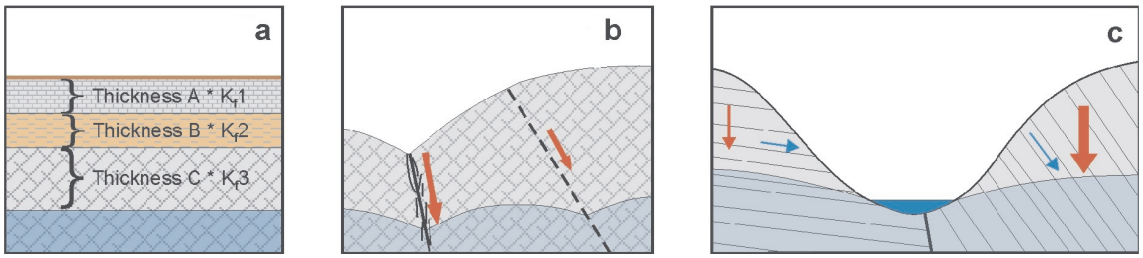

Figure 20. Factors influencing Time: a) The hydraulic conductivity and the thickness of each stratum result in the basic travel time; b) Faults are often the most important factor influencing travel time. Different correction factors should be used for different types and sizes of faults; c) In layered rock, the travel time is often influenced by bedding planes. Its significance depends on the degree and type of inclination (towards runoff or groundwater) (adapted from Zwahlen, 2004).

INPUT (groundwater recharge) calculating

The second main factor, INPUT (groundwater recharge), is classified as a correction factor. In low recharge quantities, there are high correction factors, increasing the time, whereas high recharge quantities reduce the time and increase vulnerability (Kralik & Keimel, 2003).

The quantitative input to the groundwater is expressed as groundwater recharge in mm/year. The simple water balance calculates it (Kralik & Keimel, 2003):

Groundwater recharge = Precipitation – (Surface flow + Inter flow + Evapotranspiration)

The calculation of this factor depends on the amount of precipitation, the solar radiation input, the slope inclination and aspect, the vegetation, the type and thickness of the soil, and the catchment area (Figure 21).

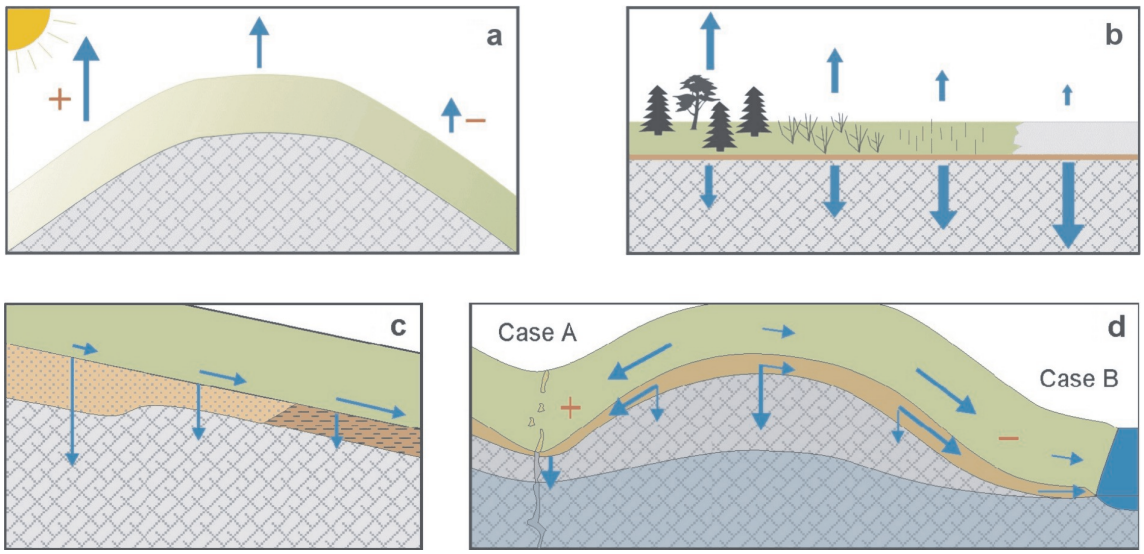

Figure 21. Factors influencing INPUT: a) Influence of solar radiation-input (determined by slope inclination and slope orientation) on evapotranspiration; b) Influence of vegetation type on evapotranspiration; c) Soil thickness and soil type and influencing the ratio between runoff and infiltration; d) Dependence of slope inclination and catchment area on runoff ratio (surface runoff and interflow *vs* infiltration): case A sinking stream—accumulation of runoff to groundwater recharge; case B surface water—no accumulation of runoff to groundwater recharge, (adapted from Zwahlen, 2004).

This vulnerability assessment method differs from others by expressing the vulnerability in real-time and not displaying it in dimensionless numbers, so the results are more easily verified, and the evaluation process is more transparent.

2.7.1. INPUT (recharge) in an urban area

The process of groundwater recharge is key to understanding how contamination can occur and classifying aquifer units according to their contamination vulnerability. Moreover, without an understanding of recharge, namely its quantity, its seasonality, and the routes the recharge may take through the subsoil and the unsaturated zone, it is impossible to correctly manage groundwater resources or individual groundwater sources (Robins, 1998).

The groundwater recharge mechanisms include the soil infiltration process, the flow rates, and pathways through the vadose (unsaturated) zone to phreatic aquifers and the vertical leakage through confining beds to semi-confined aquifers (Foster, 1998). It is important to recognize that groundwater contamination and recharge are directly related as contaminated dispersed groundwater is directly affected by recharge and dilution. The greater the recharge, the more efficient the transport from the surface to the water table (Robins, 1998). In urban areas, many factors control groundwater recharge (Lerner,1990, Hibbs, 2016)) as Table 7 shows:

Table 7. Urban controls on groundwater recharge (adapted from Lerner,1990, Hibbs, 2016)

Urban Factors Increasing Recharge Urban	**Urban Factors Decreasing Recharge Urban**
Impervious cover reducing evapotranspiration	Impervious cover limiting rain recharge
Changing urban microclimate (+)	Changing urban microclimate (-)
Urban runoff dry wells and catch basins	Infiltration to sewer and water pipes
Artificial recharge wells and basins	Infiltration to storm sewers
The concentrated density of septic tanks	Extraction and export to other basins
Exfiltration from sewer and water pipes	
Exfiltration from storm sewers	
Import water return flow	
(Wiles & Sharp Jr, 2008) noted that leakage through impervious cover must also be considered	

According to Freitas et al. (2019b), to map the Urban Infiltration Potential Index (IPI-Urban) in urban areas, it is necessary to have the following layers:

i. geology and morphotectonics;

ii. climate and hydrology;

iii. urban hydrogeology and hydrogeomorphology; and

iv. urban hydraulics and sanitary features.

The IPI-Urban consists of a weighted sum of eight factors, namely: hydrogeological units, slope, land use, tectonic lineament density, drainage network density, sewer network density, stormwater network density, and water supply network. In addition, the index included urban hydraulics and sanitary features as one of the last three factors. Figure 22 shows the methodology to calculate the IPI-Urban and recharge in an urban area.

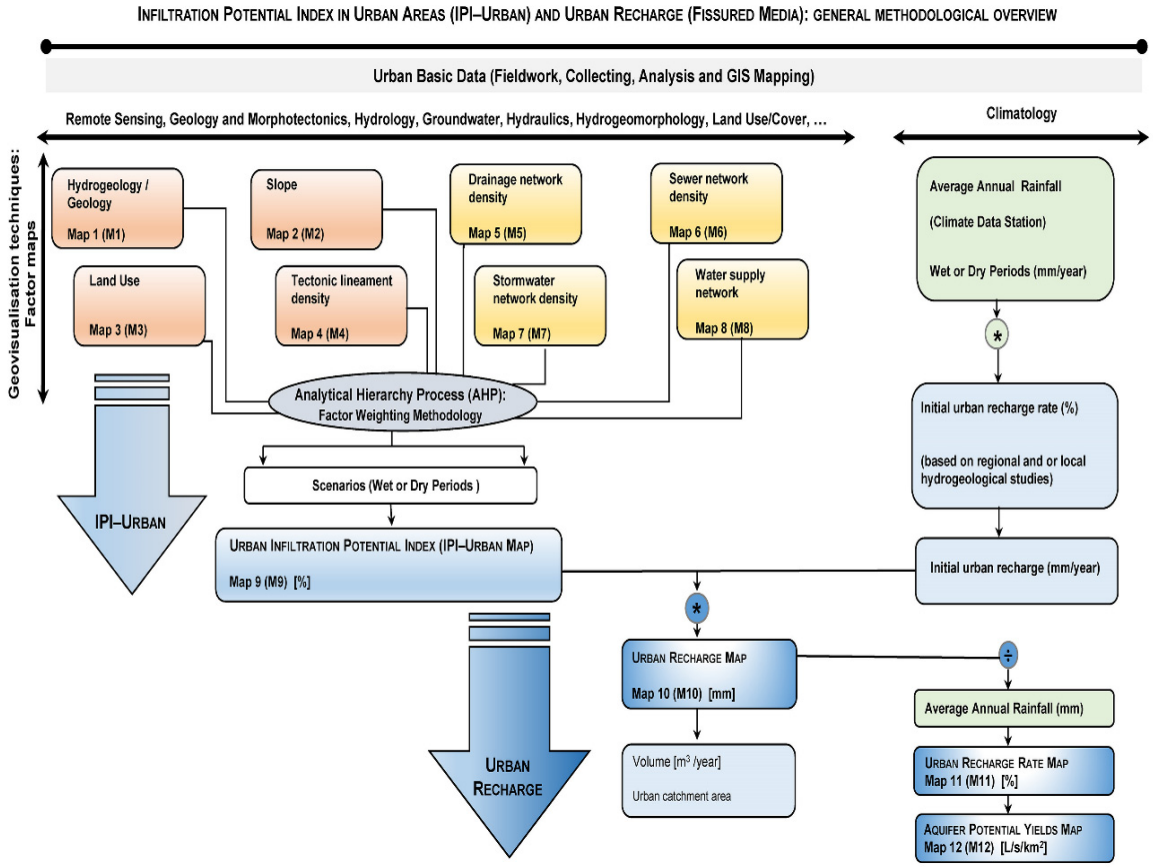

Figure 22. Methodological overview to determine the Urban Infiltration Potential Index in Urban Areas (IPI-Urban) and Urban Recharge in fissured media (Freitas et al., 2019b).

2.8. Reconstruction of safeguard zones of groundwater sources

Source water assessments begin by delineating (or mapping) the land area that contributes water to the drinking water supply and determining where contamination from human activities or natural sources is of greatest concern for the quality of the drinking water supply. This delineated

area is often considered a source water protection area or zone of concern. The area of protection zones may vary based on various hydrogeological, environmental, regulatory, and management factors (USEPA, 2021).

Various methods are used to delineate groundwater source protection zones. Some methods are more scientifically complex and accurate than others. Several factors should influence the appropriate choice of delineating method, including access to technical resources, availability of data (e.g., hydrogeologic data), cost, and desired level of effort (USEPA, 2021).

According to (USEPA, 1987), delineating a water head protection area is based on five criteria: distance, drawdown, travel time, flow system boundaries, and aquifer capacity to assimilate contaminants. In addition, they classified the methods for safeguard zones delineation into six categories in the ascending order of their complexity and cost: (a) arbitrary radii, (b) fixed calculated radius, (c) simplified variable shapes, (d) analytical methods, (e) hydrogeological mapping, and (f) numerical flow and transport models.

In fractured aquifers, delineating protection zones poses a challenge because of heterogeneity and anisotropy in hydraulic conductivity, making predictions of groundwater flow organization and velocities difficult. Researchers in various fields of hydrogeology are currently trying to understand better groundwater flow in fractured rocks, but groundwater protection still needs much improvement (e.g., Pochon et al., 2008).

2.9. The Time-Dependent Model (TDM)

The time-dependent model (TDM) for groundwater source protection zoning, developed at the Faculty of Mining and Geology at the University of Belgrade (Živanović et al., 2016), has been designed to assess source vulnerability based on surface water and groundwater travel times. TDM was initially created for karst groundwater sources but is also applicable to other types of aquifers. It considers three main components:

i. surface water travel time (t_s) for areas in the source catchment where surface runoff is predominant;

ii. vertical travel time (t_v) through the unsaturated zone, or the overlying low-permeability strata in the case of a confined aquifer; and

iii. horizontal travel time (t_h) through the saturated zone to the intake groundwater sources.

According to Živanović et al. (2021), all types of surface water travel time (ts) depend on the flow length, terrain slope and roughness, and precipitation intensity and can be calculated by applying hydrology analysis in GIS tools. While the vertical travel time (t_v) can be calculated using the TIME-INPUT method (Kralik & Keimel, 2003), and the horizontal travel time (th) should include both matrix and fractured flow in hard-rock aquifers.

It is possible to calculate some components of the total travel time directly (from dye-tracing tests) or indirectly (based on karst hydrogeological system characterizations, such as hydrograph analysis and time series analysis).

2.9.1. Vertical travel time

The vertical travel time through the unsaturated zone is influenced by the characteristics of the unsaturated zone and the recharge process. It is considered that aquifers that receive water (and contaminants) from the land surface readily and rapidly are more vulnerable than aquifers that receive water (and contaminants) more slowly and in smaller quantities since all groundwater is hydrologically connected to the land surface and vulnerability to contamination is determined in part by the effectiveness of this connection to the land surface. According to the Irish groundwater vulnerability mapping scheme (Lee et al., 2020), the intrinsic vulnerability of groundwater depends on the following:

i. the time of travel of infiltrating water (and contaminants);

ii. the relative quantity of contaminants that can reach the groundwater; and

iii. the contaminant attenuation capacity of the geological materials through which the water and contaminants infiltrate.

According to the Polish approach to groundwater vulnerability assessment (Witczak et al., 2014), the transport time of conservative contaminants is one of the essential elements of the vulnerability assessment and mapping since the travel time of groundwater is long-term, on several average tens of years. Consequently, long-term contamination of groundwater, in turn, results in a slower response of surface waters to alterations in groundwater baseflow quality. Table 8 shows the time scale of the Polish approach.

For vulnerability assessments to be effective, the time lag associated with contaminant transport must be considered since when contaminants take longer to reach the groundwater table or the groundwater receptor, the more dilution, retardation, and attenuation they have. Water's mean residence time is a pragmatic indication of the groundwater's potential vulnerability and the

several terms used to describe the temporal aspects of mass transport (travel time, residence time, transit time, turnover time). The mean residence time equals the turnover time of water and, thus, the water volume ratio in the reservoir to water flux. In contrast, the mean travel or transit time of water can be evaluated using Darcy's law, representing the advective flow timescale. That study by Wachniew et al. (2016) focused on reviewing the vulnerability methods that rely on the evaluation of timescales of groundwater flow since the relevance of vulnerability assessments to the present requirements of water resources management depends on their ability to address time lags associated with contaminant transport. Besides, incorporating timescales in groundwater vulnerability mapping facilitates the transfer of knowledge and information to decision-makers.

Table 8. The time scale of the Polish approach for Vulnerability assessment (Witczak et al., 2014).

Vulnerability Class	Definition	Vertical Travel Time to aquifer [Years]	Color on the map
Very high	The aquifer is vulnerable to most water pollution with rapid impact in many pollution scenarios	<5	Red-Orange
High	Aquifers are vulnerable to many pollutants, except those strongly absorbed or readily transformed, in many pollution scenarios	5-25	Pink
Moderate	The aquifer is vulnerable to some pollutants, but only when continuously discharged or leached	25-50	Yellow
Low	Aquifers are only vulnerable to conservative pollutants in the long term when continuously and widely discharged or leached	50-100	Light Olive-Green
Very low	Aquifer confining beds present with no significant vertical groundwater leakage	>100	Olive-green

In this study, the Time-Input method was developed by Kralik & Keimel (2003) to calculate the vertical travel time, as discussed in section 2.7.

2.9.2. Surface travel time

The surface travel time or time of concentration is a concept used in hydrology to measure the response of a watershed to a rain event. It is the time needed for water to flow from the most

remote point in a watershed to the watershed outlet. It is a function of the topography, geology, and land use within the watershed (Staff, 2010).

The main factors affecting surface travel time (Time of Concentration) include(Fang et al., 2007; Staff, 2010):

i. **Surface Roughness:** One of the most significant effects of urban development on overland flow is the lowering of retardance to flow, causing higher velocities. Urban development has modified undeveloped areas with the very slow and shallow overland flow (sheet flow and shallow concentrated flow) through vegetation. Flow is then delivered to streets, gutters, and storm sewers that rapidly transport runoff downstream. Travel time through the watershed is generally decreased;

ii. **Channel Shape**: In small non-urban watersheds, much travel time results from overland flow in upstream areas. Typically, urbanization reduces overland flow lengths by conveying storm runoff into a channel as soon as possible. Since channel designs have efficient hydraulic characteristics, runoff flow velocity increases and travel time decreases; and

iii. **Slope**: Slopes may be increased or decreased by urbanization, depending on the extent of site grading or the extent to which storm sewers and street ditches are used in the water management system design. The slope will tend to increase when channels are straightened and decrease when the overland flow is directed through storm sewers, street gutters, and diversions.

Urbanization usually decreases the time of concentration, thereby increasing the peak discharge. However, the concentration time can be increased by ponding behind small or inadequate drainage systems (including inlets and road culverts) or by reducing land slope through grading.

There are many methods available to estimate the time of concentration. This research applied the NRCS velocity method (NRCS 1972, 1986) to the study to estimate the concentration-time.

2.9.2.1. NRCS Velocity Method

The Natural Resources Conservation Service NRCS velocity method (NRCS 1972, 1986) is commonly used to estimate the concentration-time for hydrologic analysis and design. The NRCS velocity method applies the physical concept that travel time is a function of runoff flow length and flow velocity.

Travel time (T_t) is when it takes water to travel from one location to another. The travel time between two points is determined using the following relationship:

$$T_t = \frac{l}{v}$$

Where:

Tt = travel time;

ℓ = flow length; and

V = average velocity

Surface water flow through the watershed has three different flow types: sheet flow, shallow concentrated flow, and open channel flow. The NRCS Velocity Method assumes that time of concentration (T_c) is the sum of travel times for each flow segment along the hydraulically most distant flow path.

$$T_c = T_s + T_c + T_o$$

Where:

Tc = time of concentration (hours);

Ts = travel time for sheet flow (hours);

Tc = travel time of shallow concentrated flow (hours); and

To = travel time for open channel flow (hours).

Sheet *flow* is defined as the flow over plane surfaces. Sheet flow usually occurs in the headwaters of a stream near the ridgeline that defines the watershed boundary. Typically, sheet flow occurs for no more than 30 m before transitioning to S*hallow concentrated flow*, collecting in swales, small rills, and gullies. *Shallow concentrated flow* is assumed not to have a well-defined channel and has a flow depth of 3-15 cm.

Manning's equation or water surface profile information can estimate average flow velocity. Manning's equation is:

$$v = \frac{1.49 * r^{\frac{2}{3}} * s^{\frac{1}{2}}}{n}$$

Where:

V = average velocity;

r = hydraulic radius, r=a /P_w ;

a = cross-sectional flow area;

P_w = wetted perimeter;

s = slope of the hydraulic grade line (channel slope); and

n = Manning's n value for open channel flow, which is a unitless coefficient representing the conduit's roughness or friction factor.

Equations for estimating shallow concentrated flow velocity according to runoff type, flow depth, surface roughness (n), and slopes (s) were developed according to specific figures for estimating the velocity (Staff, 2010) (Table 9). The developed equations give velocity in ft/s, and then the conversion into metric units should be done.

The *Open Channel Flow* in open channels (swales, ditches, storm sewers, and tiles not flowing full) is assumed to begin where surveyed cross-sectional information has been obtained, where channels are visible on aerial photographs.

Table 9. Equations and Assumptions for calculating flow velocity (Staff, 2010).

Flow Type	Depth of flow (ft)	Manning's roughness Coefficient, n	Velocity Equation (ft/s)
Pavement and small upland gullies	0.2	0.025	$V=20.238(S)^{0.5}$
Grassed waterway (and unpaved urban areas)	0.4	0.050	$V=16.135(S)^{0.5}$
Nearly bare and untilled (overland flow); and alluvial fans	0.2	0.051	$V=9.965(S)^{0.5}$
Cultivated straight-row crops	0.2	0.058	$V=8.762(S)^{0.5}$
Short-grass prairie	0.2	0.073	$V=6.962\ (S)^{0.5}$
Minimum tillage cultivation, contour or strip-cropped, and woodlands	0.2	0.101	$V=5.032(S)^{0.5}$
Forest with heavy ground litter and hay meadows	0.2	0.202	$V=2.516(S)^{0.5}$

2.9.3. Horizontal travel time and groundwater flow in fractured hard-rocks aquifers

Horizontal travel dominates when infiltrated water or potential contaminants reach the saturated zone. In fractured rock aquifers, groundwater pathways and residence times are controlled by aquifer flow and storage properties, characterized by high spatial heterogeneity in weathered/fractured hard rock aquifers (Comte et al., 2019). Hydraulic conductivity and flow rate

in fractured rock aquifers are highly variable spatially, and Hydraulic properties can also be highly anisotropic, so directional information must be used in conjunction with hydraulic properties. The water flow through individual fractures can be extremely high, but the fractures usually occupy a small fraction of the aquifer. Therefore, even when water velocities through individual fractures are high, volumetric flow rates through the aquifer can be quite low on average. This heterogeneity makes some traditional techniques for describing porous media aquifer systems of limited value in fractured rock aquifers (Cook, 2003).

A fractured rock aquifer comprises a network of fractures that cut through the rock matrix (Figure 23). Characterizing fractured rock aquifers requires information about the fractures and the rock matrix. Fractures can be classified by their dimensions (e.g., aperture, length, width), their location (orientation, spacing, etc.), and the characteristics of their walls (e.g., roughness). In contrast, the rock matrix is classified by its pore size distribution, often expressed in terms of porosity and hydraulic conductivity. The fracture porosity is defined as the volume of the aquifer occupied by open fractures that are, in most cases, greater than the matrix porosity, the porosity of the rock matrix.

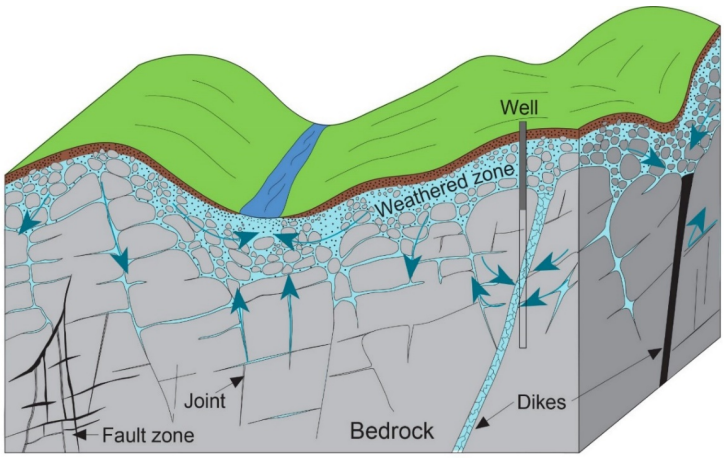

Figure 23. Generalized groundwater flow in a fractured-rock aquifer (modified from Freeze and Cherry, 1979).

Groundwater flow in a single fracture can be calculated using Darcy's law as the following: (Singhal, 2008):

$$V = K_f * I$$

Where:

K_f is the hydraulic conductivity of the fracture; and

I is the hydraulic gradient.

The fractured rock formations can be classified according to their porosity and permeability, into four groups, as Figure 24 shows (Singhal, 2008):

a. purely fractured medium;
b. fractured formations;
c. double porosity medium; and
d. heterogeneous medium.

With a purely fractured medium, porosity and permeability can only be attributed to interconnected fractures, and blocks are impervious, but in a dual-porosity medium, both fractures and matrix blocks contribute to groundwater flow, but fractures are the main contributor. In the case of fractures filled with clay or silt, the permeability of the fracture is considerably reduced, giving it the name heterogeneous medium.

Cook (2003) describes the main approaches for modelling groundwater flow and solute transport in fractured rock aquifers. The main issue is how to describe the heterogeneity associated with fractures. Several approaches exist, but most can be grouped into three classes:

i. the equivalent porous media approach;
ii. the dual-porosity approach; and
iii. the discrete fracture network approach.

In an equivalent porous media approach, the hydraulic properties of the system are modelled using equivalent coefficients such as permeability and effective porosity to represent the volume-average behavior of many fractures within a fractured rock body. Therefore, individual fracture details are not necessary. In contrast, in a discrete network approach, the details of individual fractures are explicitly accounted for in the model simulation. Using a dual-porosity approach, equivalent properties of porous media are assigned separately to fracture and matrix elements, and an exchange coefficient is calculated for transfer between the two zones based on simplified fracture geometry.

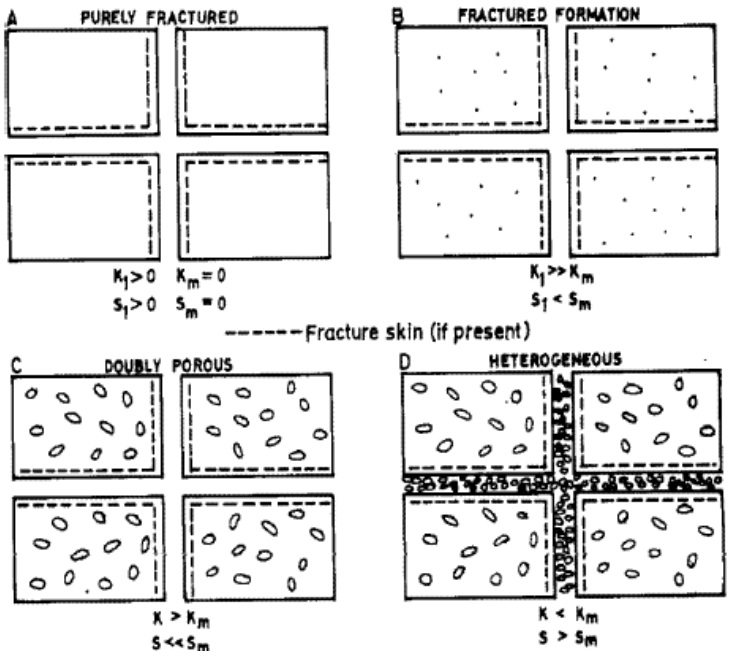

Figure 24. Hydrogeological classification of fractured media. Kf and Km are the fractures' and matrix hydraulic conductivities, respectively. Sf and Sm represent the fluid storativities of the fractures and the matrix (Cook, 2003).

(página propositadamente em branco)

Chapter III: Porto Urban Area: Paranhos and Salgueiros Water Galleries

(página propositadamente em branco)

3.1. Geographical and historical background

Porto city became an important metropolis in the 12th century, although its history dates back at least to the 6th century (De Oliveira Marques, 1972). The water supply of Porto city was, for more than 600 years, provided by fountains supplied by abundant springs. Throughout the centuries, several underground galleries were excavated on the fissured granitic rock substratum to capture the water of these springs and protect it from contamination. Paranhos and Salgueiros spring waters were among the most important water supply sources, in quantitative and qualitative terms, by the end of the 18th century. The primary gallery, transporting Paranhos and Salgueiros waters, is 3.2 km long at has a maximum depth of 20 m below ground level (e.g., Bourbon e Noronha 1885; Carteado Mena 1908; Fontes 1908; Afonso et al. 2010a, b, 2016; Chaminé et al. 2010, 2014; Afonso 2011; Freitas et al. 2014), (Figure 25). Urban water systems with proper sanitation infrastructures and hygienic practices were absent until the late 19th century, and they were implemented only in the period 1860 to 1920 (e.g., Silva & Matos 2004, Chaminé et al., 2010, 2014, Freitas et al., 2014, Afonso et al., 2018).

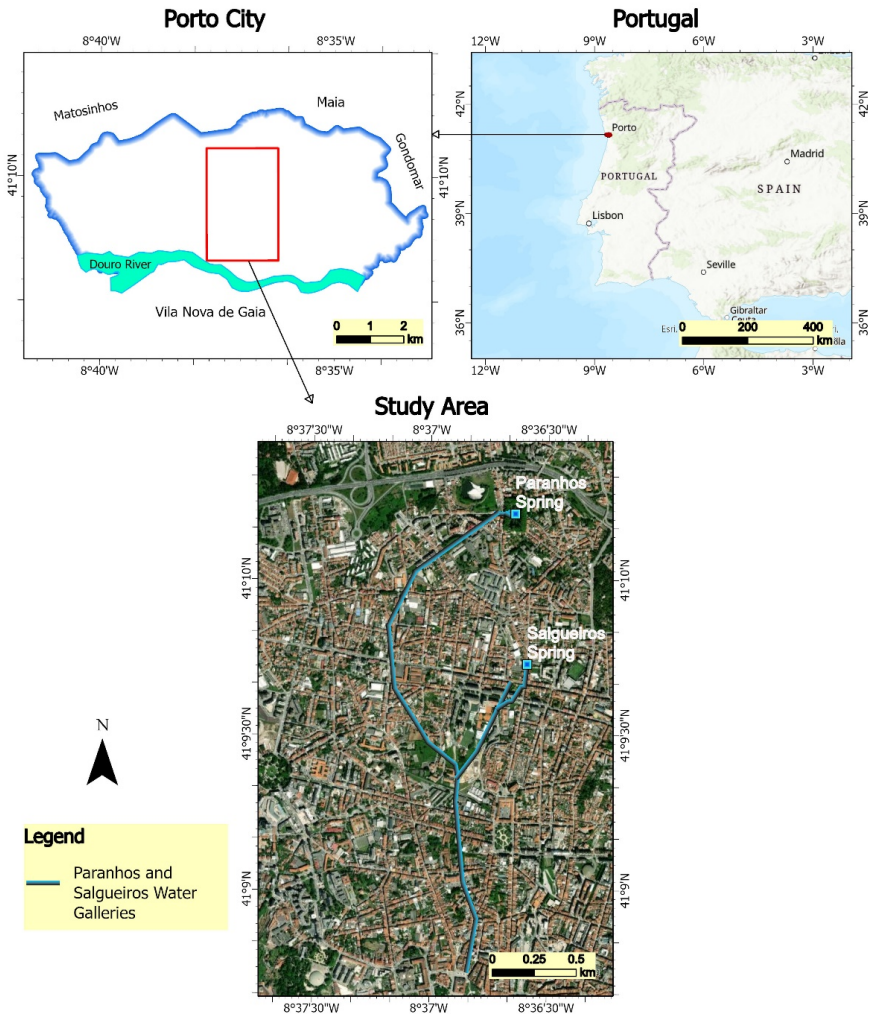

Figure 25. The geographical location of the study area.

3.2. Climate, geomorphology, and drainage network

The climate in Porto city is temperate, with a dry and warm summer (Köppen climate classification Csb). The average annual temperature is 15.2 °C. The average annual rainfall is 1236.8 mm/year, reaching 181 mm in December (the wettest month) and 20.4 mm in July (the driest month) (Afonso et al., 2019; IPMA 2022).

Concerning geomorphology, the study area is on the western border of the highest plateau of Porto City. Most of the highest elevations are concentrated in the NE area, and the maximum elevation is about 155 m to the east of the Salgueiros Spring (Figure 26A). Most of the area has a gentle to very gentle slope (< 6°) (Figure 26B).

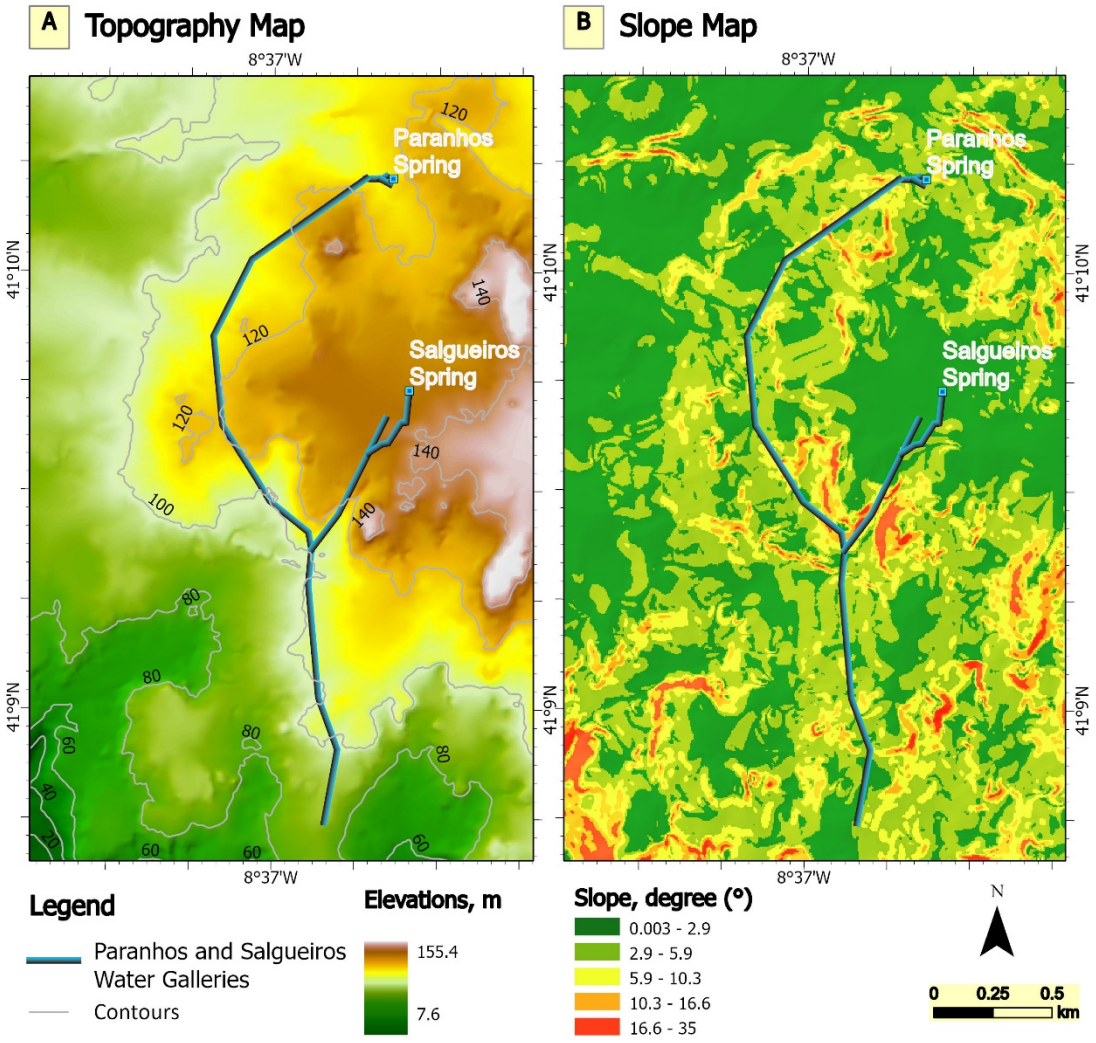

Figure 26. (A) Digital elevation model; and (B) slopes (^{0}) in the study area.

Regarding drainage, the study area is crossed by a network of streamlines corresponding to canalized and/or actual streamlines (Figure 27). The drainage density is between 0 and 38.5 km/km^2.

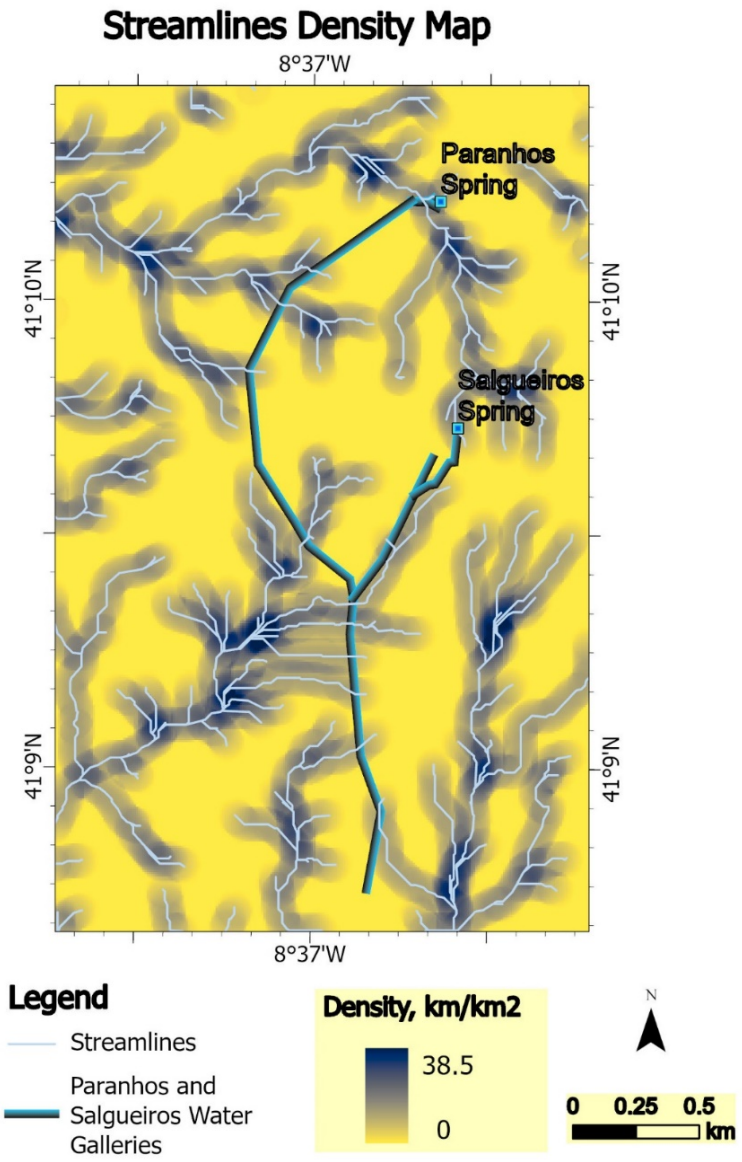

Figure 27. Drainage density map in the study area.

3.3. Hydrogeology and hydrogeochemical background

The hydrogeotechnical units in the surrounding area of Paranhos and Salgueiros water galleries are (Afonso et al. 2010, 2019; Chaminé et al. 2010), (Figure 28):

- Alluvial deposits: They consist mainly of sands and silts with low to moderate permeability (< 2 m/day); the thickness of these deposits is less than 6 m;
- Saprolite: Most of these are kaolinitic silty sands firmly related to the Porto granite with very low permeability (< 0.1 m/day); and
- Porto granite: This unit is intersected by crushed quartz veins (thicknesses of millimetres to several centimetres) and occurs weathered, from fresh rock to slightly weathered ($W_{1–2}$) to

highly weathered ($W_{4–5}$), but predominantly, moderately weathered (W_3); the permeability is low to moderate (< 1 m/day).

According to the hydrogeochemistry, Paranhos and Salgueiros spring waters are neutral, with a median pH of 6.7, and nitrate enriched, with a median NO_3 higher than 50 mg/L. There are two main groups of water, the SO_4-Ca-type and the HCO_3-Ca-type. Paranhos and Salgueiros spring waters are shallow groundwaters with quick responses to precipitation events (Afonso et al., 2016).

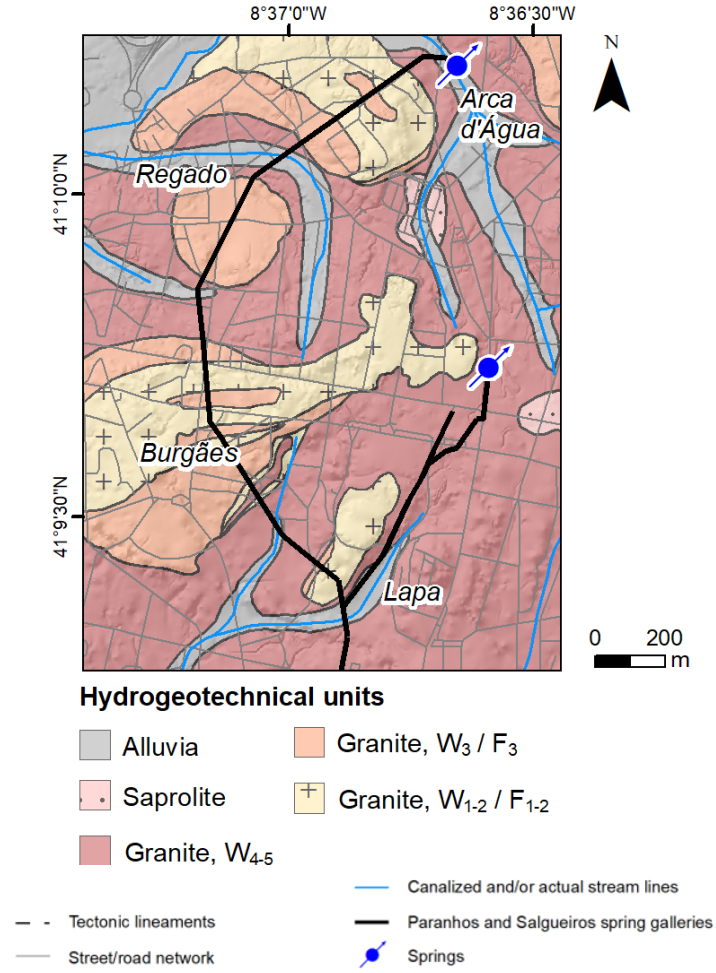

Figure 28. Hydrogeotechnical units in the study area (adapted from Afonso et al., 2019).

3.4. Water supply, sewers, and stormwater systems

Porto urban area already had fountains for more than six centuries for public use, albeit without hygienic conditions. However, with the growth of the population and consequent concentration, the problems became worse, being necessary to take advantage of the Paranhos spring, located in the basement of the Jardim da Praça 9 de Abril, better known as Jardim da Arca d'Água (Águas e Energia do Porto, n.d.).

The plumbing began and was completed in 1607, allowing water to be transported to the city through water Galleries, feeding various sources along its route.

In 1825, a new route was approved, that of Salgueiros originating in the current street of Antero de Quental. The new gallery, with a length of about 3.5 km, was completed in 1838 and ended at Arca de Sá Noronha.

Before what would become a home water supply, most of the population resorted to public fountains, but the wealthier ones established contracts with "aguadeiros" (“watermen”) who had escaped from military service and sold water. After that, water contamination, transmitted diseases, the evolution of health care, and even the demands on the quality of life imposed a radical transformation of the system.

From 1855 onwards, several companies began to apply for the design and execution of works for capturing, lifting, transporting, and distributing households.

In the XIX century, Porto had no sewers or stormwater systems. The first reports noting serious problems with urban water and sanitation in Porto were published between (1833-1855), and in 1903, the sanitation network was established in Porto (Chaminé et al., 2014).

Figure 29 depicts, for the present-day, the water supply system line density (A), the sewers network line density (B), and the stormwater network line density (C) in the study area. As can be seen in Figure 29, the water supply system network has a higher line density than sewers and stormwater networks, which have approximately the same line density.

3.5. Land uses and potential contamination sources

The city structure changed greatly during the last decades from mainly agriculture to urban settings. One hundred years ago, green and agricultural spaces occupied the study area, while the present-day urban sites covered most of this region (Madureira et al., 2011), leading to the inevitable increment of contamination sources.

In the surrounding area of Paranhos and Salgueiros spring galleries, 107 potential contamination sources were inventoried. Most of them correspond to automobile repair shops and school/university buildings. Most of the contamination sources have moderate contamination loads and correspond to point sources (Afonso et al., 2016; Freitas et al., 2019a,b) (Figure 30). Additionally, the sewer system in this area is over 50 years old, which makes it highly susceptible to leaks, and it crosses spring galleries frequently.

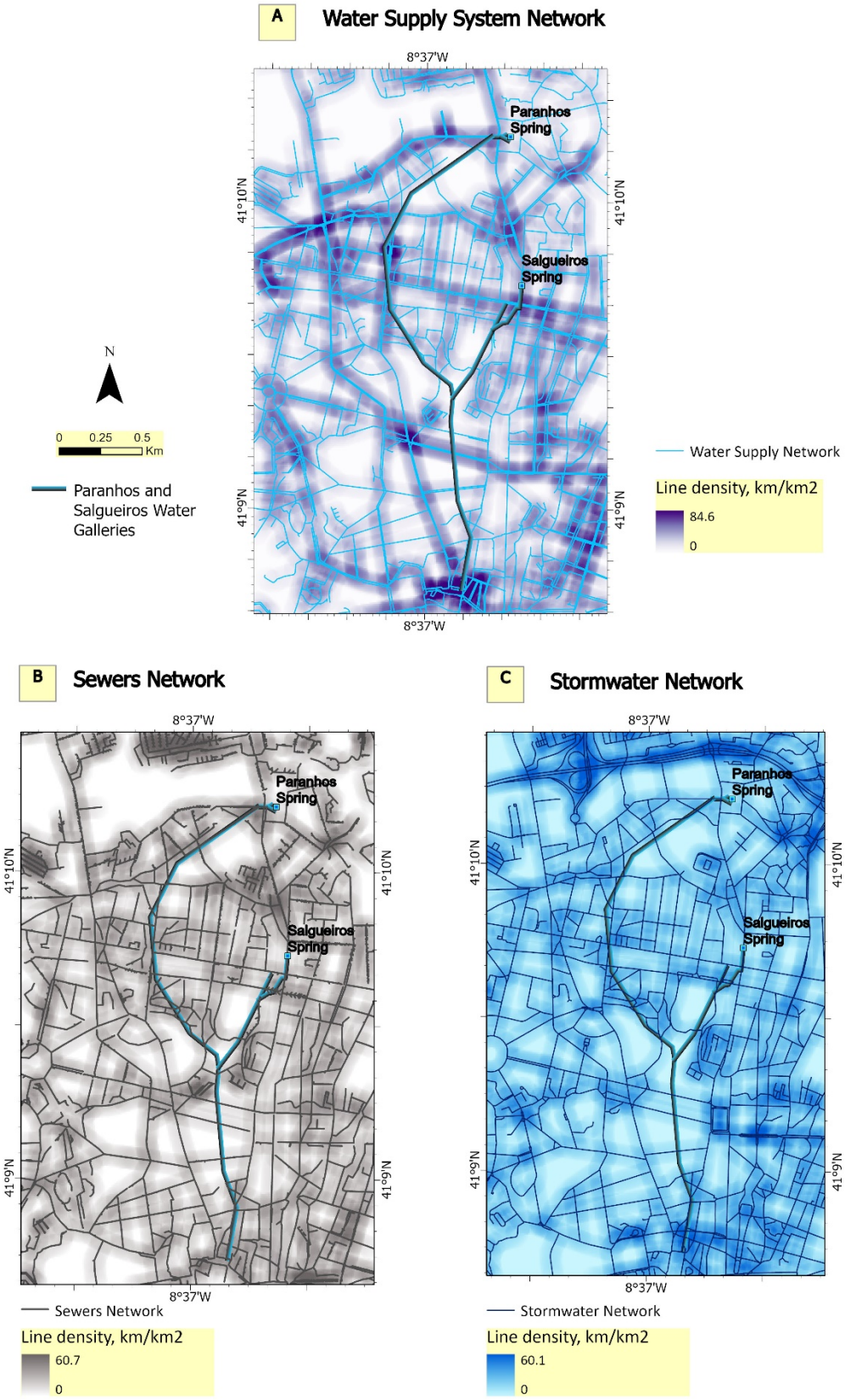

Figure 29. Hydraulics in the study area. (A) Water Supply System line density; (B) Sewers System line density; (C) Stormwater systems line density (adapted from COBA, 2003).

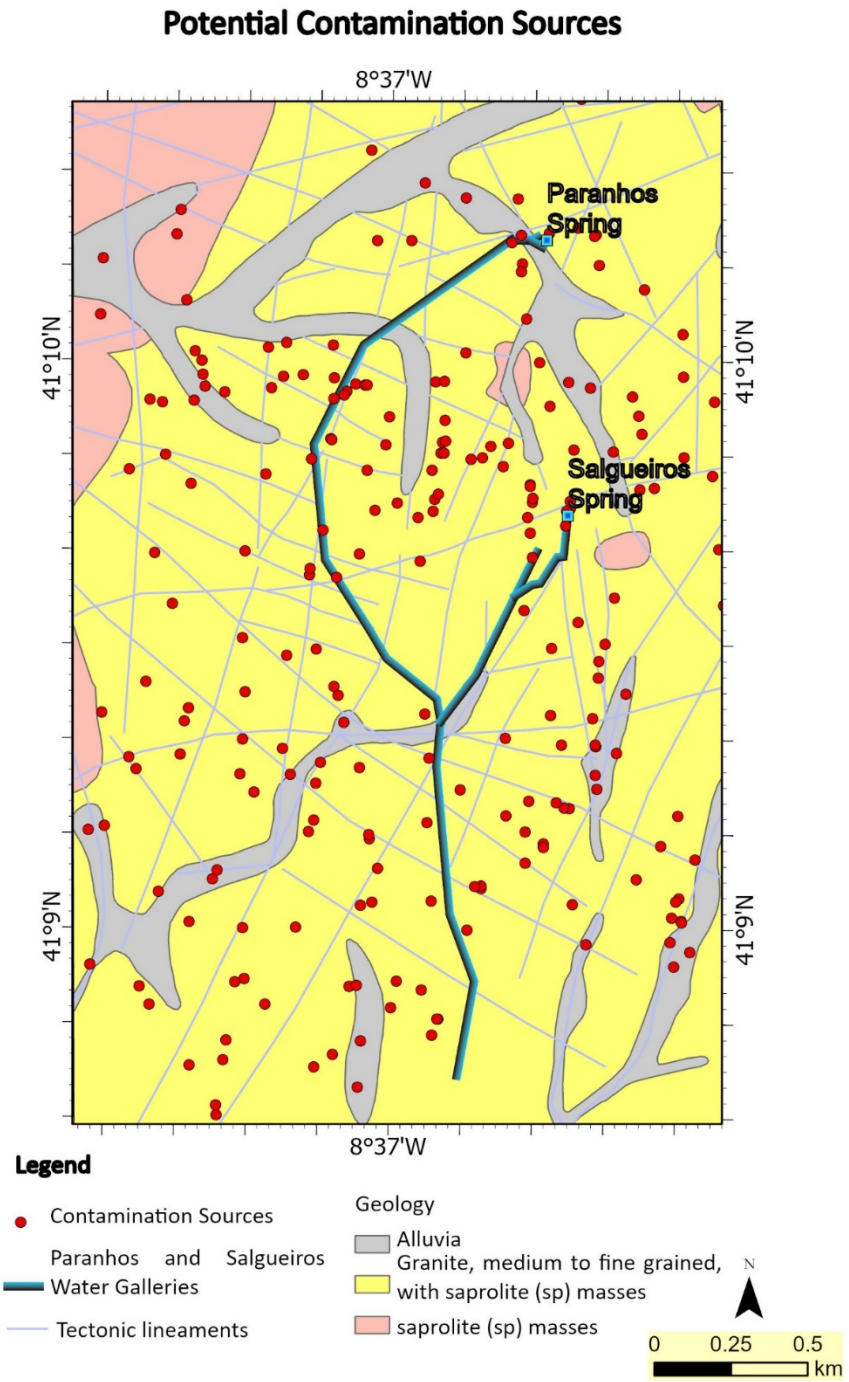

Figure 30. Geology and potential contamination sources around Paranhos and Salgueiros water galleries (adapted from Afonso et al., 2016; Freitas et al., 2019 a,b).

3.6. Methodology

As part of the process of reconstruction of the historical groundwater maps and identifying spatiotemporal changes in intrinsic vulnerabilities and safeguard zones in the study area, the maps and spatiotemporal changes of groundwater vertical travel time in unsaturated zones, groundwater horizontal travel time in the saturated zone, and surface travel time have been

analyzed using GIS-based mapping techniques. This was accomplished using two main methods, presented in sections 2.72.9:

1) The TIME-INPUT method by Kralik & Keimel (2003) identifies the intrinsic vulnerability by identifying the vertical travel time (t_v) of groundwater from the surface to the saturated zone;

2) The time-dependent method (Živanović et al., 2016) identifies the protection zones by considering the surface water travel time (t_s) for areas in the source catchment where surface runoff is predominant; vertical travel time (t_v) through the unsaturated zone or the overlying low-permeability strata in the case of a confined aquifer; and horizontal travel time (t_h) through the saturated zone to the intake groundwater sources.

Two-time scenarios were used to compare how intrinsic vulnerability and safeguard zones changed after and before urban expansion and the city's growth.

Scenario 1: Before the urban expansion and the growth of the city (XIXth century)

Conditions:

- Urban groundwater was still used for drinking
- There were no sanitary sewers or water supply systems.

Scenario 2: After the urban expansion and the growth of the city (XXIst century)

Conditions:

- Urban groundwater is no longer used for drinking
- There are sanitary sewers, stormwater networks, and water supply systems.

An integrated, multidisciplinary, and simplified GIS-based methodology has been conducted to prepare groundwater maps in urban hard-rock aquifers, as Figure 31 shows. Implementing the GIS-based model consists of an integrated three-phased approach: i) Data Collection, ii) Analysis and Development, and iii) Implementation. Each phase is outlined as an independent vertical process flow with a concurrent horizontal process between the model and the GIS application.

The data was collected from different sources, and then ArcGIS pro has been used for mapping, analyzing, and developing models for displaying and comparing the results.

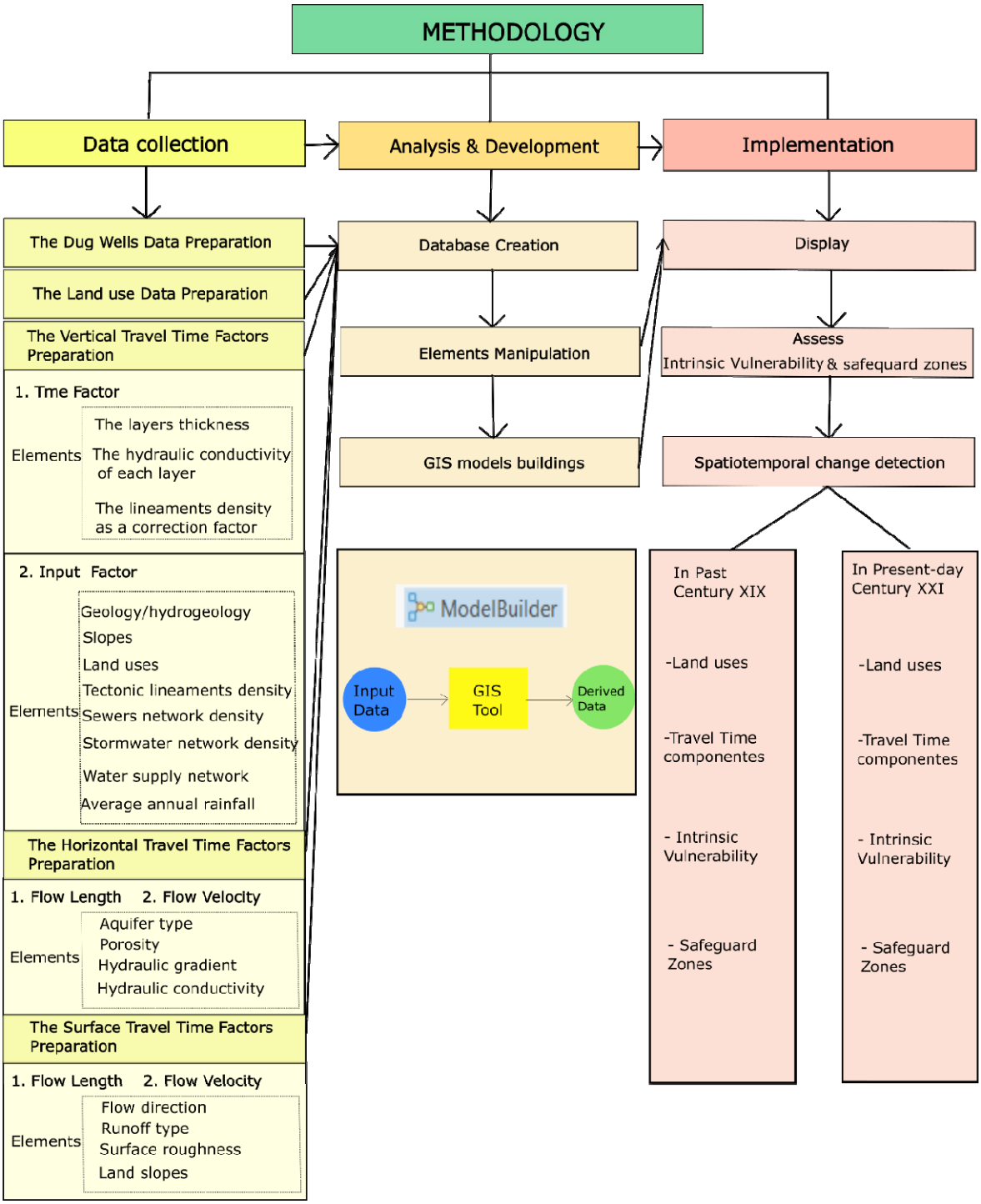

Figure 31. Research methodology.

3.6.1. Data Collection

The fundamental data for calculating the vertical and the horizontal travel time for groundwater and the surface travel time are collected from existing geological and hydrogeological maps, remote sensing data, field measurements, and field observations. All these data are usually stored in a computerized database (Kralik & Keimel, 2003). Data sources are presented in Table 10.

Table 10: Research data type, format, scale, and source

GIS layer	Format	Scale	Source
Dug-wells data	.shp (point)	1:500	Carteado Mena (1908).
Land use (1892)	raster	1:500	Telles Ferreira (1892); Madureira (2001); Madureira et al. (2011).
Land use (2018)	.shp (polygon)	Multiscale	IGP (2010); Caetano et al. (2009).
Geological and hydrological data	.shp (point, polygon, polyline)	1:50 000	Carrígnton da Costa & Teixeira (1957); Pereira et al. (1989); COBA (2003); Chaminé et al. (2003).
Topographic data	Digital Elevation Model (DEM)	1:5 000	COBA (2003).
Hydraulics Networks (water supply, sewer, stormwater networks)	.shp (polyline)	1:5 000	COBA (2003).
Potential contamination sources	.shp (point)	Field inventory	Freitas, et al. (2019 a,b).
Meteorological data (rainfall)	Tabular data	-	IPMA (2022).

3.6.1.1. Dug wells data preparation

To estimate the thicknesses of the unsaturated, the saturated zones, and the fissured layer, the dug wells inventory developed by Carteado Mena (1908) was applied. This historic inventory shows several hydroparametric measurements and quantification, such as geographic coordinates, the total depth of the dug well, the width of the dug well, the water table's depth, the water column's thickness, air temperature, and groundwater temperature (Table 11). Figure 32 shows a longitudinal section of a dug well with some of the parameters measured and calculated:

- (a) The water depth - is the length from the ground surface to the water table in the dug well; represents the thickness of the unsaturated zone (above the groundwater table);

- (b) The water column thickness - is the length from the water table to the bottom of the dug well; represents the minimum thickness of the saturated zone in the fissured layer that lies directly beneath the unsaturated zone;

- (c) The dug well depth - is the length from the ground surface to the bottom of the dug well;

- (A) The ground surface elevation level above sea level; can be calculated by the Digital Elevation Model (DEM) of the study area;

- (B) The water table level above sea level - is the upper surface of the saturated zone; it can be calculated by subtracting the water depth (a) from the ground surface elevation (A); and

- (C) The dug well depth level above sea level; can be calculated by subtracting the dug well depth (c) from the ground surface elevation (A).

Table 11. Data from the 29 dug wells inventoried in the study area (adapted from Carteado Mena, 1908; Freitas 2010).

Well No.	X coordinate	Y coordinate	Air Temperature, °C	Water Temperature, °C	Water Depth (a), m	Water Column Thickness (b), m	Well Depth (c), m	Ground Surface Level above sea level (A), m	Water Table Level above sea level (B), m	Well depth above sea level (C), m
1	159800	464400	14.00	17.90	2.20	4.77	6.97	64.29	62.09	57.32
2	160000	464400	13.00	26.30	4.07	2.23	6.30	71.77	67.70	65.47
3	160100	464500	13.50	17.50	2.65	5.30	7.95	83.56	80.91	75.61
4	160100	464200	14.50	20.00	2.07	1.36	3.43	70.27	68.20	66.84
5	160200	464300	14.50	14.70	5.43	1.38	6.81	79.14	73.71	72.33
6	160200	464500	16.50	16.00	3.80	1.65	5.45	79.33	75.53	73.88
7	160300	464400	17.00	14.90	5.46	1.70	7.16	86.37	80.91	79.21
8	160300	464600	14.50	14.80	8.85	1.50	10.35	89.85	81.00	79.50
9	160400	464600	17.50	15.70	8.07	0.43	8.50	92.25	84.18	83.75
10	160400	464600	16.00	15.20	9.75	1.10	10.85	94.73	84.98	83.88
11	160200	464900	14.00	15.60	8.55	1.30	9.85	93.86	85.31	84.01
12	159900	464900	13.50	15.40	2.02	3.15	5.17	96.45	94.43	91.28
13	160400	464700	15.50	15.80	1.70	10.55	12.25	99.70	98.00	87.45
14	160300	467400	16.50	15.60	4.05	0.68	4.73	119.91	115.86	115.18
15	160300	467300	15.50	15.50	5.35	0.71	6.06	116.85	111.50	110.79
16	160200	466900	19.00	14.80	15.78	0.97	16.75	130.42	114.64	113.67
17	159900	466700	18.50	14.40	7.73	1.76	9.49	120.53	112.80	111.04
18	160300	466700	20.00	14.90	24.25	0.32	24.57	143.30	119.05	118.73
19	159800	466200	19.00	15.00	12.20	2.20	14.40	132.72	120.52	118.32
20	159500	466400	17.00	14.60	23.50	0.25	23.75	132.22	108.72	108.47
21	159600	466400	17.00	15.40	16.30	0.50	16.80	130.12	113.82	113.32
22	159900	466000	16.50	15.00	8.42	0.36	8.78	139.88	131.46	131.10
23	159700	465700	16.00	15.00	23.70	1.70	25.40	140.73	117.03	115.33
24	160000	465400	17.00	14.90	7.20	1.25	8.45	119.36	112.16	110.91
25	160200	465500	18.50	15.80	7.23	1.43	8.66	129.06	121.83	120.40
26	160200	465700	21.00	14.40	9.52	1.63	11.15	144.25	134.73	133.10
27	160300	465700	15.00	14.60	8.92	1.60	10.52	144.37	135.45	133.85
28	159900	465800	19.00	15.00	14.25	0.65	14.90	140.08	125.83	125.18

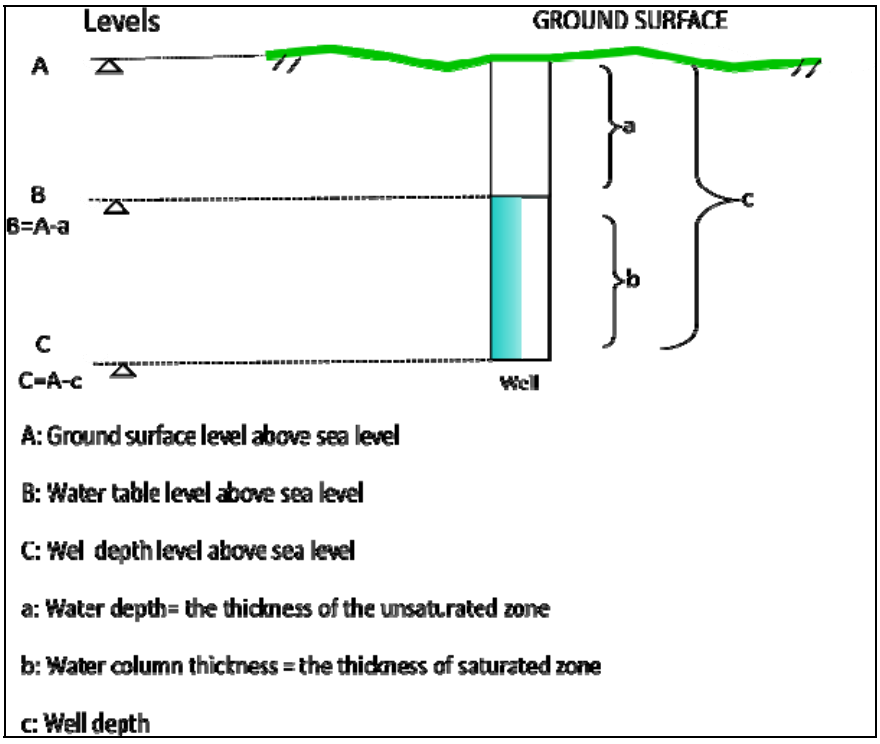

Figure 32. Some of the parameters measured and calculated in each dug well.

An important and special note must be emphasized on this point. Since groundwater was being tapped mostly through the age-old practice of hand-dug well structures, the depth of dug wells (c) was controlled by the thickness of the weathered zone, so this length represents the minimum thickness of the weathered layer of the fissured granite.

Therefore, considering the geological units in the study area, it was possible to evaluate the thickness of the top layer, alluvia, and saprolite deposits, as well as the thickness of the weathered layer of the fissured granite (Figure 33).

The kriging interpolation process in ArcGIS Pro was used for mapping the thickness of the fissured layer, the water table levels, the thickness of the unsaturated zone, and the thickness of the saturated zone using the dug wells data in the study area (Carteado Mena, 1908) (Figure 33 and Figure 34).

According to Afonso et al. (2016), the thickness of the top layer, alluvia, and saprolite deposits is around 3 meters (Figure 33B). According to the dug wells data, the estimated thickness of the fissured layer is between 0.18 m and 19 m (Figure 33C), the predicted water table levels above sea level are between 32 m and 136.6 m above sea level (Figure 34A), the estimated thickness of the unsaturated zone is between 2.8 m to 19 m (Figure 34B), and for the saturated zone is between 0.28 m to 9.7 m (Figure 34C).

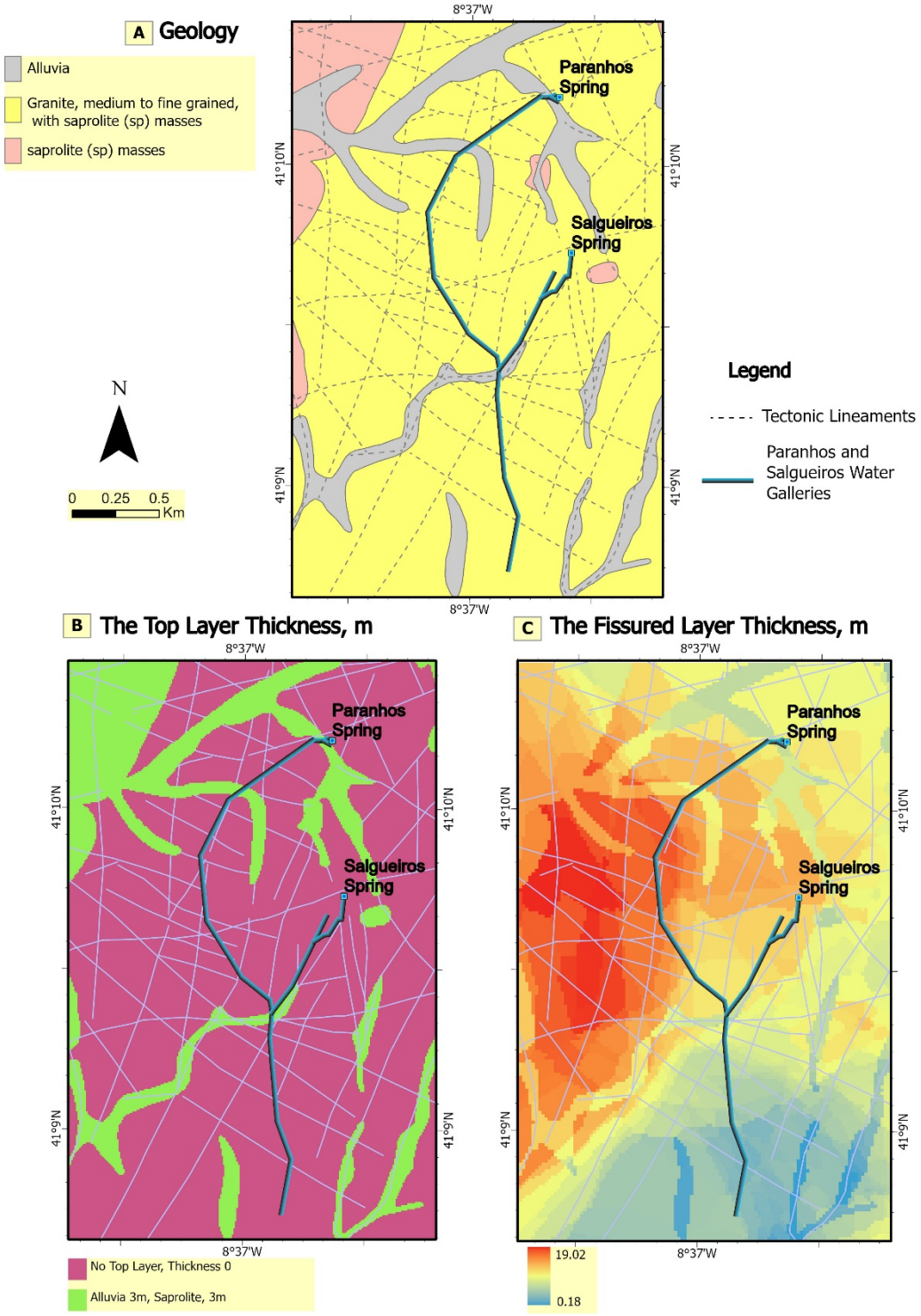

Figure 33. (A) Geological units of the study area; (B) The thicknesses of the top layer (m); and (C) The thickness of the weathered layer of the granite (m).

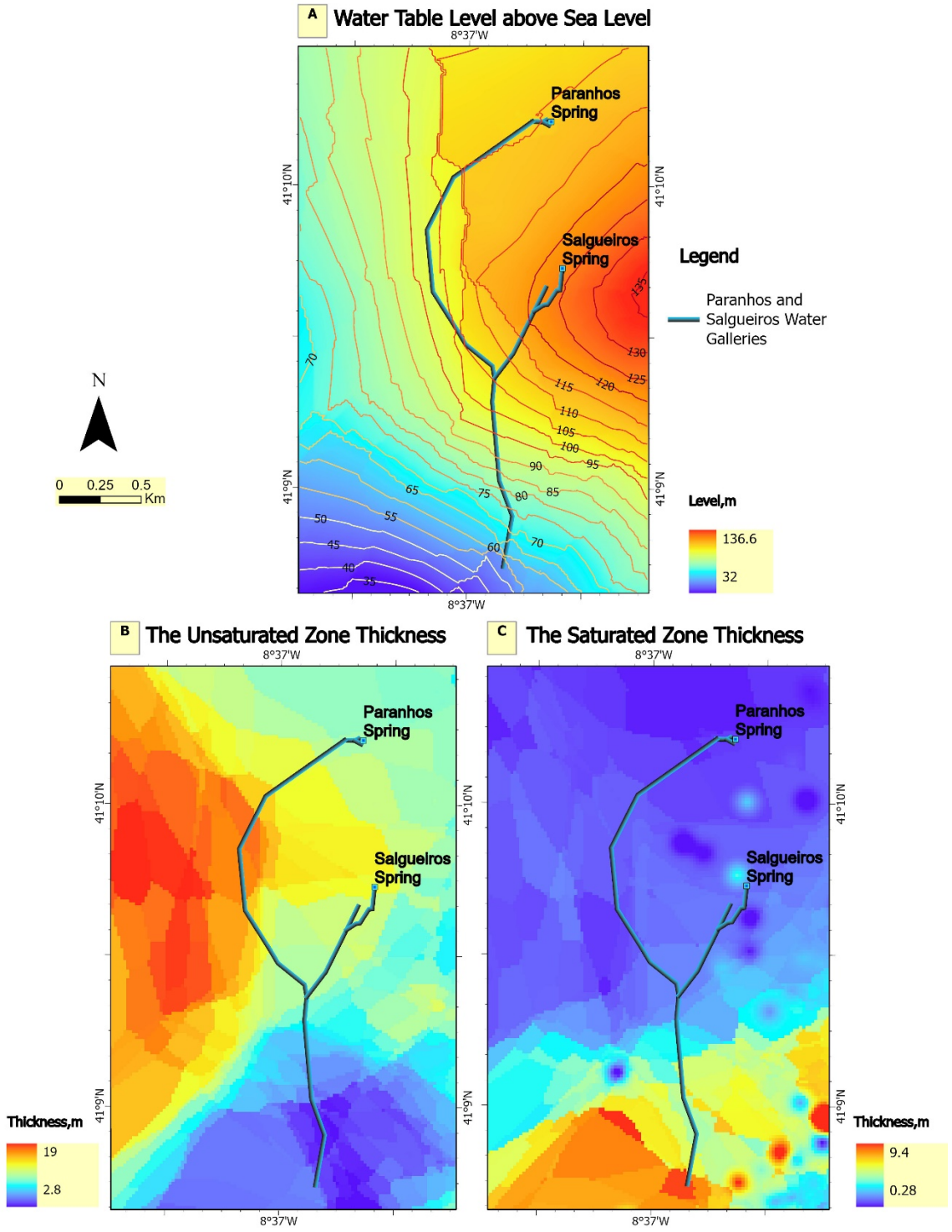

Figure 34. (A)Water table levels (m); (B) The thicknesses of the unsaturated zone (m); and (C) The thickness of the saturated zone (m).

3.6.1.2. Land use data preparation

To evaluate the spatiotemporal changes in land uses between the past and present-day, two different maps that represent the land use types in the XIXth century and XXIst century were used.

In the XIXth century, a topographic map of Porto, the Carta Topographica da Cidade do Porto (1:5.000 scale) from 1892, was used, which was the first map of Porto presenting an accurate

representation of its administrative boundaries, drafted under the responsibility of Telles Ferreira (Telles Ferreira, 1892; Madureira, 2001; Madureira et al., 2011). Four categories of green areas were defined and vectorized on the original map: agricultural and green areas, green areas related to edification, public gardens and urban areas, outcrops, and streets/roads. In the XXIst century, a multiscale digital map in 2018 was used (adapted from IGP, 2010; Caetano et al., 2009).

3.6.1.3. Vertical travel time factors preparation:

Vertical travel time (t_v) in the unsaturated zone heavily depends on the unsaturated zone. Several parameters, such as precipitation, evapotranspiration, runoff, vegetation, soil, overlaying rocks, and many others, impact recharge processes and should be assessed too. The two main factors, travel time (TIME) and recharge (INPUT), are combined by the simple equation (Kralik & Keimel, 2003):

$$Vulnerability = Time\ [s] * Inputs\ [factor\ based\ on\ recharge\ (mm)]$$

TIME Factor:

In the study area, the basic data to calculate the TIME Factor, which represents the travel time from the ground surface to the saturated zone, are the thickness and the hydraulic conductivity of each layer of the unsaturated zone. The mean travel time can be calculated by dividing the thickness by the hydraulic conductivity of the layers. Information about the tectonic lineaments is also important as the hydraulic conductivity will be much enhanced by faults in hard-rock aquifers (Kralik & Keimel, 2003).

The thickness of the layers and their hydraulic conductivity (k-values) were estimated from the geological map and previous studies (e.g. Afonso et al., 2016).

There are two main layers in the study area. The bottom layer is the fissured layer, and the top layer covers the fissured layer in some places and consists of either saprolite or alluvia. The surface soil is so thin and absent in most of the area, so its effect on the travel time was ignored. Table 12 explains the geological layers in the study area with their thickness and hydraulic conductivity.

Table 12: Geological layers in the study area, thickness, and hydraulic conductivity (Adapted from Afonso et al., 2016).

Layers	Thickness (m)	Hydraulic conductivity, K (m/d)
Alluvia	3	1.5
Saprolite	3	0.1
Fissured granite	0.18 – 19	1.0

The TIME factor = The thickness of layer / hydraulic conductivity

Regarding the discontinuities parameter (Figure 35), most of the area is characterized by low permeability, and most discontinuities have a slow connection to the springs. Therefore, lineaments will enhance the hydraulic conductivity in the bedrock strata. Therefore, a correction factor according to tectonics was applied (Table 13). Because most of the area is characterized by low permeability, and most discontinuities have a slow connection to the springs (Meerkhan et al., 2021), the lineaments were classified and ranked according to their connectivity to the springs and line density.

Table 13. Tectonic lineaments correction factor

Lineament density (km/km^2)	Rank	Correction Factor
0-39	1	1
39-112	2	5
112-185	3	10
185-271	4	15
271-432	5	20

INPUT Factor

To calculate INPUT Factor (the recharge), the Urban Infiltration Potential Index (IPI-Urban) in urban areas was used (Freitas et al., 2019a) (Figure 22). An integrated approach of Geographical Information System (GIS) and Analytical Hierarchy Process (AHP) was used for geospatial mapping of groundwater (IPI-Urban) and then recharge, according to the following steps:

i. Defining the influencing parameters according to the period of the study. Several factors influence groundwater recharge in urban areas. In the XIXth century, five parameters were used to define the potential recharge areas: hydrogeology/geology, slopes, land use, tectonic lineaments density, and drainage network density. Three more parameters were used in the XXIst century after the urban expansion in addition to the five ones used in the XIXth century, which are stormwater network, sewers network, and water supply network;

ii. Calculating the weights of the influencing parameters. For the first period (XIXth century), an Analytic Hierarchy Process (AHP) was used to determine the priorities of variables using an open-source Excel-based software version 15.09 of Goepel (2018) (Table 14), while for the second period (XXIst century), the weights were adapted from (Freitas et al., 2019a) (Table 15); and

iii. Finally, ArcGIS Pro was used to produce the final groundwater (IPI-Urban) map and the urban recharge map.

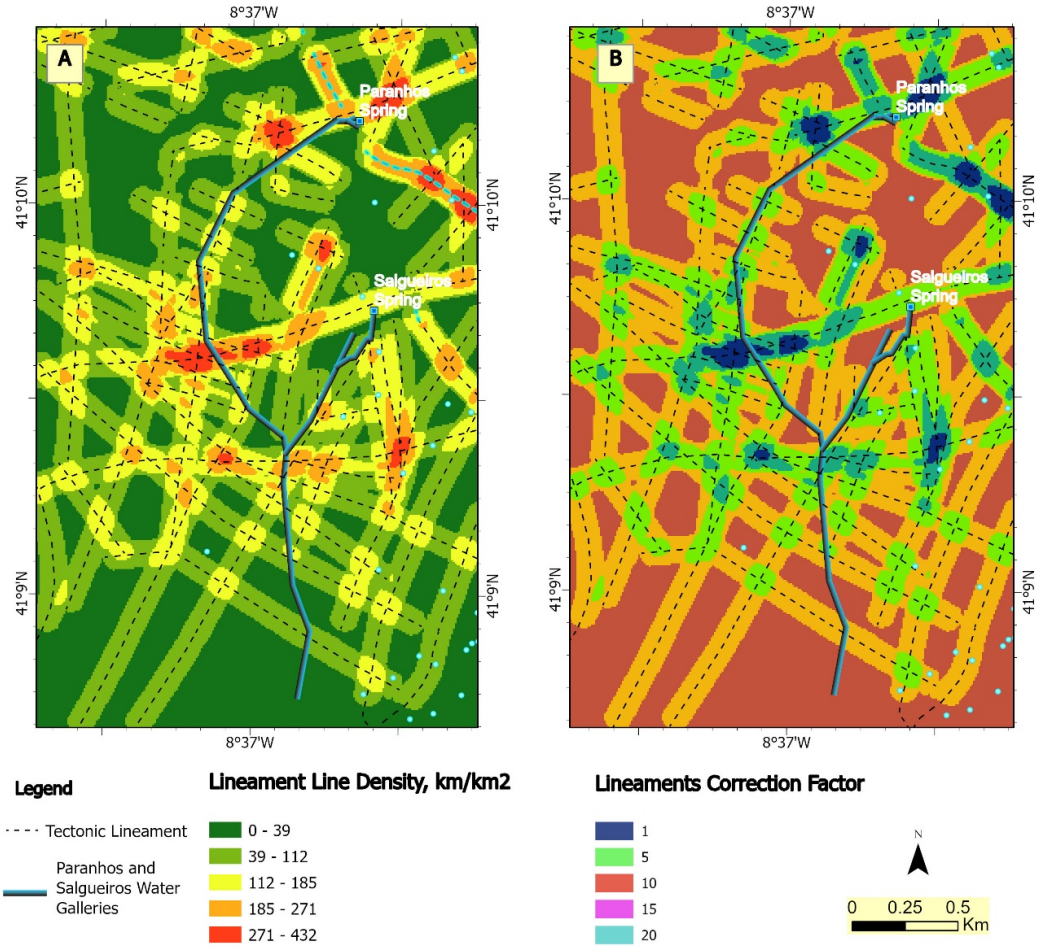

Figure 35. Tectonic lineaments in the study area. (A) tectonic lineaments density; (B) Tectonic lineaments correction factor.

Table 14. Weights assigned for different groundwater potential infiltration control parameters in the XIXth century.

Parameter	Classes	Weight	Influence %	Rank
Hydrogeology / Geology	Alluvia	0.41	41	5
	Granite, medium to fine-grained			3
	Saprolite			1
Slopes (°)	0-2.9	0.11	11	5
	2.9-5.9			4
	5.9-10.4			3
	10.4-16.7			2
	16.7-35			1
Drainage density (km/km^2)	0-2.4	0.12	12	1
	2.4-7			2
	7-12			3
	12-19			4
	19-38.6			5
Land use/cover	Urban areas, outcrops, and streets/roads	0.19	19	1
	Agricultural and green areas			5
	Green areas related to edification			4
	Public gardens			4
Tectonic lineament density (km/km^2)	0-39	0.17	17	1
	39 -112			2
	112-185			3
	185-271			4
	271-432			5

Table 15. Weights assigned for different groundwater potential infiltration control parameters in the XXIst century.

Parameter	classes	weight	Influence %	Rank
Hydrogeology	Alluvia	0.23	23	5
	Granite, medium to fine-grained			3
	Saprolite			1
Slopes (degree)	0-2.9	0.13	13	5
	2.9-5.9			4
	5.9-10.4			3
	10.4-16.7			2
	16.7-35			1
Drainage density (km/km^2)	0-2.4	0.05	5	1
	2.4-7			2
	7-12			3
	12-19			4
	19-38.6			5
Land use/cover	Urban areas, outcrops, and streets/roads	0.16	16	1
	Agricultural and green areas			5
	Green areas related to edification			4
	Public gardens			4
Tectonic lineament density (km/km^2)	0-39	0.16	16	1
	39 -112			2
	112-185			3
	185-271			4
	271-432			5
Storm Water Network (km/km^2)	0-7.06	0.13	13	1
	7.06-14.84			2
	14.48-22.61			3
	22.61-32.26			4
	32.26-60			5
Water Supply Network density (km/km^2)	0-10.2	0.06	6	1
	10.2-21.1			2
	21.1-31.97			3
	31.97-45.5			4
	45.5-84			5
Sewers Network (km/km^2)	0-5.91	0.06	6	1
	5.91-14.21			2
	14.21-22.02			3
	22.02-32.2			4
	32.2-60.38			5

Then, the INPUT factor maps were produced following recharge rates, as the author of the TIME–INPUT method suggested. As a result, three classes of INPUT factors were assigned (1.0, 0.75, and 0.5). Recharging quantities that are low have high correction factors, which increases time. Recharging quantities that high reduce time, which causes an increase in vulnerability.

TIME-INPUT Factor

The TIME-INPUT Factor or the vertical travel time was calculated by combing both factors, the travel-time (TIME; about 60%) and the recharge (INPUT; about 40%), giving the travel time slightly higher importance than the groundwater recharge (Kralik & Keimel, 2003).

3.6.1.4. Surface travel time factors preparation:

Surface water can be rapidly transported to the sinking zones in aquifers, and potential contaminants' travel time to the springs needs to be assessed. There are many methods available to estimate the surface travel time or time of concentration which is a concept used in hydrology to measure the response of a watershed to a rain event and is defined as the time needed for water to flow from the most remote point in a watershed to the watershed outlet. It is a function of the topography, geology, and land use within the watershed. The NRCS Velocity method (Fang et al., 2007; Staff, 2010) is one of the most used methods for determining the time of concentration (see description in section 2.9.2.1).

It was assumed that the flow in the study area is Shallow Concentrated Flow. The flow length and velocity are the main factors affecting surface travel time. The flow length is estimated using ArcGIS Spatial Analyst Hydrology Tools. A Digital Elevation Model (DEM) and the flow direction raster must be prepared first. Then, using the Flow Length tool creates a raster where each pixel value represents the upstream length L of the flow.

The runoff type, flow depth, surface roughness (n), and slopes (s) control the flow velocity. Table 16 contains the equations used for velocity calculation as described in section 2.9.2.

Table 16. The equation for velocity estimation according to land use types (Staff, 2010).

Land use	Velocity Equation
Urban areas, outcrops, and streets/roads	$V=20.238\ (S)^{0.5}$
Agricultural and green areas	$V=5.032(S)^{0.5}$
Green areas related to edification	$V=16.135(S)^{0.5}$
Public gardens	$V=6.962(S)^{0.5}$

3.6.1.5. Horizontal travel time factors preparation:

Horizontal travel predominates when infiltrated water or potential contaminants reach the saturated zone, and the travel time to the groundwater source should be analyzed.

The main factors that affect the horizontal travel time in the saturated zone and the flow velocity are controlled by the aquifer type, porosity, hydraulic gradient, and hydraulic conductivity.

The mutual relationship between matrix and channel flow systems, which can be described as inverse flow, was partially ignored, and the duality of groundwater flow was presented as the result of the drainage of small fissures and the matrix system into the channel system. Travel times from the matrix system to the nearest fractures were estimated using the Euclidian

Distance tool in ArcGIS Pro Spatial Analyst. The initial values of 1m/day for matrix flow velocity were taken from Devlin (2020).

3.6.1.6. Total travel time data preparation

The total travel time of surface and groundwater flow, and likewise potential contaminants from the ground surface to the springs, can be estimated as follows (Živanović et al., 2016):

- For flow in the matrix system of the fissured layers, it equals the sum of vertical and horizontal travel time; and
- For flow in channels and fractures/fissures, it equals the sum of the surface travel time in the catchment of the fracture/fissure and the horizontal travel time in the fracture/fissure.

3.6.2. Analysis and development

The creation and manipulation of data elements, as a design and build function, is closely associated with the data collection process. Information collected is either in a raw format that requires extraction or is available in a digital format that can be tailored to the specific requirement of the model parameters.

From this point forward, GIS tools are used almost exclusively to integrate model elements for analysis and display. The analysis and development methodology includes: i) Database creation, ii) Manipulating elements, and iii) Model building.

3.6.2.1. Database creation

Before geographic data can be used in a GIS, the data must be converted into a suitable digital format. The process of converting data from paper maps or aerial photographs into computer files is called digitizing (ESRI, 2021a). Modern GIS technology can automate this process fully for large projects using scanning technology; smaller jobs may require manual digitising, requiring a digitizing table. Creating databases for representation within a GIS is accomplished by compiling data from several dissimilar sources into a common format or editing GIS point and vector attribute tables (ESRI,2021b). An attribute table is a tabular file that identifies geographic features as rows and attributes of that feature in columns. A well, for example, as a geographic feature, may consist of several columns of attributes (e.g., depth, location, aquifer media) that make up the information for a particular well. The second case of database creation is accomplished by editing the attribute tables within existing GIS vector files. A database has been created for each type of travel time in this study area.

3.6.2.2. Manipulating data

Data manipulation is taking data and applying logic or computations to it to get a different collection of data than the original. GIS must manipulate data because different maps have different projections and formats. The projected coordinate system defines spatial reference for all data elements: Lisboa Hayford Gauss IGeoE. Data elements exist in GIS point, vector, and raster formats. Manipulation of individual elements produces the integrated model that is the focus of this investigation. To create this integrated model, databases undergo various transformations. The tools within the GIS perform the geoprocessing operations required to produce layers that represent the model elements (Zhen et al., 1993).

Familiarity with software functionality and individual data files within this study area dictates the strategy for data manipulation. The Spatial Analyst extension within the ArcGIS software package provides many operation selections for manipulating the elements (ESRI, 2021c). In the case of well locations that exist as GIS point files, the kriging spatial interpolation technique is used to transform depth to the water information into a continuous surface. In addition to the kinging functionality, many other analysis tools were used, like the surface analysis tool for calculating the per cent slope from a Digital Elevation Model (DEM) of the study area, the Line Density tool to calculate the density of linear features in the neighbourhood of each output raster cell, the Hydrology tools to model the flow of water across a surface, the spatial analyst tools to calculate, for each cell, the Euclidean distance to the closest source, etc.

3.6.2.3. GIS models building

This study involves intensive spatial data processing, where the logical sequence of tasks (geoprocessing workflows) must be performed and documented. GIS technology is essential in this effort, providing geoprocessing tools to perform the necessary spatial analyses. GIS spatial models make the process easier as they automate the workflows by connecting tasks and processes together; they allow executing a workflow, modifying it, and repeating it multiple times with one click of the mouse, making it easier to manage the workflow and increasing the efficiency of geoprocessing (Goodchild, 2005).

The geoprocessing tools in GIS allow spatial analysis and managing data, while the ModelBuilder in GIS is used to create, edit, and manage geoprocessing models that automate those tools (ESRI, 2021d). Therefore, conversion to a raster format for all vector data is necessary to integrate the model elements within the GIS. First, the cell size of the model raster is defined. Then, since the input layers will be in different numbering systems with different ranges, to combine them in a single analysis, each cell for each criterion must be reclassified into a common preference scale,

such as 1 to 5, with 5 being the most favorable. Finally, the data layers representing each model element will be combined using the ArcGIS Spatial Analyst extension (ESRI, 2021c).

3.6.2.4. Modelling the *Time* factor (Travel time)

The model diagram represents a geoprocessing workflow with one or multiple processes strung together. Each process consists of a tool and its parameter values (e.g., input and output data, reclassification table). The model components, or elements, are represented in the Model Builder interface by different symbols: inputs as blue ovals, outputs as green ovals, tools (operations to be performed on the input data) as yellow rectangles, and connecting arrows that indicate the processing sequence, and text labels that explain the model

The model for estimating the Time factor was developed with the following steps (Figure 36):

- ✓ Calculating the travel time in the top layer using the raster calculator tool;
- ✓ Calculating the travel time in the fissured layer using the raster calculator tool;
- ✓ Calculating the tectonic lineament correction factor using line density and reclassifying spatial analyst tools; and
- ✓ Calculating the total travel time using the raster calculator tool.

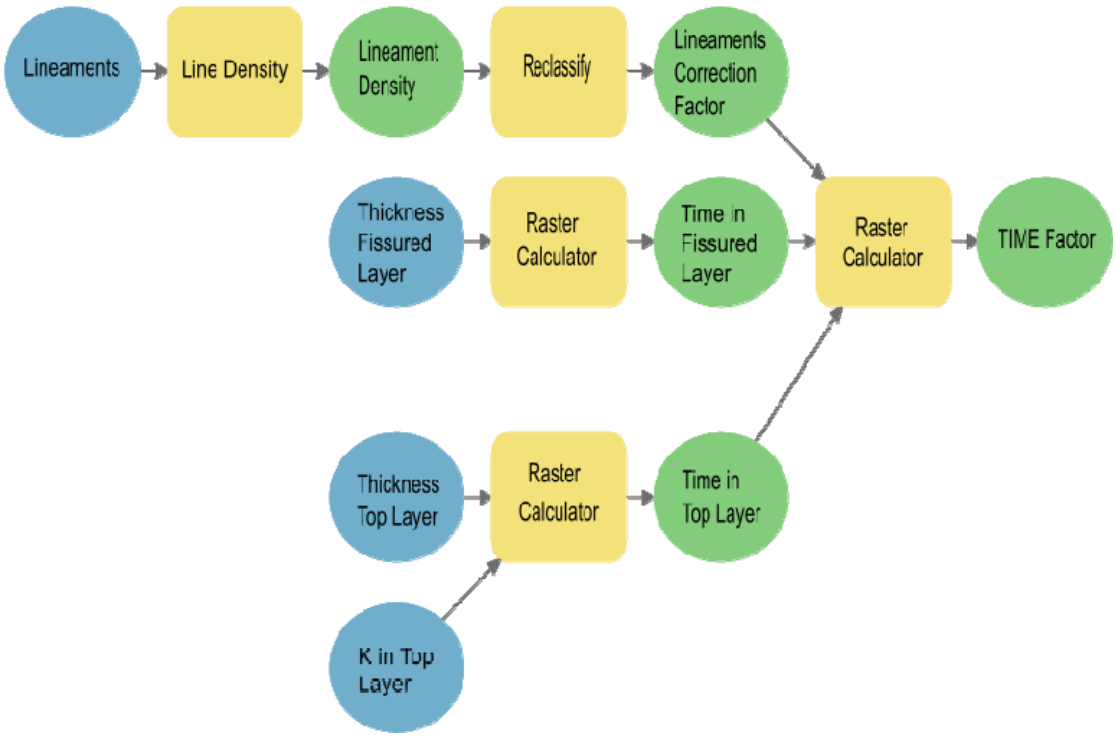

Figure 36. GIS model for estimating Time Factor.

3.6.2.5. Modelling *the recharge (INPUT Factor)*

The diagrams in Figure 37 and Figure 38 show the GIS models used to calculate the recharge and INPUT factor as a correction to travel time in the XIXth and the XXI^{st,} respectively. The number of influencing factors is the only difference between the two models. Each model contains the following steps:

- ✓ Calculating the line density for the vector recharge influencing factors;
- ✓ Reclassifying the recharge influencing factors using the reclassify tool;
- ✓ Combining the factors using the weighted overlay tool to calculate the IPI-Urban;
- ✓ Calculating the recharge using the raster calculator tool; and
- ✓ Reclassifying the recharge and calculating the recharge correction factor.

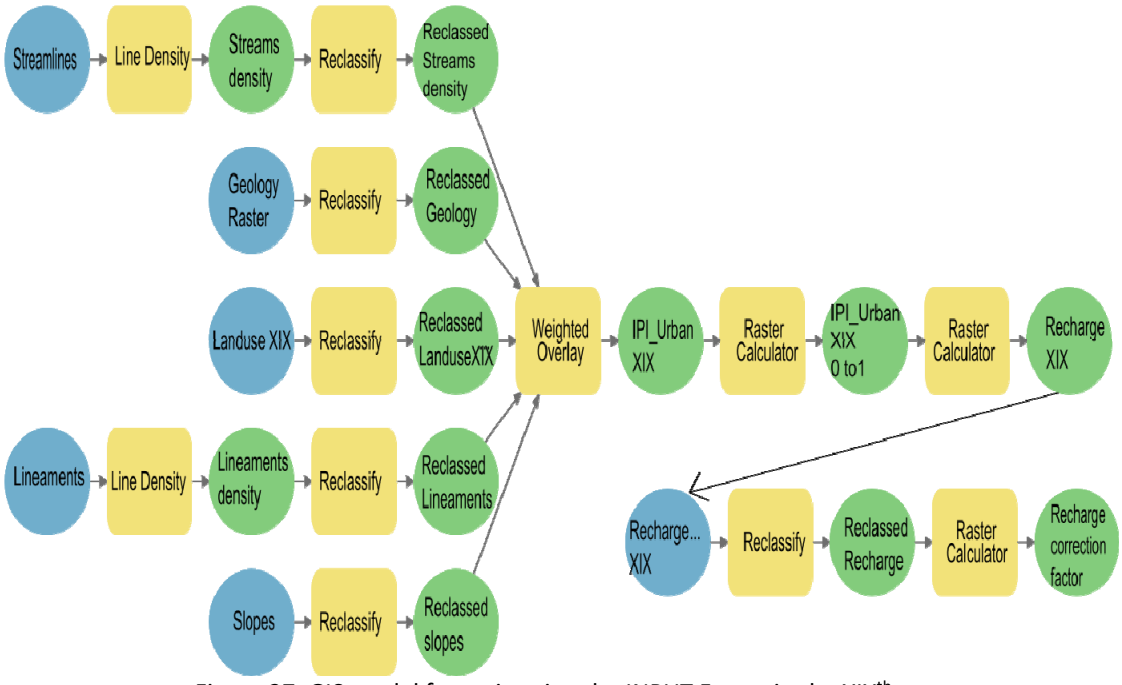

Figure 37. GIS model for estimating the INPUT Factor in the XIXth century.

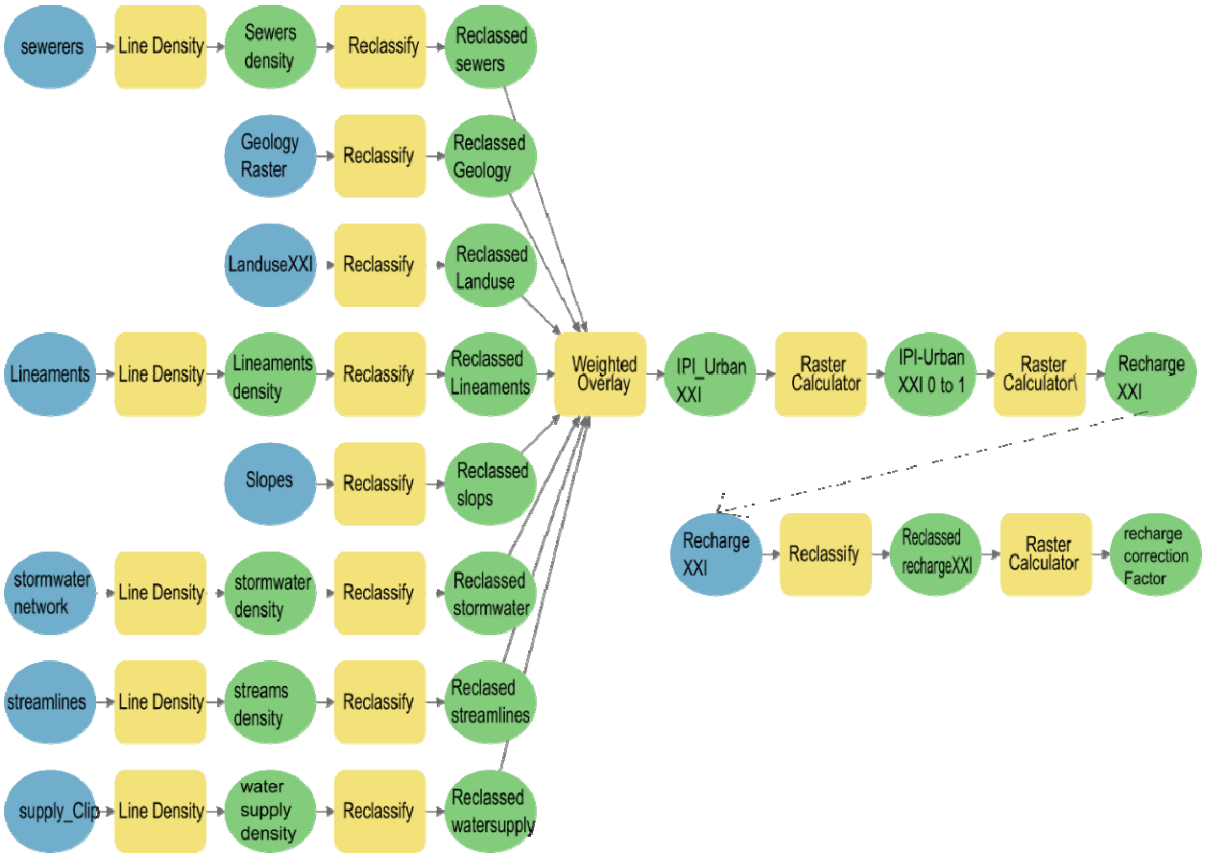

Figure 38. GIS model for estimating the INPUT Factor in the XXIst century.

3.6.2.6. Modelling *the TIME-INPUT* factor *(the intrinsic vulnerability)*

To map the Time-Input factor, the two main factors, travel time and input, are combined by the previously mentioned equation: Vulnerability =TIME*60%(s)* INPUT*40%(mm), giving the travel-time slightly higher importance than the groundwater recharge (Kralik & Keimel, 2003). Then, the Raster Calculator tool was used in ArcGIS pro to calculate the TIME-INPUT Factor (Figure 39).

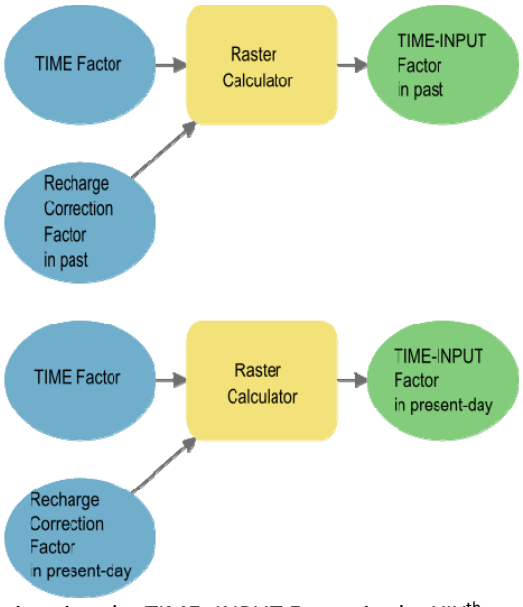

Figure 39. GIS model for estimating the TIME- INPUT Factor in the XIXth century and the XXIst century.

3.6.2.7. Modelling the *Surface travel time*

To map the surface travel time using the NRCS Velocity method, the following steps were defined (Figure 40):

- ✓ Defining the flow direction and length using the hydrological analysis tools in ArcGIS Pro Fill, Flow Direction, and Flow Length;
- ✓ Mapping the slopes of the study area using the Slope tool;
- ✓ Defining the velocity of flow using the Raster Calculator tool according to (Runoff type, Surface roughness, and land Slopes) see Table 16; and
- ✓ Finally, the raster calculator tool was used to produce surface travel time maps.

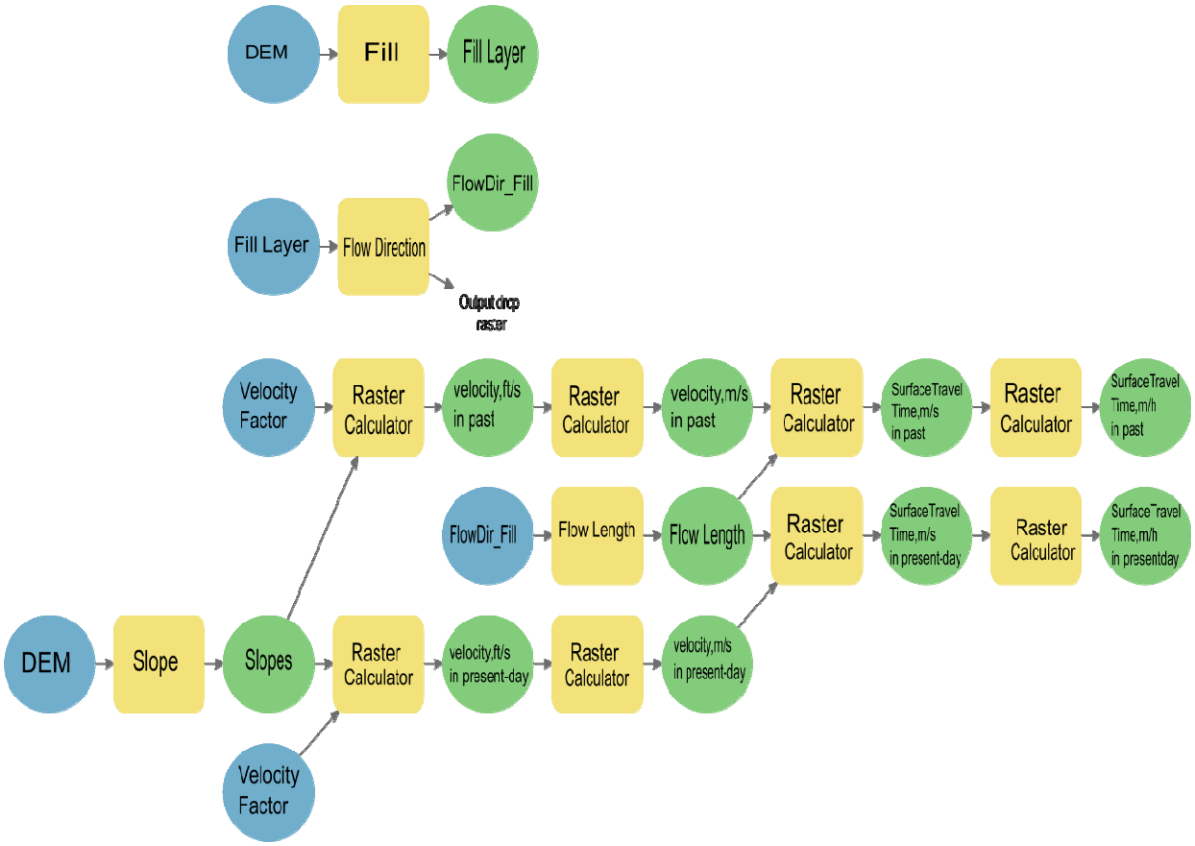

Figure 40. GIS model for estimating surface travel time.

3.6.2.8. Modelling horizontal travel time

The horizontal travel time from the matrix system to the nearest fractures was estimated using the Euclidian Distance tool in ArcGIS Pro Spatial Analyst (Figure 41). As previously mentioned, the initial values for matrix flow velocity were 1 m/day.

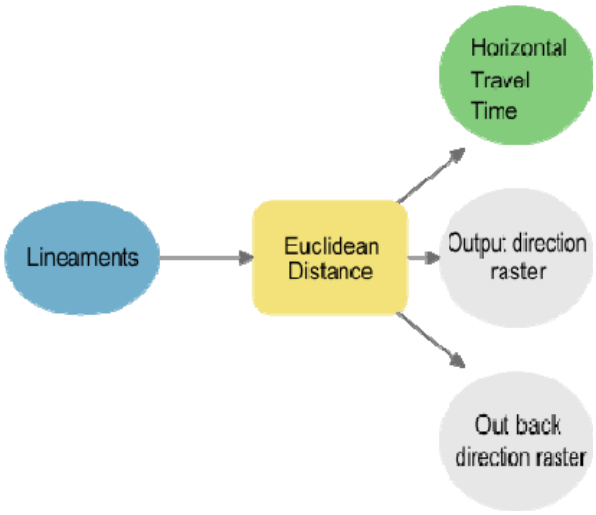

Figure 41. GIS model for estimating horizontal travel time.

3.6.2.9. Modelling the *total travel time*

The GIS model presented in Figure 42 includes using the Raster Calculator tool in ArcGIS Pro to calculate the total travel time.

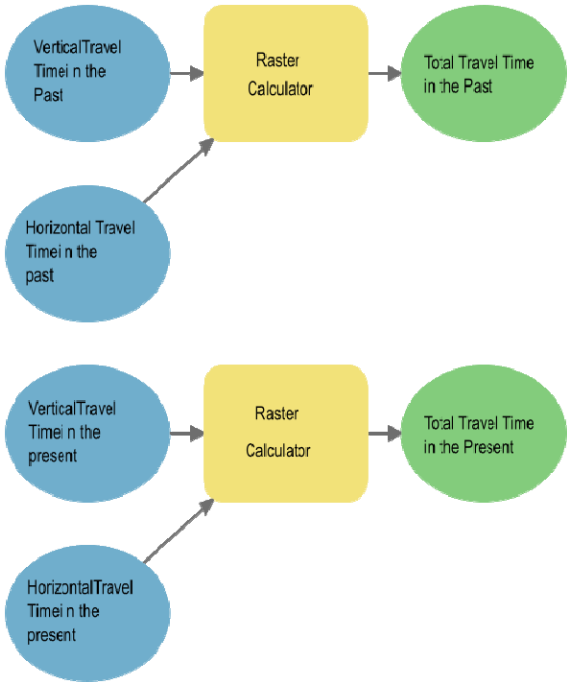

Figure 42. The total travel time model

3.6.3. Implementation

3.6.3.1. Display

ArcGIS Pro is the software package used to create models. Existing as point and vector files, the model feature for each file is converted into a raster format. Individually, each layer developed

allows for a display of how a particular element impacts the model. Adding each raster layer together using the raster calculator function provides an integrated model. Model inputs and outputs can be automatically added to the ArcMap after model execution using the “Add to Display” option (ESRI,2021d).

3.6.3.2. Assess vulnerability and safeguard zones

Vulnerability and safeguard zones assessment is the process of identifying, classifying, and prioritizing the aquifer areas of greater groundwater vulnerability from areas of lesser groundwater vulnerability. A comprehensive assessment evaluates whether the water table is exposed to known vulnerabilities, assigns severity levels to identified vulnerabilities, and recommends remediation or mitigation steps where required (Moraru et al., 2018).

In conjunction with the display of the integrated raster dataset is the assessment of the vulnerability of groundwater. Integrating the data layers results in a range of values based on the grid cell values of each element. Higher values will represent higher groundwater travel time and lower vulnerability relative to higher values. From this quantified data, a classification scheme is implemented based on the statistical grouping of data (ESRI,2021e). Classifying the data based on categories provides a useful division of values that demonstrate relative vulnerability without excessive attempts at precision (more classifications) for a region where data accuracy is variable. The potential map that emerges from the assessment methodology provides a mechanism for comparison analysis of vulnerability and safeguard zones' potential with land use practices from the past and currently in place or under consideration for future implementation.

3.6.3.3. Comparison analysis

Comparative analysis is comparing items to one another and distinguishing their similarities and differences. Given a set of maps of the same location captured at different times, the main focus of comparison analysis and change detection is to identify the significant change that has occurred over a series of maps. These significant changes contribute to the generation of the change map (ESRI,2022).

The data types used for a comparative analysis between the past and the present time include known detections of land use and land cover data, the vertical travel time factors, the horizontal travel time, and the surface travel time.

(página propositadamente em branco)

Chapter IV: Results

(página propositadamente em branco)

4.1. Land use changes in the study area

The spatiotemporal study shows past land use composition and configuration changes in Porto urban area (Figure 43). Urbanization has significantly contributed to this area's rapid land use change (Table 17). Large urban areas have replaced agriculture lands within the study period. Agricultural areas of 35.4% in 1892 were reduced to 0.6% in the present day. On the other hand, urban land use has significantly increased from 45.4% in the past to 92% in the present time. Meanwhile, green areas related to edification decreased by 15.6% due to increasing urban land use in this region, while public garden areas increased by 3.8%.

Table 17. Land use changed between 1892 and the present day.

Land use Classes	1892		Present day		Land use changes	
	Area (km^2)	Area (%)	Area (km^2)	Area (%)	Area (km^2)	Area (%)
Agricultural and green areas	2.60	35.4%	0.04	0.6%	2.56	- 34.8%
Green areas related to edification	1.37	18.6%	0.21	3.0%	1.15	- 15.6%
Public gardens	0.05	0.6%	0.32	4.4%	-0.27	+ 3.8%
Urban areas, outcrops, and streets/roads	3.33	45.4%	6.59	92.0%	-3.25	+ 46.6%

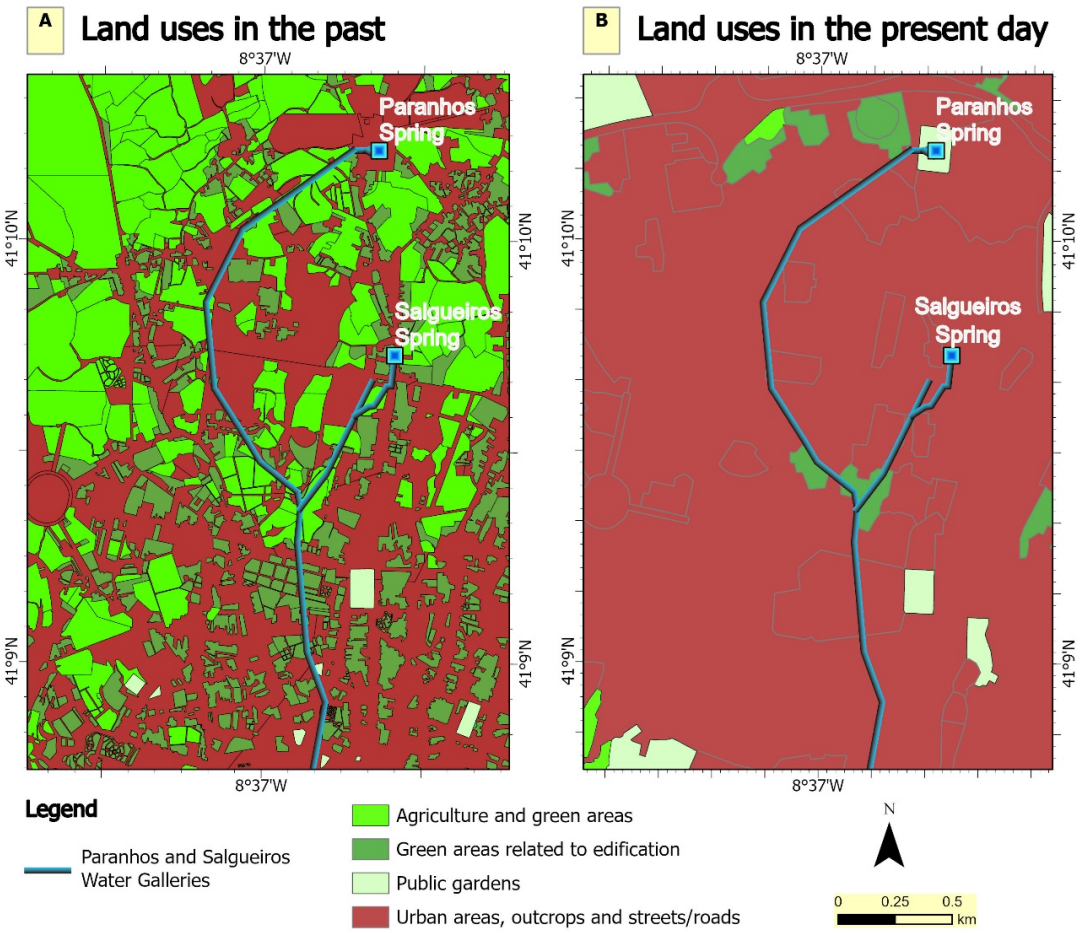

Figure 43. Land use in the surroundings of Paranhos and Salgueiros spring galleries. (A) 1892 (adapted from Telles Ferreira, 1892; Madureira et al., 2011; Afonso et al., 2016); (B) Present day (Adapted from Corine Land Cover 2006).

4.2. Spatiotemporal changes in vertical travel time (intrinsic vulnerability)

Vertical travel time components (t_v) from the ground surface to the saturated zone were estimated for each specific point (pixel) of the fissured urban area of the Paranhos and Salgueiros springs catchment in two different time scenarios before urbanization in the XIXth century and the XXIst century after the urbanization and the growth of the city.

The TIME Factor includes calculating the travel times of water flow through the soil and the cover of the unsaturated zone. The travel time of water flow through the unsaturated zone was calculated according to layers' thickness and hydraulic conductivity for each pixel in the raster map of the spring catchment.

To include the influence of tectonic structures, a correction factor was used to shorten the travel times of vertical flow using fault pattern analysis obtained by field measurements, remote sensing, quantitative geomorphologic analysis, and a DEM.

The results obtained indicate that the time factor is less than 5 days in the top layer, alluvia and/or saprolite (Figure 44A), less than 19 days in the fissured layer (Figure 44B), being the total time factor in the unsaturated zone less than 22 days (Figure 44C).

The INPUT Factor represents the groundwater recharge, and it was used as a factor to enhance the travel time. To predict the INPUT Factor, several components were considered: five parameters in the XIXth century were used to define the potential recharge areas, which are Hydrogeology/ geology, slopes, land use, lineaments density, and drainage network density. Three more parameters were used in the XXIst century after the urban expansion, and the five ones used in the XIXth century: stormwater network, sewers network, and water supply network. INPUT Factor was prepared using an integrated Geographical Information System (GIS) and the Analytical Hierarchy Process (AHP) approach.

Low recharge values have high correction factors, which increases time. High recharge values reduce time, which causes an increase in vulnerability (Kralik & Keimel, 2003).

Table 18 shows that areas with higher recharge values have decreased from 13% in the past to 2% in the present day, while the areas with lower recharge have increased.

The TIME-INPUT Factor or the Vertical travel time (t_v) was obtained by overlaying the TIME and INPUT maps and multiplying both values at each point (Figure 46). The map produced for vertical travel time (t_v) represents the study area's resource vulnerability map (TIME–INPUT method).

The results indicate that the total vertical travel time component (t_v) is less than 12 days and that areas around the tectonic lineaments are the most vulnerable as they have the lowest travel time

values (Figure 46). It is also noted that the spatiotemporal changes between the past and present-day are very small (Table 19).

Table 18. recharge change in the study area between the past in the XIXth century and the present day.

Recharge, mm	INPUT Correction Factor	XIXth century		Present day		Changes	
		Area, km^2	Area, %	Area, km^2	Area, %	Area, km^2	Area, %
> 60	0.5	0.90	13%	0.12	2%	-0.78	-11%
50 - 60	0.75	3.64	51%	4.11	58%	+0.47	+7%
17.1 - 50	1	2.54	36%	2.85	40%	+0.31	+4%

Table 19. Vertical travel time change in the study area between the past in the XIXth century and the present day.

Vertical Travel Time, days	XIXth century		Present day		Changes		Vulnerability
	Area, km^2	Area, %	Area, km^2	Area, %	Area, km^2	Area, %	
< 2	4.63	65%	4.64	65%	+0.01	0%	▲ increase
2 - 4	0.92	13%	0.79	11%	-0.13	-2%	
4 - 6	0.79	11%	0.60	8%	-0.19	-3%	
6 - 8	0.51	7%	0.63	9%	+0.12	+2%	
8 - 12	0.30	4%	0.49	7%	+0.19	+3%	▼ decrease

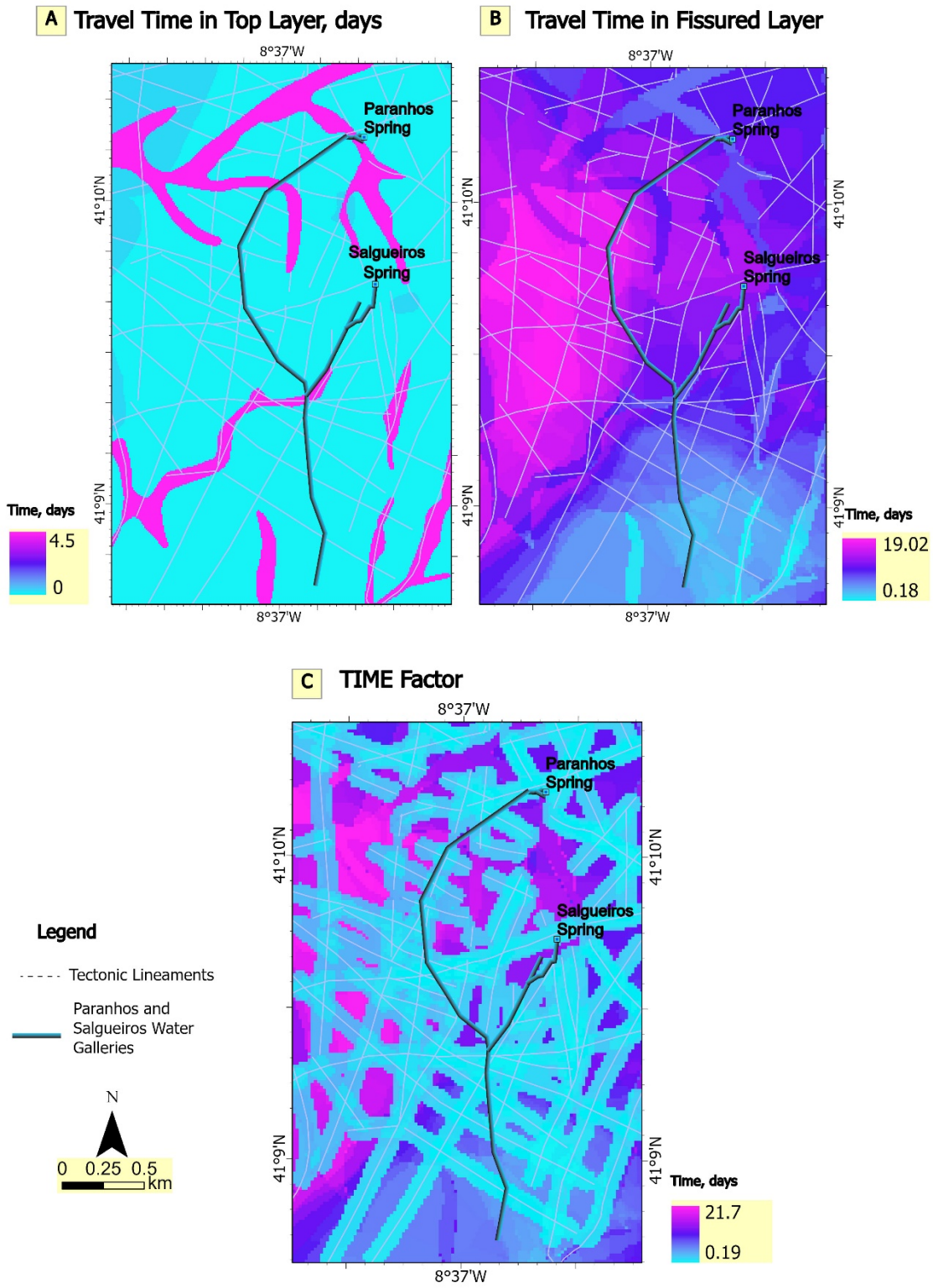

Figure 44. TIME Factors for the unsaturated zone. (A) Travel time in the top layer (days), saprolite, and alluvia; (B) Travel time in the fissured layer (days); (C) Total Time factor (days).

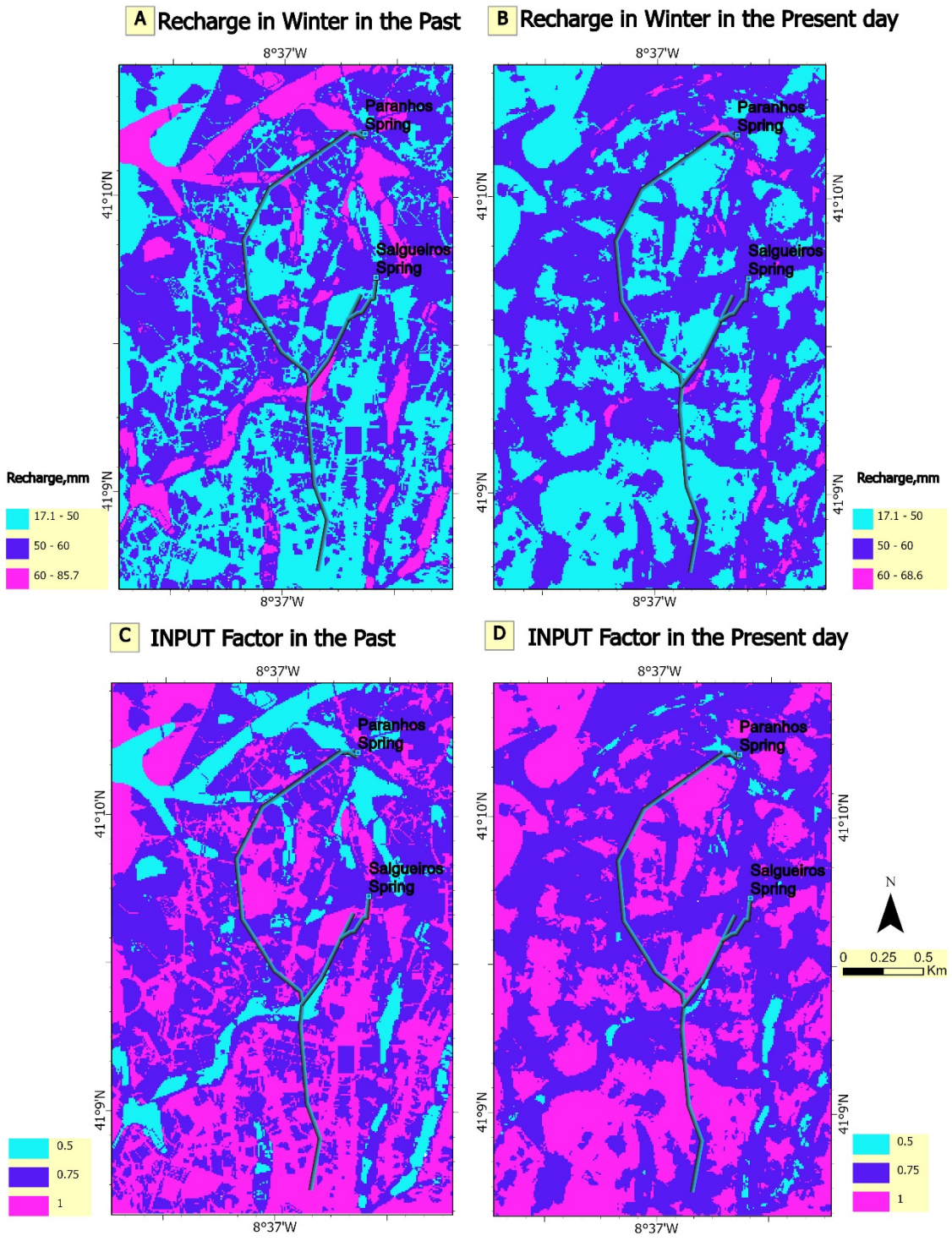

Figure 45. Recharge and INPUT Factors in the study area. (A) Recharge in the XIXth century; (B) Recharge in the XXIst century; (C) INPUT Factor in the XIXth century; (D) INPUT Factor in the XXIst century.

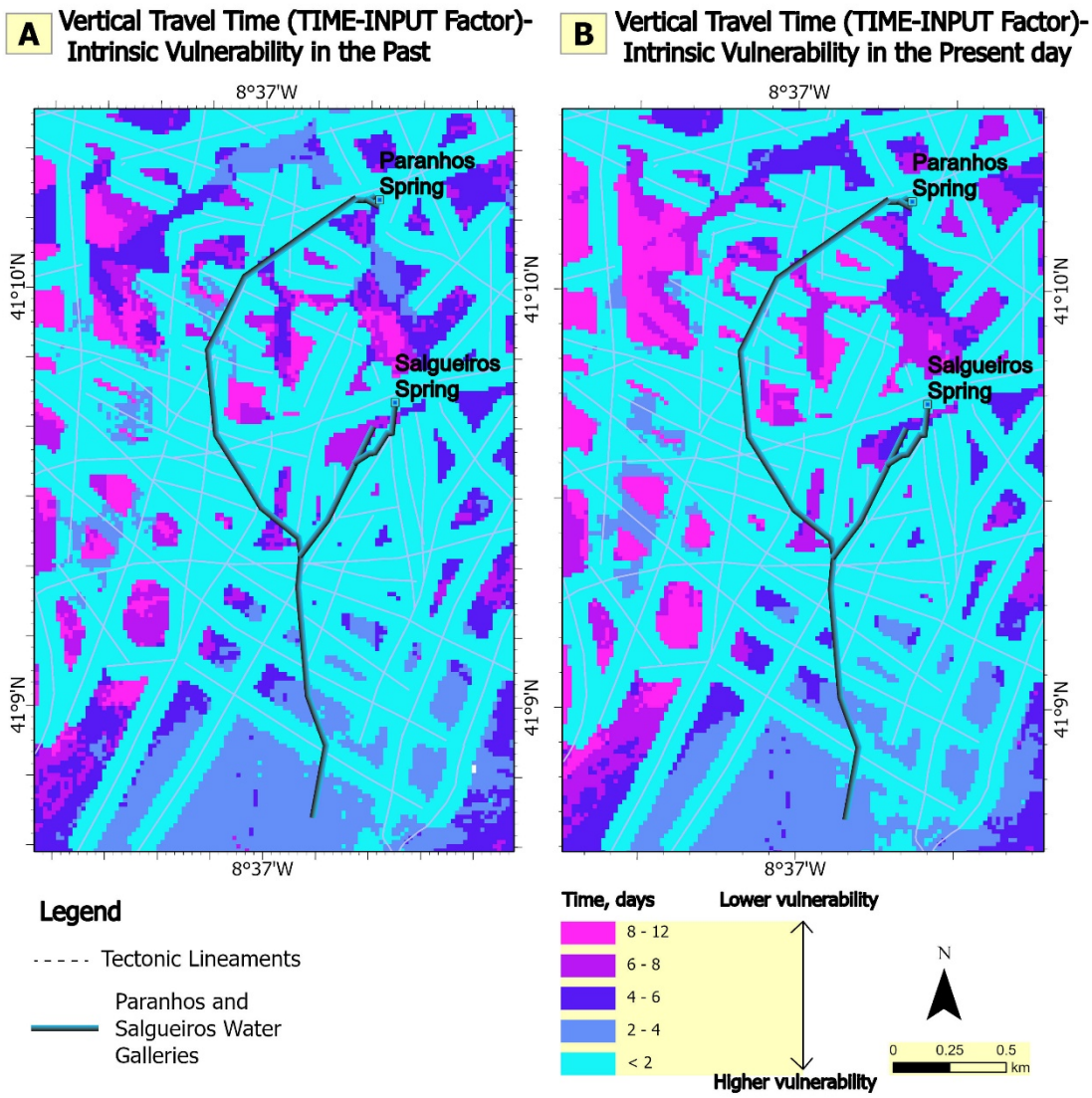

Figure 46. Vertical Travel Time (TIME-INPUT Factor) or the intrinsic vulnerability in the study area. (A) Map in the XIXth century; (B) Map in the XXIst century.

4.3. Spatiotemporal changes in surface travel time

The Surface flow travel time (t_s) represents the lateral flow from any specific point in the study area. This time component represents the shallow concentrated flow in this study area. The final map of surface travel time represents the time needed for the surface water, and thus for contaminants, to reach the springs.

To calculate the surface travel time, the flow length was calculated first. Then, the flow velocity was estimated. The results show that the flow length is up to 3620 m in the study area, and the highest values are in the streams, while most areas with low flow length, as (Figure 47A) show. Furthermore, the flow velocity in the past is between 0.18 m/s and 34.4 m/s (Figure 47B), while in the present day, it is slightly higher and between 0.32 m/s to 35.6 m/s (Figure 47C).

The map obtained for surface travel time indicates that the surface travel time in the study area takes a maximum of 1 h in the past while it only takes 0.5 h in the present time (Figure 48). This means that surface travel time becomes faster after urbanization growth. Table 20 and Table 21 show the area of each surface travel time class in the XIXth and the XXIst centuries.

Table 20. Surface Travel time in the study area in the XIXth century.

Surface Travel Time (hours)	XIXth century	
	Area, km^2	Area, %
< 0.016	6.73	94.9%
0.016 - 0.04	0.26	3.6%
0.04 - 0.06	0.05	0.7%
0.06 - 0.97	0.05	0.7%

Table 21. Surface Travel time in the study area in the XXIst century.

	XXIst century	
Surface Travel Time (hours)	Area, km^2	Area, %
< 0.01	6.77	95.5%
0.01 - 0.016	0.22	3.1%
0.016 - 0.025	0.05	0.7%
0.025 - 0.56	0.05	0.7%

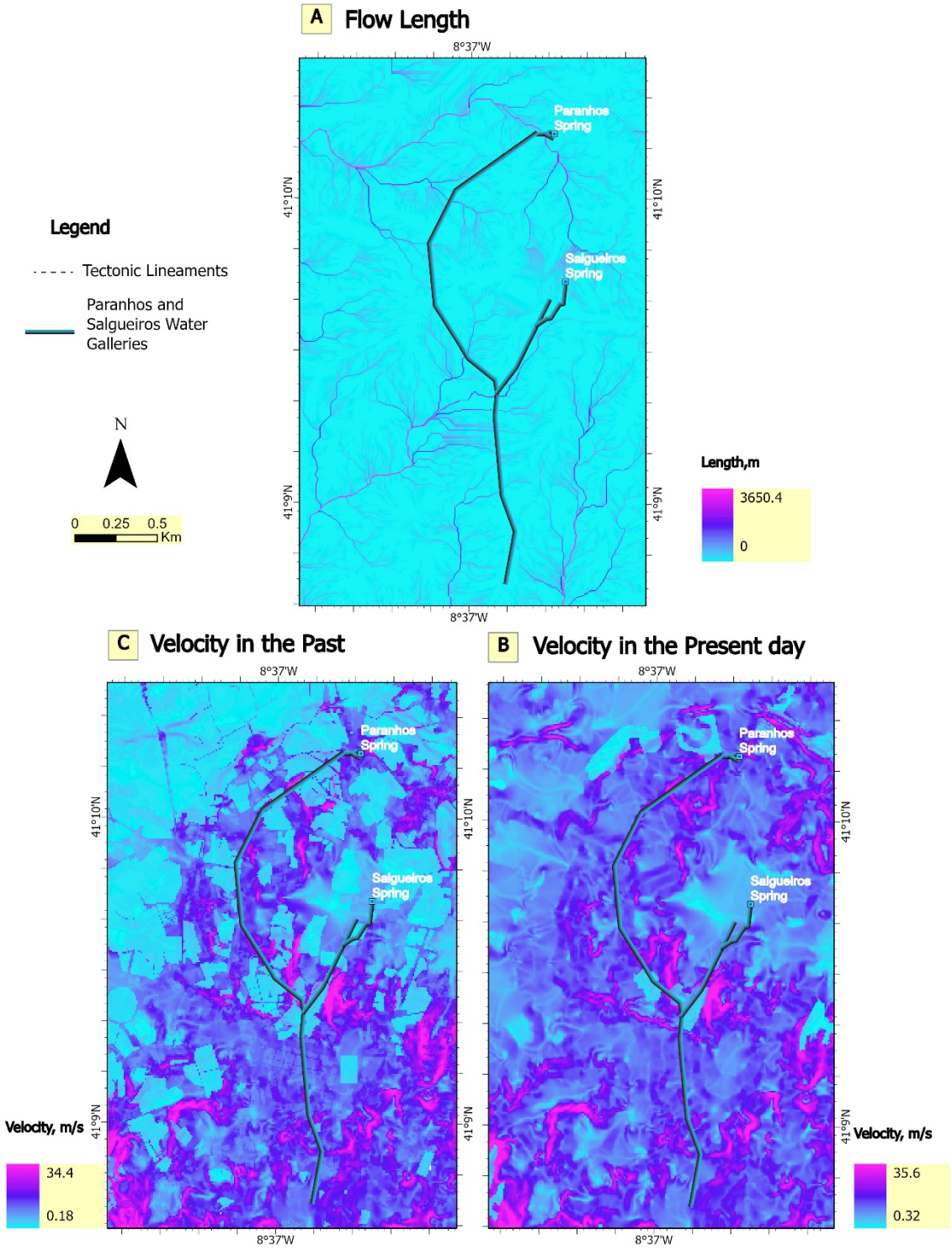

Figure 47. Flow length and flow velocity in the study area. (A) Flow length (m); (B) Flow velocity in the XIXth century (m/s); (C) Flow velocity in the XXIst century (m/s).

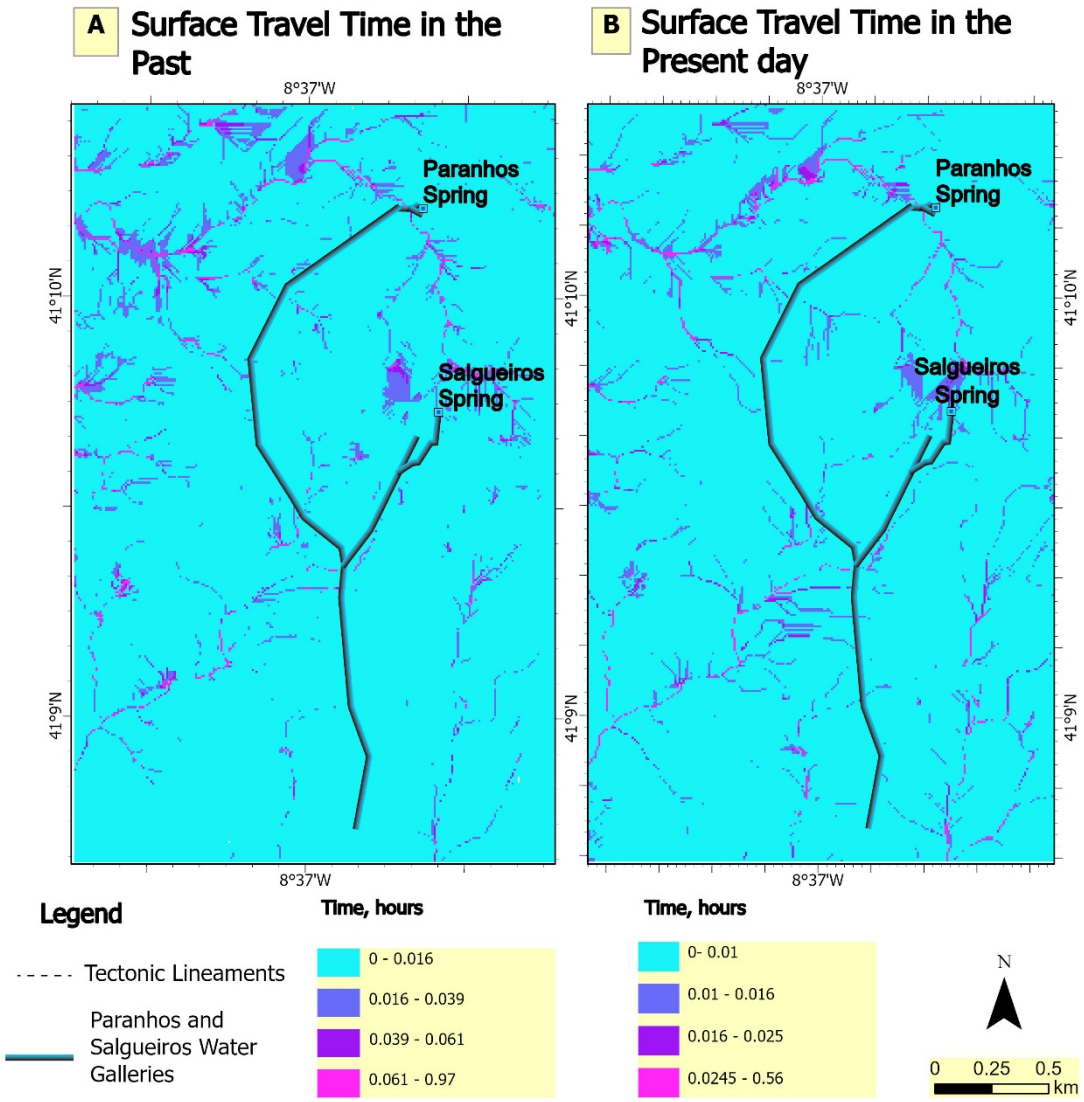

Figure 48. Surface Travel Time (h) in the study area. (A) Map in the XIXth century; (B) Map in the XXIst century.

4.4. Spatiotemporal changes in horizontal travel time

Travel times from the matrix system to the nearest fissures were estimated using the Euclidian Distance tool in ArcGIS Spatial Analyst, and an initial value of 1 m/day for matrix flow velocity was taken from Devlin (2020).

Considering that the hydrogeological characteristics of the study area have not changed between the past and the present-day, there are no spatiotemporal changes in the horizontal travel time. The results indicate that the horizontal travel time has a maximum value of 487 days, i.e., nearly 1 year and 4 months (Figure 49). Nevertheless, in most of the area, the horizontal travel time is less than 50 days, even in the surroundings of the Paranhos and Salgueiros springs.

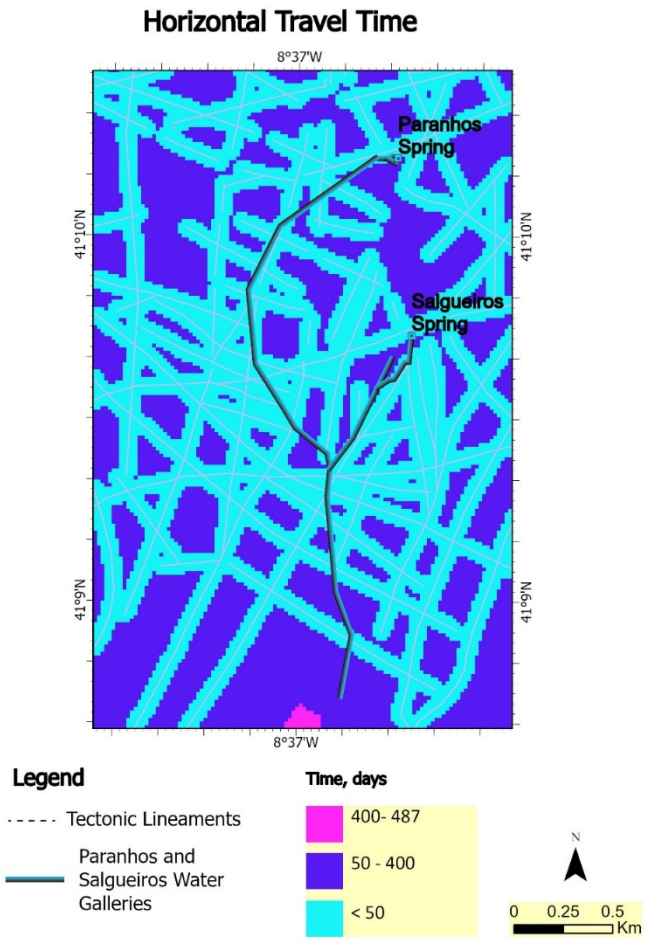

Figure 49. Horizontal travel time (days) in the study area.

4.5. Spatiotemporal changes in total travel time (safeguard zones)

By combining the vertical and horizontal travel time, the total travel time was estimated for each specific point (pixel) of the fissured urban area of the Paranhos and Salgueiros. The surface travel time was ignored here because of its small values compared to other travel time values and because the information about the watersheds of the main tectonic faults connected to the spring are missing.

The results show small spatiotemporal changes in the study area's total travel time between the past and present day. The results indicate that the total travel time has a maximum value of 489 days, i.e., nearly 1 year and 4 months (Figure 50). Nevertheless, in more than half of the area, the total travel time is less than 50 days, even in the surroundings of the Paranhos and Salgueiros springs. Table 22 shows the spatiotemporal changes in the total travel time in the study area.

Table 22. Total travel time changes in the study area between the XIXth century and the XXIst century.

Total Travel Time, days	Past		Present day		Changes	
	Area, km^2	Area, %	Area, km^2	Area, %	Area, km^2	Area, %
< 50	4.10	57.31%	4.09	57.25%	0.004	0.1%
50 to 400	3.04	42.44%	3.04	42.51%	-0.005	-0.1%
400-489	0.02	0.25%	0.02	0.25%	0.000	0.0%

The delineation of sanitary protection zones is much easier when we have the total travel time. According to the (Environment Agency Bristol, 2019), the safeguard zones can be divided into zones. The first two zones are based on the travel time of potential contaminants through the saturated zone; the third zone represents the recharge area. All the zones should cover the maximum possible extent based on that abstraction.

The Inner first Protection Zone is defined by a 50-day travel time from any point below the water table to the source or a minimum 50-meter radius from the source and is used to control a wide range of activities that could pose a significant risk to groundwater.

The second Outer Protection Zone is defined as a 400-day travel time. The 400-day travel time is based loosely on consideration of the minimum time required to provide delay, dilution, and attenuation of slowly degrading pollutants.

The third Protection Zone or Source Catchment Protection Zone also referred to as the total catchment, Total Capture Zone, or Catchment Protection Zone, is defined as the area needed to support the projected yield from long-term groundwater recharge.

Therefore, different travel time classes can be easily transformed into a sanitary protection zone map. Figure 50 shows the first protection zone, up to 50 m, around the tectonic lineaments and covers around 57% of the entire study area (Table 22). The second protection zone is up to 400m and covers around 42% of the entire study area, and the third protection zone which is over 400 days and covers around 0.25% of the entire study area.

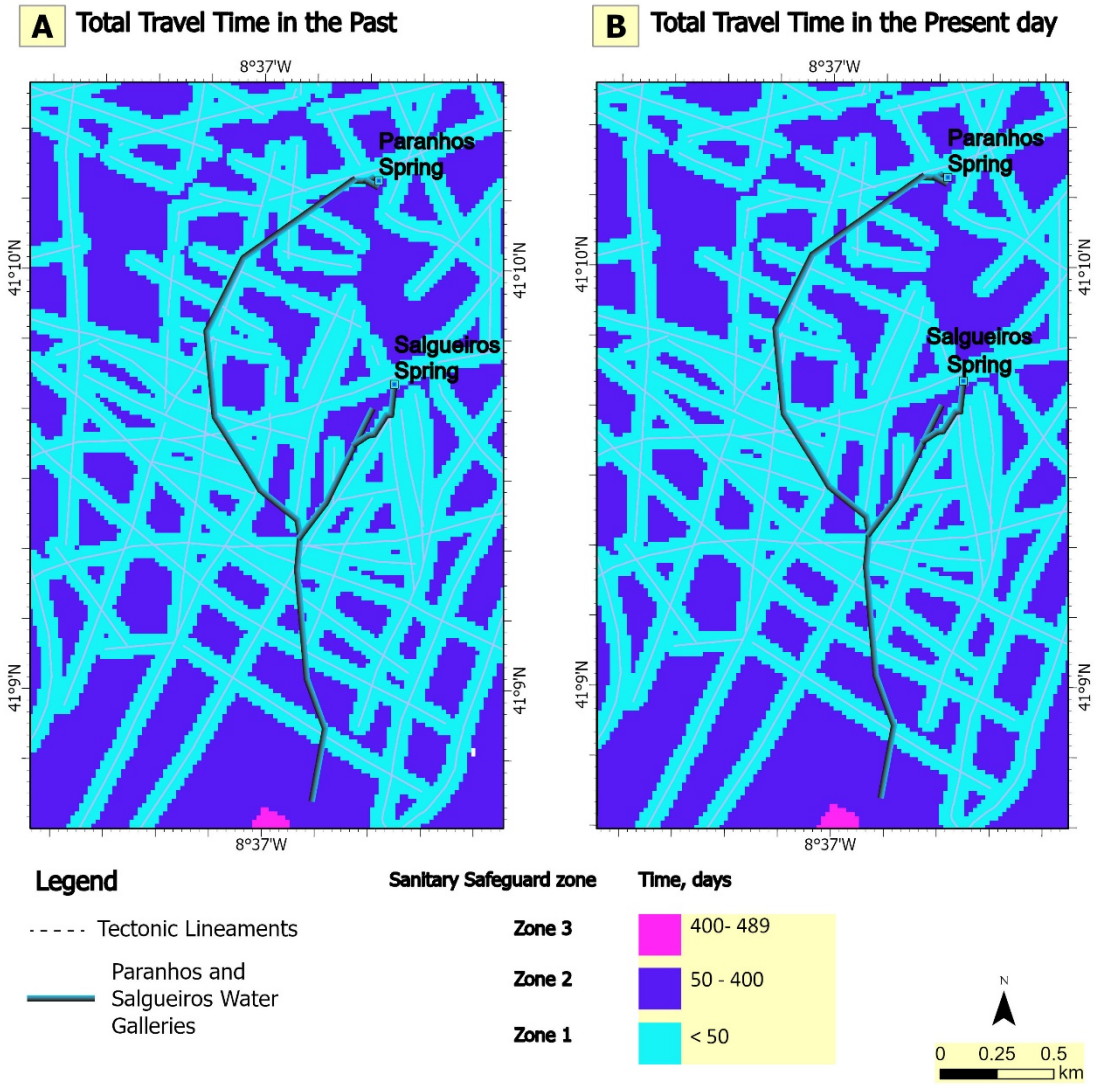

Figure 50. Total Travel Time (days) in the study area. (A) Map in the XIXth century; (B) Map in the XXIst century.

Chapter V: Conclusion and suggestions for future research

(página propositadamente em branco)

5.1. Conclusions

To predict the spatiotemporal changes of the groundwater vulnerability and the safeguard zones according to the TIME-INPUT method by Kralik & Keimel (2003) and the Time-Dependent Model (Živanović et al., 2016) in the urban fractured aquifers of Porto city and compare the results after and before the urban expansion of the city, many GIS-based models were developed to reconstruct and calculate the groundwater recharge, the groundwater vertical and horizontal travel time, and the surface travel time. Then, the models were integrated to calculate the total travel time (Kralik & Keimel, 2003).

Therefore, the following results were obtained:

i. The TIME-INPUT method applies to urban fractured hard-rock aquifers when predicting groundwater vulnerability. Its main factors are (1) the travel-time (TIME) from the surface to groundwater (about 60%) enhanced by (2) the amount of groundwater recharge (INPUT; about 40%), giving the travel time slightly higher importance than the groundwater recharge (Kralik & Keimel, 2003).

ii. The basic data to calculate the main factor travel-TIME are the thickness and the hydraulic conductivity of each layer of the unsaturated zone. Besides, the influence of tectonic structures was used as a correction factor as they accelerated the travel time.

iii. The main factor INPUT (groundwater recharge) is classified as a correction factor. Low recharge quantities have high correction factors, thus increasing time, whereas high recharge quantities reduce time and increase vulnerability. Several factors were used to predict the INPUT factor (Kralik & Keimel, 2003), including Hydrogeology/ geology, slopes, land use, lineaments density, and drainage network density. In addition, several updated elements have been added to enhance the calculation of the INPUT Factor in urban areas in the present-day, such as the maps of hydraulic networks.

iv. The results are not based on categories of unitless numbers but rather on travel times. Therefore, the level of subjectivity in assessing vulnerability is reduced as ranking and parameterization of vulnerability were partially avoided;

v. The Time-Dependent Model can also be applied to fractured hard-rock aquifers in urban areas to estimate the safeguard zones of springs which are completely assessed using flow travel time components. This model includes horizontal and vertical groundwater flow components and considers a surface flow component.

vi. The vertical travel time through the unsaturated zone was calculated using the TIME-INPUT method. Next, the horizontal travel time in the saturated zone was estimated using the Euclidian Distance tool in ArcGIS Spatial Analyst, and an initial value of 1 m/day for matrix flow velocity was taken from Devlin (2020). Next, the surface travel time, which is a function of the topography, geology and land use within the watershed, was predicted using the NRCS velocity method (Staff, 2010). Then, the total travel time was calculated by combing the travel time components.

vii. The results are based on travel times rather than categories of unitless numbers. Therefore, converting the total travel time map into a sanitary protection zone map is very simple. This is because most countries consider sanitary protection zones based on water or particle travel times;

viii. Land use in the study area has changed over time. Urbanisation rapidly grew from the past in the XIXth century to the present in the XXIst century. It was shown that the parameter values most affected by land use change were the recharge (INPUT Factor) and surface travel time;

ix. The results indicate that the total vertical travel time component is less than 12 days and that areas around the tectonic lineaments are the most vulnerable as they have the lowest travel time values. It is also noted that the spatiotemporal changes between the past and present-day are very small. Considering that the hydrogeological characteristics of the study area have not changed between the past and the present-day, there were no spatiotemporal changes in the horizontal travel time, and it has a maximum value of 487 days, i.e., nearly 1 year and 4 months. Nevertheless, in most of the area, the horizontal travel time is less than 50 days, even in the surroundings of the Paranhos and Salgueiros springs. The surface travel time in the study area takes a maximum of 1 h in the past while it only takes 0.5 h in the present-time, and this means that it becomes faster after the urbanization growth;

x. The total travel time has a maximum value of 489 days, i.e., nearly 1 year and 4 months. Nevertheless, in more than half of the area, the total travel time is less than 50 days, even in the surroundings of the Paranhos and Salgueiros springs. The areas around the tectonic lineaments have the lowest travel time values and, therefore, the highest levels of vulnerability;

xi. The overall spatiotemporal changes in vulnerability and safeguard zones were small in the study area between the past and present time; and

xii. The proposed GIS-based methodology can be applied at different data levels, even with limited data. However, with the possibility of improving it and enhancing the quality of data acquisition, the method becomes more flexible, and the level of uncertainty in prediction decreases.

5.2. Future recommendations

To improve the model's prediction of different travel time components, and, therefore, the vulnerability and safeguard zones assessment, the following recommendations can be made through further research studies:

i. Enhancing the data quality will enhance the prediction results of the GIS models. This can be achieved by reducing the sources of uncertainties in data acquisition. Uncertainties relate mostly to estimating the thickness and hydraulic conductivities of the unsaturated zones due to insufficient geophysical investigations and boreholes. Besides, only detailed hydrogeological field observations and structural analysis supported by aerial photographs make it possible to analyze the important fault zones responsible for rapid travel time to groundwater (Kralik & Keimel, 2003). Defining the watershed area for the important tectonic fissures in the study area connected to the springs is also important to estimate the surface travel time and include it in calculating the total travel time. To increase groundwater velocity estimations and, therefore, horizontal travel times, natural tracers and tracer experiments are essential;

ii. Calibration and sensitivity analysis is important so that the model simulates the aquifer system to a desired degree of accuracy. The calibration process involves matching water levels, water-level changes, hydraulic gradients, flow rates, volumetric budgets, or a combination of these; and

iii. The methodology can be enhanced using mathematical and computer-based models, as the computer-based models are the most sophisticated tools available for simulating aquifer behavior and understanding groundwater flow.

(página propositadamente em branco)

Chapter VI: References

(página propositadamente em branco)

6. References

Acreman, M., Albertengo, J., Amado, T., Amis, M., Anderson, A., Bacchur, I., ... & Yakushina, E. (2012). Report of the work of the expert group on maintaining the ability of biodiversity to continue to support the water cycle.

Afonso, M. J., Freitas, L., Devy-Vareta, N., Teixeira, J., Fontes, G., & Chaminé, H. I. (2018). Cartografia subterrânea dos antigos mananciais de Paranhos e Salgueiros para o abastecimento de água à cidade do Porto (NW de Portugal): Contexto e marcos históricos. Xeomorfoloxía e paisaxes xeográficas: catro décadas de investigación e ensino, homenaxe a Augusto Pérez-Albertí.

Afonso, M. J., Freitas, L., & Chaminé, H. I. (2019). Groundwater recharge in urban areas (Porto, NW Portugal): The role of GIS hydrogeology mapping. Sustainable Water Resources Management, 5(1), 203–216.

Afonso, M. J., Freitas, L., Marques, J. M., Carreira, P. M., Pereira, A. J. S. C., Rocha, F., & I. Chaminé, H. (2020). Urban Groundwater Processes and Anthropogenic Interactions (Porto Region, NW Portugal). Water, 12(10), 2797.

Afonso, M.J., Freitas, L., Pereira, A., Neves, L., Guimarães, L., Guilhermino, L., Mayer, B., Rocha, F., Marques, J., & Chaminé, H.I. (2016). Environmental Groundwater Vulnerability Assessment in Urban Water Mines (Porto, NW Portugal). Water, 8(11), 499.

Afonso, M.J. (2011). Hidrogeologia e Hidrogeoquímica da Região Litoral Urbana do Porto, entre Vila do Conde e Vila Nova de Gaia (NW de Portugal): Implicações Geoambientais. Ph.D. Thesis, Instituto Superior Técnico da Universidade Técnica de Lisboa, Lisboa, Portugal.

Afonso, M.J.; Chaminé, H.I.; Marques, J.M.; Carreira, P.M.; Guimarães, L.; Guilhermino, L.; Gomes, A.; Fonseca, P.E.; Pires, A.; Rocha, F. (2010). Environmental issues in urban groundwater systems: A multidisciplinary study of the Paranhos and Salgueiros spring waters, Porto (NW Portugal). Environ. Earth Sci., 61, 379–392.

Afonso, M.J.; Pires, A.; Chaminé, H.I.; Marques, J.M.; Guimarães, L.; Guilhermino, L.; Rocha, F. (2010). Aquifer vulnerability assessment of urban areas using a GIS-based cartography: Paranhos groundwater pilot site, Porto, NW Portugal. In Global Groundwater Resources and Management; Paliwal, B.S., Ed.; Scientific Publishers: Jodhpur, India, pp. 259–278.

Águas e Energia do porto. (n.d.). Contextualização Histórica. Retrieved September 6, 2022, from https://www.aguasdoporto.pt/abastecimento-de-agua/contextualizacao-historica.

Alam, F., Umar, R., Ahmed, S., & Dar, F. A. (2014) A new model (DRASTIC-LU) for evaluating groundwater vulnerability in parts of central Ganga Plain, India. Arabian Journal of Geosciences, 7(3), 927–937.

Albinet, M., & Margat, J. (1970) Cartographie de la vulnérabilité à la pollution des nappes d'eau souterraine. Bull. BRGM, 2(3), 4.

Albuquerque, M. T. D., Sanz, G., Oliveira, S. F., Martínez-Alegría, R., & Antunes, I. M. H. R. (2013). Spatio-Temporal Groundwater Vulnerability Assessment—A Coupled Remote Sensing and GIS Approach for Historical Land Cover Reconstruction. Water Resources Management, 27(13), 4509–4526.

Albuquerque, T., Roque, N., Rodrigues, J., Antunes, M., & Silva, C. (2021) DRASTICAI, a New Index for Groundwater Vulnerability Assessment—A Portuguese Case Study. Geosciences, 11, 228.

Aller, L. (1985). DRASTIC: a standardized system for evaluating ground water pollution potential using hydrogeologic settings. Robert S. Kerr Environmental Research Laboratory, Office of Research and Development, US Environmental Protection Agency.

Alley, W. M., Reilly, T. E., & Franke, O. L. (1999). Sustainability of ground-water resources (Vol. 1186). US Department of the Interior, US Geological Survey.

Bachmat, Y., & Collin, M. (1987). Mapping to assess groundwaters vulnerability to pollution. . Atti Int. Conf. Vulnerab. of Soil and Groundwater to pollutants, RIVM Proc. And Inf. 38; 297-307 pp.

Barbulescu, A. (2020). Assessing Groundwater Vulnerability: DRASTIC and DRASTIC-Like Methods: A Review. Water, 12(5), 1356.

Bourbon e Noronha T (1885). As aguas do Porto. Escola Médico-Cirúrgica do Porto, Porto (Graduation´s Dissertation) http:// hdl. handle.net/ 10216/ 16634

Caetano, M., Nunes, V., & Nunes, A. (2009). CORINE land cover 2006 for continental Portugal. Instituto Geográfico Português.

Carríngton da Costa, J., & Teixeira, C. (1957). Notícia explicativa da Carta Geológica de Portugal, na escala de 1/50000, Folha 9-C (Porto). Serviços Geológicos de Portugal.

Carteado Mena, J. (1908). Contribuição para o estudo da Hygiene do Porto: Analyse sanitaria do seu abastecimento em água potável. III. Estudo sobre os poços do Porto. Unpublished Report.

Chaminé, H. I., Afonso, M. J., & Freitas, L. (2014). From historical hydrogeological inventory through GIS mapping to problem solving in urban groundwater systems. European Geologist Journal, 38, 33–39.

Chaminé, H. I., Afonso, M. J., Robalo, P. M., Rodrigues, P., Cortez, C., Monteiro Santos, F. A., ... & Rocha, F. (2010). Urban speleology applied to groundwater and geo-engineering studies: underground topographic surveying of the ancient Arca D'Água galleries catchworks (Porto, NW Portugal). International Journal of Speleology, 39(1), 1.

Chaminé, H. I., Pereira, L. G., Fonseca, P., Moço, L., Fernandes, J., Rocha, F., Flores, D., De Jesus, A. P., Gomes, C., & De Andrade, A. S. (2003). Tectonostratigraphy of Middle and Upper Palaeozoic

black shales from the Porto-Tomar-Ferreira do Alentejo shear zone (W Portugal): New perspectives on the Iberian Massif. Geobios, 36(6), 649–663.

Civita MV (1994). Le carte della vulnerabilità degli acquiferi all'inquinamento: teoria & pratica. Pitagora Editrice, Bologna

Civita MV (2010). The combined approach when assessing and mapping groundwater vulnerability to contamination. J Water Resour Prot 2:14–28

Civita MV, De Maio M (2000). Valutazione e cartografia automatica della vulnerabilità degli acquiferi all'inquinamento con il sistema parametrico: SINTACS R5. Pitagora Editrice, Bologna

Civita MV. (2008). An improved method for delineating source protection zones for karst springs based on analysis of recession curve data. Hydrogeology Journal, 16(5), 855–869.

Civita, M., & De Regibus, C. (1995). Sperimentazione di alcune metodologie per la valutazione della vulnerabilità degli aquiferi. Q Geol Appl Pitagora Bologna, 3, 63–71.

Clement, T. P. (2011). Complexities in hindcasting models—When should we say enough is enough? Groundwater, 49(5), 620–629.

COBA—Consultores de Engenharia e Ambiente, SA (2003). Carta geotécnica do Porto, 2nd edn. COBA/FCUP/CMP, Porto

Comte, J.-C., Ofterdinger, U., Legchenko, A., Caulfield, J., Cassidy, R., & Mézquita González, J. A. (2019). Catchment-scale heterogeneity of flow and storage properties in a weathered/fractured hard rock aquifer from resistivity and magnetic resonance surveys: Implications for groundwater flow paths and the distribution of residence times. Geological Society, London, Special Publications, 479(1), 35–58.

Cook, P. G. (2003). A guide to regional groundwater flow in fractured rock aquifers. Citeseer.

de Oliveira Marques, A. H. (1972). History of Portugal: from Lusitania to Empire (Vol. 1). Columbia University Press.

Denny, S.C.; Allen, D.N.; Journeay, J.M. (2007). DRASTIC-Fm: A modified vulnerability mapping method for structurally controlled aquifers in the southern Gulf Islands. British Columbia, Canada. Hydrogeol. J., 15, 483–493.

Devlin, J. F. (2020). Groundwater velocity. https://books.gw-project.org/groundwater-velocity.

Environment Agency Bristol (2019). Manual for the production of Groundwater Source Protection Zones.

ESRI (2021a), About preparing to digitize a paper map, Retrieved August 06, 2022, from https://desktop.arcgis.com/en/arcmap/latest/manage-data/creating-new-features/about-preparing-to-digitize-a-paper-map.htm

ESRI (2021b), An overview of geodatabase design, Retrieved August 06, 2022, from https://desktop.arcgis.com/en/arcmap/latest/manage-data/geodatabases/an-overview-of-geodatabase-design.htm

ESRI (2021c), What is the ArcGIS Spatial Analyst extension?, Retrieved August 06, 2022, from https://desktop.arcgis.com/en/arcmap/latest/extensions/spatial-analyst/what-is-the-spatial-analyst-extension.htm

ESRI (2021d), Use ModelBuilder, Retrieved August 06, 2022, from https://pro.arcgis.com/en/pro-app/latest/help/analysis/geoprocessing/modelbuilder/modelbuilder-quick-tour.htm

ESRI (2021e), Data classification methods, Retrieved August 06, 2022, from https://pro.arcgis.com/en/pro-app/latest/help/mapping/layer-properties/data-classification-methods.htm

ESRI (2022), Change detection in ArcGIS Pro, Retrieved August 06, 2022, from https://pro.arcgis.com/en/pro-app/latest/help/analysis/image-analyst/change-detection-in-arcgis-pro.htm

Fang, X., Thompson, D. B., Cleveland, T. G., & Pradhan, P. (2007). Variations of Time of Concentration Estimates Using NRCS Velocity Method. Journal of Irrigation and Drainage Engineering, 133(4), 314–322.

Findell, K. L., Berg, A., Gentine, P., Krasting, J. P., Lintner, B. R., Malyshev, S., Santanello, J. A., & Shevliakova, E. (2017). The impact of anthropogenic land use and land cover change on regional climate extremes. Nature Communications, 8(1), 989.

Fitts, C. R. (2013). Hydrology and Geology. Groundwater Science, 123-186.

Fletcher, T. D., Andrieu, H., & Hamel, P. (2013) Understanding, management and modelling of urban hydrology and its consequences for receiving waters: A state of the art. Advances in Water Resources, 51, 261–279.

Fontes, A. (1908). Contribuição para a Hygiene do Porto: analyse sanitaria do seu abastecimento em água potavel. I. Estudo dos Mananciaes de Paranhos e Salgueiros. Bachelor's Thesis, Escola Médico-Cirúrgica do Porto, Porto, Portugal. (In Portuguese)

Foster, S., Hirata, R., & Andreo, B. (2013). The aquifer pollution vulnerability concept: Aid or impediment in promoting groundwater protection? Hydrogeology Journal, 21(7), 1389–1392.

Foster, S., Witkowski, A., Kowalczyk, A., & Vrba, J. (2007). Aquifer pollution vulnerability concept and tools–use, benefits and constraints. Groundwater Vulnerability Assessment and Mapping. IAH-Selected Papers, 11, 2–9.

Foster SD, Hirata R, Gomes D, D'Elia M, Paris M (2002). Groundwater quality protection: a guide for water utilities, municipal authorities, and environment agencies. The World Bank, Washington, DC

Foster, S. (1998). Groundwater recharge and pollution vulnerability of British aquifers: A critical overview. Geological Society, London, Special Publications, 130(1), 7–22.

Foster, S. (1987). Fundamental concepts in aquifer vulnerability, pollution risk and protection strategy. In: Duijvenbooden W van, Waegeningh Hg van (eds): TNO Committee on Hydrological Research, The Hague. Vulnerability of soil and under groundwater to pollutants, Proceedings and Information, 38: 69-86.

Francés A, Paralta E, Fernandes J, Ribeiro L (2001). Development and application in the Alentejo region of a method to assess the vulnerability of groundwater to diffuse agricultural pollution: the susceptibility index. In: Ribeiro L (ed) Proceedings 3rd International Conference

Freitas, L. (2010). Análise hidro-histórica das águas subterrâneas do Porto, Séculos XIX a XXI: inventário, base de dados e cartografia SIG. Universidade do Porto.

Freitas, L., Afonso, M. J., Devy-Vareta, N., Marques, J. M., Gomes, A., & Chaminé, H. I. (2014). Coupling Hydrotoponymy and GIS Cartography: A Case Study of Hydrohistorical Issues in Urban Groundwater Systems, Porto, NW Portugal: Historical Issues in Urban Groundwater Systems. Geographical Research, 52(2), 182–197.

Freitas, L., Afonso, M. J., Pereira, A. J. S. C., Delerue-Matos, C., & Chaminé, H. I. (2019a). Assessment of sustainability of groundwater in urban areas (Porto, NW Portugal): A GIS mapping approach to evaluate vulnerability, infiltration and recharge. Environmental Earth Sciences, 78(5), 140.

Freitas, L., Chaminé, H. I., & Pereira, A. J. S. C. (2019b.) Coupling groundwater GIS mapping and geovisualisation techniques in urban hydrogeomorphology: Focus on methodology. SN Applied Sciences, 1(5), 490.

Freitas, L., Chaminé, H. I., Afonso, M. J., Meerkhan, H., Abreu, T., Trigo, J. F., & Pereira, A. J. S. C. (2020). Integrative Groundwater Studies in a Small-Scale Urban Area: Case Study from the Municipality of Penafiel (NW Portugal). Geosciences, 10(2), 54.

Gatwaza, O. C., Cao, X., & Beckline, M. (2016). Impact of Urbanization on the Hydrological Cycle of Migina Catchment, Rwanda. OALib, 03(07), 1–12.

Goepel, K.D. (2018). Implementing the Analytic Hierarchy Process as a Standard Method for Multi-Criteria Decision Making in Corporate Enterprises—A New web-based AHP Excel template software 15.09.2018 version with Multiple Inputs. California, USA. http://bpmsg.com.

Goldscheider, N. I. C. O., Klute, M., Sturm, S., & Hötzl, H. (2000). The PI method–a GIS-based approach to mapping groundwater vulnerability with special consideration of karst aquifers. Z Angew Geol, 46(3), 157-166.

Goodchild, M. F. (2005). GIS and modeling overview. GIS, Spatial Analysis, and Modeling. ESRI Press, Redlands, 1–18.

Guan, J., Maslia, M. L., & Aral, M. M. (2009). A Methodology to Reconstruct Groundwater Contamination History with Limited Field Data. In ASCE World Environmental and Water Resources Congress, Kansas City, MO, published on CD.

Hasan, M., Shang, Y., Jin, W., & Akhter, G. (2019). Assessment of aquifer vulnerability using integrated geophysical approach in weathered terrains of South China. Open Geosciences, 11(1), 1129-1150.

Hibbs, B. J. (2016). Groundwater in Urban Areas. Journal of Contemporary Water Research & Education, 159(1), 1–4.

Hibbs, B. J., & Sharp, J. M. (2012) Hydrogeological impacts of urbanization. Environmental & Engineering Geoscience, 18(1), 3–24.

Hölting, B., Haertlé, T., Hohberger, K.-H., Nachtigall, K. H., Villinger, E., Weinzierl, W., & Wrobel, J.-P. (1995). Konzept zur Ermittlung der Schutzfunktion der Grundwasserüberdeckung (Vol. 63). Schweizerbart.

IGP – Instituto Geográfico Português (2010). Carta de uso e ocupação do solo de Portugal Continental para 2007 (COS2007). Memória Descritiva, 87 pp.

IPMA—The Portuguese Institute for Sea and Atmosphere (2022). Air temperature and rainfall, Climate Normals, Porto – Serra do Pilar 1981–2010. Retrieved August 2022, from http://www.ipma.pt/pt/oclima/norma is. clima/1981–2010/ 014/.

Jani, J. (2012). GIS as a tool for modelling groundwater flow. 2012 IEEE Symposium on Business, Engineering and Industrial Applications, 513–517.

Kralik, M., & Keimel, T. (2003). Time-input, an innovative groundwater-vulnerability assessment scheme: Application to an alpine test site. Environmental Geology, 44(6), 679–686.

Kresic, N., & Mikszewski, A. (2012). Hydrogeological conceptual site models: Data analysis and visualization. CRC press.

Lachassagne, P., Dewandel, B., & Wyns, R. (2021). Review: Hydrogeology of weathered crystalline/hard-rock aquifers—guidelines for the operational survey and management of their groundwater resources. Hydrogeology Journal, 29(8), 2561–2594.

Lachassagne, P., Wyns, R., & Dewandel, B. (2011). The fracture permeability of Hard Rock Aquifers is due neither to tectonics, nor to unloading, but to weathering processes. Terra Nova, 23(3), 145–161.

Lee, M., Kelly, C., Meehan, R., Hickey, C., & Williams, N. H. (2020). Irish groundwater vulnerability mapping and Groundwater Protection Schemes. In A. J. Witkowski, S. Jakóbczyk-Karpierz, J. Czekaj, & D. Grabala (Eds.), Groundwater Vulnerability and Pollution Risk Assessment (1st ed., pp. 197–206). CRC Press.

Lerner, D. N. (1990) Groundwater recharge in urban areas. Atmospheric Environment. Part B. Urban Atmosphere, 24(1), 29–33.

Lubis, R. F. (2018). Urban hydrogeology in Indonesia: A highlight from Jakarta. IOP Conference Series: Earth and Environmental Science 118(1):012022.

Machiwal, D., Jha, M. K., Singh, V. P., & Mohan, C. (2018) Assessment and mapping of groundwater vulnerability to pollution: Current status and challenges. Earth-Science Reviews, 185, 901–927.

Madureira, H. (2001). Processos de transformação da estrutura verde do Porto. Revista da Faculdade de Letras — Geografia, I série, vol. XVII-XVIII, Porto, 137-218.

Madureira, H., Andresen, T., & Monteiro, A. (2011). Green structure and planning evolution in Porto. Urban Forestry & Urban Greening, 10(2), 141–149.

Majandang, J., & Sarapirome, S. (2013). Groundwater vulnerability assessment and sensitivity analysis in Nong Rua, Khon Kaen, Thailand, using a GIS-based SINTACS model. Environmental Earth Sciences, 68(7), 2025–2039.

Margat, J. (1968). Vulnerabilité des nappes d'eau souterraine a la pollution. Bases de al Cartographie (Doc.), 68.

Marsalek, J. (2014). Urban Water Cycle Processes and Interactions. CRC Press.

Martin, S. L., Hamlin, Q. F., Kendall, A. D., Wan, L., & Hyndman, D. W. (2021). The land use legacy effect: Looking back to see a path forward to improve management. Environmental Research Letters, 16(3), 035005.

Martin, S. L., Hayes, D. B., Kendall, A. D., & Hyndman, D. W. (2017). The land-use legacy effect: Towards a mechanistic understanding of time-lagged water quality responses to land use/cover. Science of The Total Environment, 579, 1794–1803.

McGrane, S. J. (2016). Impacts of urbanisation on hydrological and water quality dynamics, and urban water management: A review. Hydrological Sciences Journal, 61(13), 2295–2311.

Meerkhan, H., Freitas, L., Teixeira, J., Rocha, F., Pereira, A. J. S. C., Afonso, M. J., & Chaminé, H. I. (2021). DISCO-Urban: An updated GIS-based vulnerability mapping method for delineating groundwater protection zones in historic urban areas. Mediterranean Geoscience Reviews, 3(3), 361–377.

Meerkhan, H., Teixeira, J., Espinha Marques, J., Afonso, M.J., & Chaminé, H.I. (2016). Delineating Groundwater Vulnerability and Protection Zone Mapping in Fractured Rock Masses: Focus on the DISCO Index. Water, 8(10), 462.

Morais, A. R. L., & Galvão de Carvalho, C. A. (2018). Porto (in)visível: Redescobrir os antigos mananciais. Reflexão sobre a sua relevância. in genius loci lugares e significados places and meanings (vol. 3, pp. 129–144).

Moraru, C., Hannigan, R. (2018). Overview of Groundwater Vulnerability Assessment Methods. In: Analysis of Hydrogeochemical Vulnerability. Springer Hydrogeology. Springer, Cham.

Morris, B. L., Lawrence, A. R., Chilton, P., Adams, B., Calow, R. C., & Klinck, B. A. (2003). Groundwater and its susceptibility to degradation: A global assessment of the problem and options for management. United Nations Environment Programme, 126p.

National Research Council (1993). Groundwater vulnerability assessment: Predicting relative contamination potential under conditions of uncertainty. National Academies Press.

Natural Resources Conservation Service (NRCS) (formerly Soil Conservation Service). (1972). "Travel time, time of concentration, and lag." The national engineering handbook, Sec. 4, U.S. Dept. of Agriculture, Washington, D.C.

Natural Resources Conservation Service (NRCS). (1986). "Urban hydrology for small watersheds." Technical release No. 55, U.S. Dept. of Agriculture, Washington, D.C.

Ó Dochartaigh, B. É., Ball, D. F., MacDonald, A. M., Lilly, A., Fitzsimons, V., Rio, M. D., & Auton, C. A. (2005). Mapping groundwater vulnerability in Scotland: A new approach for the Water Framework Directive. Scottish Journal of Geology, 41(1), 21–30.

Olmer, M., & Rezac, B. (1974). Methodical principles of maps for protection of groundwater in Bohemia and Moravia scale 1/200.000. Mem. IAH, 10(1), 105–107.

Palmquist, R. (1993). Groundwater vulnerability: A DRASTIC approach. 15, 91–150.

Pereira, E.; Ribeiro, A.; Carvalho, G.S.; Noronha, F.; Ferreira, N.; Monteiro, J.H (1989). Carta Geológica de Portugal, escala 1/200000. Folha 1; Serviços Geológicos de Portugal: Lisboa, Portugal.

Pochon, A., Tripet, J.-P., Kozel, R., Meylan, B., Sinreich, M., & Zwahlen, F. (2008). Groundwater protection in fractured media: A vulnerability-based approach for delineating protection zones in Switzerland. Hydrogeology Journal, 16(7), 1267–1281.

Poeter, E., Fan, Y., Cherry, J., Wood, W., & Mackay–Guelph, D. (2020). Groundwater in our water cycle–getting to know Earth's most important fresh water source. The Groundwater Project, Guelph, Ontario, Canada.

Pórcel, R. A. D., Schüth, C., León-Gómez, H. D., Hoppe, A., & Lehné, R. (2014). Land-Use Impact and Nitrate Analysis to Validate DRASTIC Vulnerability Maps Using a GIS Platform of Pablillo River Basin, Linares, N.L., Mexico. International Journal of Geosciences, 5(12), 1468–1489.

Ribeiro L, Pindo JC, Dominguez-Granda L (2017). Assessment of groundwater vulnerability in the Daule aquifer, Ecuador, using the susceptibility index method. Sci Total Environ 574:1674–1683

Robins, N. S. (1998). Recharge: the key to groundwater pollution and aquifer vulnerability. In: Robins, N. S. (ed.) Groundwater Pollution, Aquifer Recharge and Vulnerability. Geological Society, London, Special Publications, 130, 1-5.

Robins, N., MacDonald, A., & Allen, D. (2007). The vulnerability paradox for hard fractured lower palaeozoic and Precambrian rocks. In A. J. Witkowski, A. Kowalczyk, & J. Vrba (Eds.), In: Selected papers from the Groundwater Vulnerability Assessment and Mapping International Conference, Ustron, Poland (pp. 13–19). Taylor & Francis. http://nora.nerc.ac.uk/id/eprint/4221/

Schilling, K. E., & Wolter, C. F. (2007). A GIS-based groundwater travel time model to evaluate stream nitrate concentration reductions from land use change. Environmental Geology, 53(2), 433–443.

Schirmer, M., Leschik, S., & Musolff, A. (2013). Current research in urban hydrogeology – A review. Advances in Water Resources, 51, 280–291.

Silva, A.F. and Matos, A.C. (2004). The networked city: managing power and water utilities in Portugal, 1850s-1920s. Business and Economic History On-Line 2, 1–45.

Singh, A., Srivastav, S. K., Kumar, S., & Chakrapani, G. J. (2015). A modified-DRASTIC model (DRASTICA) for assessment of groundwater vulnerability to pollution in an urbanized environment in Lucknow, India. Environmental Earth Sciences, 74(7), 5475–5490.

Singhal, B. B. S., & Gupta, R. P. (2010). Applied Hydrogeology of Fractured Rocks. Springer Netherlands.

Singhal, B.B.S. (2008). Nature of Hard Rock Aquifers: Hydrogeological Uncertainties and Ambiguities. In: Ahmed, S., Jayakumar, R., Salih, A. (eds) Groundwater Dynamics in Hard Rock Aquifers. Springer, Dordrecht.

Sotornikova, R., & Vrba, J. (1987). Some remarks on the concept of vulnerability maps.

Staff, N. (2010). National Engineering Handbook Chapter 15 Time of Concentration.

Stempvoort, D. V., Ewert, L., & Wassenaar, L. (1993). Aquifer vulnerability index: A GIS-compatible method for groundwater vulnerability mapping. Canadian Water Resources Journal, 18(1), 25–37.

Swartz, C. H., Rudel, R. A., Kachajian, J. R., & Brody, J. G. (2003). Historical reconstruction of wastewater and land use impacts to groundwater used for public drinking water: Exposure assessment using chemical data and GIS. Journal of Exposure Science & Environmental Epidemiology, 13(5), 403–416.

Telles Ferreira. (1892). AG Carta Topográfica da Cidade do Porto. Direcção-Geral Dos Trabalhos Geodésicos, Topográficos, Hidrográficos e Geológicos Do Reino: Lisboa, Portugal.

UN-DESA-PV [United Nations - Department of Economic and Social Affairs - Population Division]. World Population Prospects 2019. Retrieved February 06, 2022, from https://population.un.org/wpp/Publications/

USEPA (2021). Delineate the Source Water Protection Area | US EPA. Retrieved February 18, 2022, from https://www.epa.gov/sourcewaterprotection/delineate-source-water-protection-area

USEPA. (1987). Guidelines for delineation of wellhead protection areas.

USGS (2018a). Groundwater Storage and the Water Cycle. Retrieved January 01, 2022, from https://www.usgs.gov/special-topics/water-science-school/science/groundwater-storage-and-water-cycle,

USGS (2018b). Urbanization and Water Quality. Retrieved January 01, 2022, from https://www.usgs.gov/special-topics/water-science-school/science/urbanization-and-water-quality?qt-science_center_objects=0#qt-science_center_objects.

USGS (n.d.). Wake County Groundwater. Retrieved February 13, 2022, from https://www2.usgs.gov/water/southatlantic/nc/projects/wake-county-groundwater/study.php

Stempvoort, D. V., Ewert, L., & Wassenaar, L. (1993). Aquifer vulnerability index: a GIS-compatible method for groundwater vulnerability mapping. Canadian Water Resources Journal, 18(1), 25-37.

Vázquez-Suñé, E., Sánchez-Vila, X., & Carrera, J. (2005). Introductory review of specific factors influencing urban groundwater, an emerging branch of hydrogeology, with reference to Barcelona, Spain. Hydrogeology Journal, 13(3), 522–533.

Villumsen, A., Jacobsen, O. S., & Sønderskov, C. (1984). Mapping the vulnerability of ground water reservoirs with regard to surface pollution. Arbog-Dan. Geol. Unders. (Denmark).

Vrba, J., & Zaporozec, A. (1994). Guidebook on mapping groundwater vulnerability. Heise.

Wachniew, P., Zurek, A. J., Stumpp, C., Gemitzi, A., Gargini, A., Filippini, M., Rozanski, K., Meeks, J., Kværner, J., & Witczak, S. (2016). Toward operational methods for the assessment of intrinsic groundwater vulnerability: A review. Critical Reviews in Environmental Science and Technology, 46(9), 827–884.

Wiles, T. J., & Sharp, J. M. (2008). The secondary permeability of impervious cover. Environmental & Engineering Geoscience, 14(4), 251–265.

Witczak, S., Duda, R., & Zurek, A. (2014). The Polish concept of groundwater vulnerability mapping. Groundwater Vulnerability Assessment and Mapping: IAH-Selected Papers, Volume 11, 11, 45.

Witkowski, A. J. Jakóbczyk-Karpierz, S., Czekaj J., Grabala D. (Ed.). (2020). Groundwater vulnerability and pollution risk assessment. CRC Press, Taylor & Francis Group.

Witkowski, A. J., Kowalczyk, A., & Vrba, J. (Eds.). (2007). Groundwater vulnerability assessment and mapping: Selected papers from the Groundwater Vulnerability Assessment and Mapping International Conference: Ustrón, Poland, 2004. Taylor & Francis.

Yang, Y., Zhang, S., Yang, J., Chang, L., Bu, K., & Xing, X. (2014). A review of historical reconstruction methods of land use/land cover. Journal of Geographical Sciences, 24(4), 746–766.

Živanović, V., Atanacković, N., & Stojadinović, S. (2021). Vulnerability Assessment as a Basis for Sanitary Zone Delineation of Karst Groundwater Sources—Blederija Spring Case Study. Water, 13(19), 2775.

Živanović, V., Jemcov, I., Dragišić, V., Atanacković, N., & Magazinović, S. (2016). Karst groundwater source protection based on the time-dependent vulnerability assessment model: Crnica springs case study, Eastern Serbia. Environmental Earth Sciences, 75(17), 1224.

Zhen, J., James, W., & Wang, F. (1993). Data Manipulation of GIS for Modelling and Simulation in Resource Management. Journal of Water Management Modeling.

Zwahlen, F. (2003). Vulnerability and risk mapping for the protection of carbonate (karst) aquifers. Office for Official Publications of the European Communities.

Zwahlen, F. (Ed.). (2004). COST action 620: Vulnerability and risk mapping for the protection of carbonate (karst) aquifers: final report. Office for Official Publications of the European Communities.